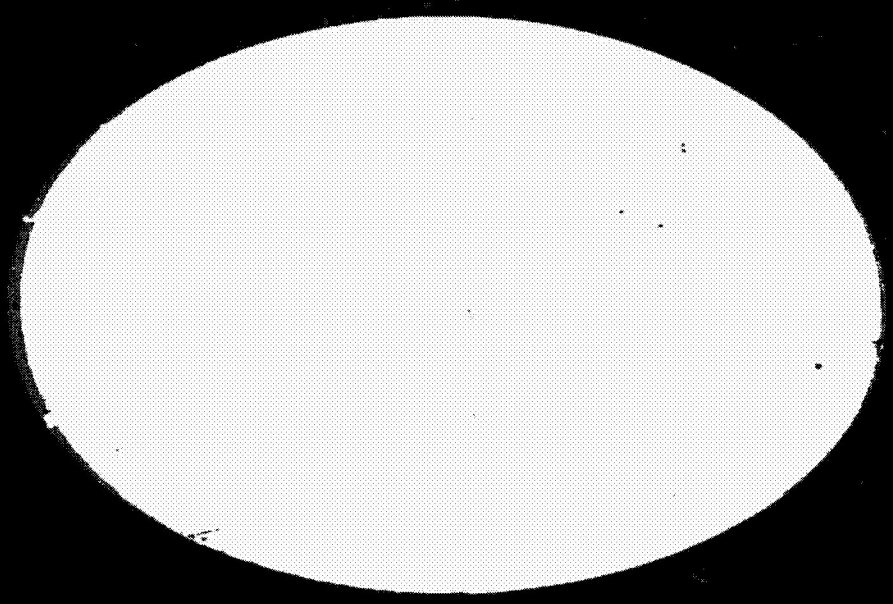

AEROTHERM CORPORATION

ADVANCES IN AEROTHERMOCHEMISTRY

Aerotherm Project 6147

Aerotherm Report 71-41

BOUNDARY CONDITION COMPUTATIONAL PROCEDURES FOR INVISCID, SUPERSONIC STEADY FLOW FIELD CALCULATIONS

by

Michael J. Abbett

Prepared for

National Aeronautics and Space Administration
Ames Research Center

Contract NAS2-6341

November 30, 1971

ABSTRACT

Results are given of a comparative study of numerical procedures for computing solid wall boundary points in supersonic inviscid flow calculations. Twenty five different calculation procedures were tested on two sample problems, a simple expansion wave and a simple compression (two dimensional steady flow). A new simple but accurate calculation procedure was developed. The merits and shortcomings of the various procedures are thoroughly discussed along with complications for three dimensional and time dependent flows.

TABLE OF CONTENTS

NOMENCLATURE

a	speed of sound
b	$\rho u^2/\sqrt{M^2 - 1}$
B	ordinate of lower wall ($y = B(x)$)
h	static enthalpy $h = \frac{\gamma}{\gamma - 1}\frac{p}{\rho}$
H	total enthalpy ($H = h + (u^2 + v^2)/2$)
M	Mach number
p	pressure
p_t, p_o	total pressure
P	$\ell n\ p/p_t$
q	velocity modulus ($q^2 = u^2 + v^2$)
S	entropy ($S = P - \gamma R$)
u,v	velocity components in x,y direction
T	ordinate of upper wall ($y = T(x)$)
x,y	Cartesian coordinates
ξ,η	transformed coordinates (computational space)
γ	isentropic exponent
$\lambda^{\pm}$	slopes characteristics in x,y space ($\lambda = dy/dx$)
δ	$T - B$

ρ	density
ρ_τ	total density
R	$\ell n\ \rho/\rho_t$
τ	streamline slope
θ	angle streamline makes with x-axis

SECTION 1

INTRODUCTION

The purpose of this study is twofold: (1) to review and evaluate techniques for handling boundary points in the numerical solution of supersonic steady flow fields with finite difference procedures, and (2) to improve an existing or develop a new technique which is simple to implement and accurate. In order to clarify and simplify the study as much as possible, attention is primarily focused on two-dimensional, steady, supersonic flow of an ideal gas. Although some implicit procedures for handling boundary conditions are considered, the object is to consider methods that fit in well with explicit differencing procedures (particularly that of MacCormack) for the interior.

The study is organized into three parts: (1) review, (2) evaluation, and (3) development. A preliminary review of current procedures was first performed, and it resulted in the categorization of the various procedures according to the basic principles incorporated. Then representative techniques from each category were compared on problems for which the exact solution is known.

Unless otherwise specified, a two-dimensional steady flow is implied, with the flow direction globally from left to right. Axes and velocity components are (x,y) and (u,v) respectively, with the x axis positive to the right. Thus, a numerical solution is obtained by marching from the left to the right.

This report begins (Section 2) with a brief review and categorization of computational procedures which are now in use, including one developed in this study. Then (Section 3) we discuss the most important elements of a computational procedure, with emphasis on boundary points. Comparative results, and a discussion of the significance, are given in Section 4. The report is concluded (Section 5) with an overview of the results of the study.

It became evident early that the procedures currently in use which give acceptable accuracy tend, in general, to be cumbersome to implement in a computer code. Also, they often require relatively long computing times per mesh point when compared to interior points. The latter is not a strong objection, since it is in the boundary calculations that the particular solution is selected from the infinity of possible solutions to the partial differential equations. However, it is important in the sense that when boundary point calculations comprise a significant portion of the computing time, improving them can result in significant savings in computational expense.

Because of the obvious need for simpler, faster, accurate procedures, efforts were directed toward understanding the factors determining a good boundary point computation procedure, particularly in the context of a predictor/corrector scheme at interior points. Subsequently, a new scheme for computing boundary points was developed. This scheme is very simple, requires little computing time, and seems to be quite accurate. It is discussed in Sections 2, 3, and 4.

SECTION 2

REVIEW

2.1 CATEGORIZATION OF METHODS

The various procedures have been classified in five categories: reflection, explicit differencing (one-sided derivatives), implicit, characteristics, and miscellaneous. Although the last category is somewhat of a grab-bag, it should not be viewed disparagingly, for that is probably where the most satisfactory procedure (from the standpoint of simplicity and accuracy) will be found.

2.2 DISCUSSION OF VARIOUS PROCEDURES TO DATE

2.2.1 Reflection

The use of this procedure is basically physically motivated. The wall boundary of an inviscid flow is essentially a slip stream, and in this sense there is no basic difference between a streamline along a solid wall and the same streamline which is located within a fluid on one side of a slip stream. On this basis, one reasons that, for computational convenience, he can replace his original problem with its solid boundary with another problem having an extended flow field which (hopefully) will include a slip stream where there was originally a solid wall (sketch).

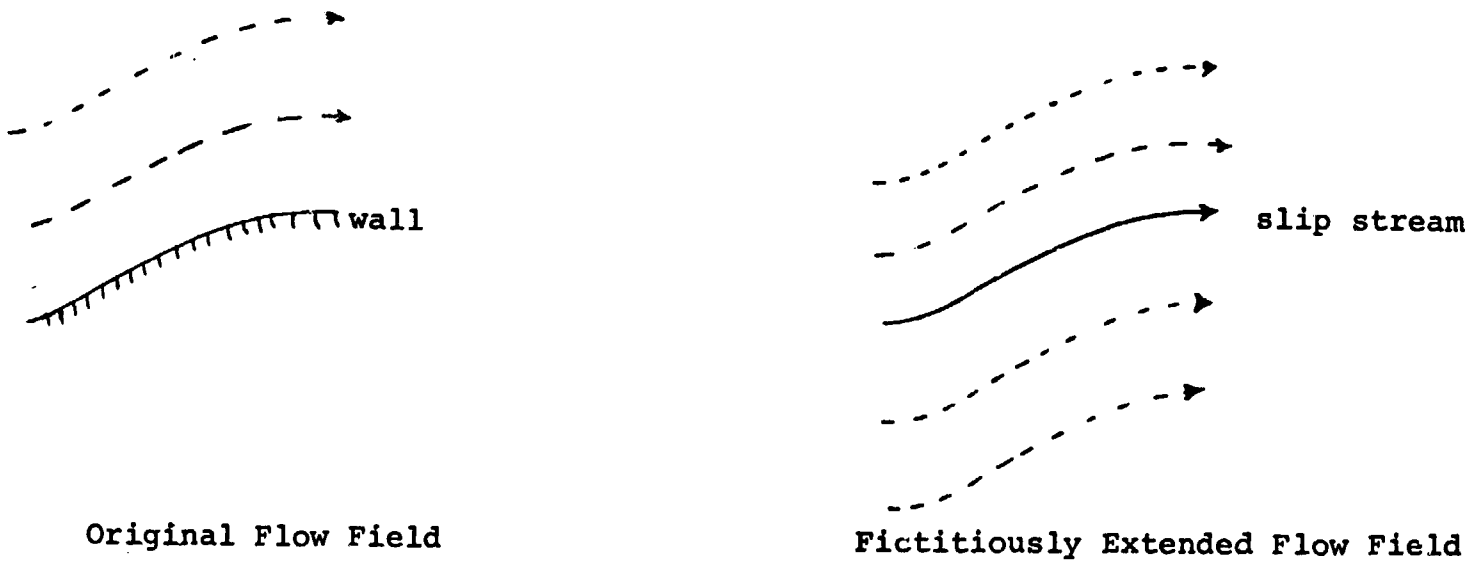

Sketch 1 The Concept of Reflection Procedures

Knowing the solution, at a given initial line, somewhat into the extended flow,* it is possible to continue the solution downstream accurately by treating the slip stream as a regular part of the interior flow. So the problem of computing the solution at the solid boundary has disappeared. Unfortunately, it has been replaced by the problem of determining the fictitiously extended flow field below the solid wall.

In looking at two-dimensional problems with straight walls, it is not difficult to construct an extended flow field which will effectively simulate the solid boundary, and there the idea of reflection enters naturally. In this case, at the wall the normal derivative of pressure vanishes along with the normal component of velocity. Therefore, the extended flow field can be constructed by simply reflecting the actual flow field about the solid wall. All quantities are reflected evenly, except the normal velocity component, which suffers odd reflection in order to impose the requirement that it vanish at the solid wall.

To carry this idea further, to flows with curved walls or to three-dimensional flows, leads to a real quagmire. Though there can be no argument in any particular case about the concept of an extended flow field, except in special cases the difficulty of constructing one which will yield an accurate solution to the posed problem is probably at least as difficult as it is to obtain more directly a solution of comparable accuracy.**

It is evident from this discussion that the biggest shortcoming of reflection procedures is that their accuracy depends so strongly on the local characteristics of the flow (and on the coordinate system used in the computation), and no one has utilized procedures reflecting this fact with enough precis However, it should be recognized that the use of body oriented coordinate ems is an attempt to accomplish this.

Reflection procedures have been used by a number of authors with varying degrees of success. The incorrect behavior of the sonic-line flow about an Apollo-like body as computed by Bohachevsky and Mates and Bohachevsky and Kostoff certainly results from poor solutions at boundary points.*** Reflection procedures in one form or another have been utilized by many other authors, including Bohachevasky and Rubin, Burstein, Eaton, Kutler, Kutler and Lomax,

---

* Note that this extended solution is not uniquely determined until one requires that the solution be continuous across the slipstream. That assumption is usually implicit.

** This will become more evident in Section 4.

*** Compare these solutions with those of Barnwell (1971), for instance.

MacCormack, Serra, Tyler and Zumwalt, and Walker and Zumwalt. In the latter report (pg 49) the following justification is made for utilizing a reflection procedure ... "The obvious advantage of the image point method (reflection) for treating boundary points is that it completely deletes the necessity of dictating a priori the values of derivatives at a surface." This statement is erroneous and misleading since exactly the opposite is true. It follows a statement (p. 42) that there are "three ways by which one can take into account the presence of boundary when a finite difference method is employed." The latter statement is also erroneous (and was in 1966) since there are far more than three possibilities. Actually, it should be clear from this discussion that image point or reflection procedures themselves do impose normal derivatives at the boundary (usually = 0 for most quantities, ≠ 0 for normal velocity component).

2.2.2 Explicit One-Sided Derivatives

It has been implied above that it would be very convenient to solve boundary points exactly as interior points, and this is one of the driving forces behind the common utilization of reflection procedures. The problem is that virtually all satisfactory difference schemes for interior points require some form of centered differencing.* However, there is no reason to require that the idea of central differences be carried over to boundary points. In fact, it violates what we know to be the physical/mathematical structure of the problem. At a solid wall, the solution along the wall is determined solely by the interaction of the wall geometry and the interior flow. Therefore, though it is not quite as convenient, it is much more natural to think in terms of one-sided derivatives at the wall if one is embarked on a course of solving the partial differential equations along the wall.

With this in mind, one can easily construct procedures for integrating one or more of the differential equations along the wall with derivatives normal to the wall in the computational space being computed by one-sided differences. The actual procedures employed can vary somewhat, particularly with respect to how many and which equations are to be integrated in this manner.

Such procedures have been employed by Barnwell (1970), Grossman and Moretti, Li, Moretti (PIBAL 70-20), and Skoglund and Guy** and they are discussed by Ciment, Eaton, and Walker and Zumwalt. Probably the most appealing aspect

---

*It need not be symmetric, and multi-step procedures are included in this rather broad interpretation of centered differencing.

**Though their procedure is more than just utilizing one-sided derivatives.

of procedures based on simple one-sided differencing of the partial differential equations is that, with the exception of reflection procedures, they most conveniently fit into schemes for integrating the equations at interior points.

2.2.3 Standard Predictor-Corrector Schemes - One-sided Derivatives

A logical extention to the simplest explicit scheme with one-sided derivatives is to consider a predictor-corrector scheme with derivatives in both the predictor and corrector steps computed as one-sided differences on the same side. Such an approach is a logical extension of a predictor-corrector scheme at interior points to boundary points. Though we can expect to have potentially more accurate calculations than those outlined in the preceding section, accuracy will be limited by the fact that no direct coupling is made between the partial differential equations and the wall geometry.

2.2.4 Implicit Schemes - One-sided Derivatives

Implicit schemes, and mixed implicit/explicit schemes, are the same as corresponding completely explicit schemes except that the derivatives "normal" to the wall are computed with the values at the next x station (i.e., $x = x_o + \Delta x$). Thus, the solution depends on the "normal" derivatives which, in turn, depend on the solution, and the solution must be determined iteratively.

There are two obvious objections to implicit schemes for our purposes: (i) since the interior points will be computed completely explicitly, it is desirable to compute the boundary points explicitly also, and (ii) computing normal derivatives implicitly "violates" the laws of the transmission of signals which are known for the hyperbolic equations under consideration. The latter is an objection concerned with accuracy, not stability, since purely implicit schemes can be unconditionally stable.

Keeping these objections in mind, it is proper that we include implicit schemes in the comparison in order to understand more completely the origin and magnitude of inaccuracies of other schemes, as well as to be certain that no approach is discarded until it has had a chance to prove itself.

2.2.5 Method of Characteristics

Gas dynamicists and numerical analysts are familiar with the method of characteristics for numerically solving [illegible]-linear hyperbolic equations for supersonic, inviscid flow. This method [illegible] on special properties of the governing partial differential equations which permit them to be reduced to ordinary differential equations (two independent variables) with variable coefficients. These ordinary differential equations hold only in special directions,

called characteristic directions, and they reflect the facts that: (i) there a are preferred directions for the propagation of signals in supersonic inviscid flow and that (ii) these signals suffer no dispersion or dissipation (at least theoretically). In most instances, the method of characteristics has been the most accurate procedure for numerically integrating the governing differential equations. It is especially convenient at boundaries where other methods require partial derivatives normal to the boundary. It's biggest shortcoming is its complexity, which results from two sources. First, to employ the method only at boundaries while utilizing other differencing procedures at interior points leads to a number of interpolations that must be made in order to integrate the equations along characteristics. Second, the equations must be combined in the form of characteristic compatibility equations, and this is inconvenient at best and time consuming* at worst. The result is that boundary points require a disproportionate amount of analytical/coding effort from the analyst/programmer.

These disadvantages are offset by the fact that the use of characteristic equations at the wall undoubtedly results, in general, in as accurate solutions as it is possible to achieve.** That they are not more commonly used reflects the fact that the inconvenience to the analyst and computer coder is substantial and results in considerable increase in code development cost. However, if large numbers of production runs are to be made, these additional costs can be more than offset by the decreased cost per run for given accuracy that can be anticipated when characteristic procedures are used at boundaries.

Characteristics methods in one form or another have been used by many investigators, including Abbett,*** Barnwell, Coakley and Porter, Kentzer, Moretti, Moretti and Abbett, Moretti and Bleich, and Kutler and Lomax (1971).

2.2.6 Miscellaneous Methods

In this category are methods which do not naturally fall into the categories of more standard techniques already described. Some of these procedures are not promising enough to receive more than passing attention; others show considerable merit.

Extrapolation

Probably the most simple is a simple extrapolation procedure where the solution at the boundary at $x = x_o + \Delta x$ is obtained by extrapolating the solution at interior points. While it is possible to construct problems in which

---

*From both analytical and computational points of view.

**This will be demonstrated in Section 4.

***Reported in Edelman, et al.

this procedure is adequate, in general it will yield completely unsatisfactory results, especially when the solution changes rapidly near the wall.

Skoglund and Guy have employed an extrapolation procedure which is somewhat more complicated than the most simple approach.

Kentzer's Scheme

A rather clever approach, first proposed by Kentzer (1970) and also used by Barnwell (1971), is based on the method of characteristics. The basic motivation seems to be to get most of the advantages of utilizing characteristics compatibility equations without some of the disadvantages. We have seen that there are basically two disadvantages of characteristics methods: (i) the added analytical work required to put the partial differential equations into characteristic form, and (ii) the additional special coding required, including a number of interpolations to get data at specific points on a characteristic. Kentzer's approach eliminates the second disadvantage while retaining the first and, hopefully, the accuracy of a complete characteristic procedure.*

The approach in its simplest form is best illustrated by looking at our basic example, supersonic, inviscid, two-dimensional flow. The governing differential equations for the momentum equations in characteristic form are are

$$\mp \frac{dp}{dx} - \frac{\rho u^2}{\sqrt{M^2 - 1}} \frac{d\tau}{dx} = 0 \tag{1}$$

along the characteristic directions

$$\lambda^{\pm} = \frac{dy}{dx} = \frac{uv \pm a\sqrt{u^2 + v^2 - a^2}}{u^2 - a^2} \tag{2}$$

with $\tau = v/u$ being the local streamline slope. Here

$$\frac{d}{dx} = \frac{\partial}{\partial x} + \frac{dy}{dx}\frac{\partial}{\partial y} = \frac{\partial}{\partial x} + \lambda \frac{\partial}{\partial y} \tag{3}$$

is a total derivative with respect to the x along the characteristic. The standard procedure for implementing this characteristic compatibility equation

*We will see in Section 4 that it is not completely successful with regard to accuracy.

at a solid boundary as indicated in the sketch. The equation is written along the characteristic between points D and C, where D is somewhere between the mesh points A and B. Since the bounding geometry is specified, τ_C is known. With τ_D and p_D obtained by interpolating between points A and B, we have

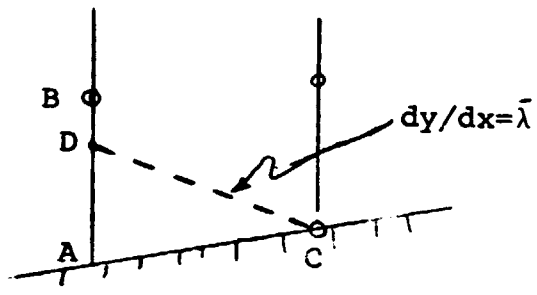

$$p_C = p_D + \bar{b}(\tau_C - \tau_D)$$

Sketch 2 Method of Characteristics at Boundary Point

with $\bar{b}$ an average value of $\rho u^2/\sqrt{M^2 - 1}$ between D and C. The inconvenience and computational time involved in locating point D and the data there are obvious, particularly when there are more than two independent variables. Kentzer's idea is to write the compatability equations in partial differential form at point A. Thus, we have

$$\mp \frac{dp}{dx} - b \frac{d\tau}{dx} = \mp \left(\frac{\partial p}{\partial x} + \lambda \frac{\partial p}{\partial y}\right) - b \left(\frac{\partial \tau}{\partial x} + \lambda \frac{\partial \tau}{\partial y}\right) = 0 \tag{4}$$

or

$$\mp \frac{\partial p}{\partial x} = \pm \lambda \frac{\partial p}{\partial y} + b \left(\frac{\partial \tau}{\partial x} + \lambda \frac{\partial \tau}{\partial y}\right) \tag{5}$$

with

$$\lambda = \frac{uv \pm a\sqrt{u^2 + v^2 - a^2}}{u^2 - a^2} \tag{6}$$

and the rest of the right-hand side evaluated at A. The interesting point is that, while Equation (5) holds generally, in the method of characteristics the derivatives in Equation (4) are treated as directional total derivatives in the directions having slopes $\lambda^{\pm}$. The hope is that by combining the equations in this special way but still retaining their partial differential character, the solution will be obtained with accuracies typical of method of characteristics calculations while retaining the simplicity of standard explicit partial derivative calculations.

Combined Equations*

Another approach, which has been used by Thomas and Thomas, et al., is to combine one or more of Euler's equations with the surface boundary condition in differential form. The object is to obtain a direct coupling of the surface boundary condition with the partial differential equation(s) to be integrated. There are many possible variations on the basic theme, and we look at some of the in Section 4.3.5.

A New Technique

The new procedure developed in this study is analytically simple, easy to code, and computationally fast. It is a predictor-corrector scheme in which the predictor step is a regular predictor step in MacCormack's scheme. All dependent variables are computed in the predictor step. The corrector step is a simple expansion or compression wave, whichever is necessary, which turns the velocity vector parallel to the wall. It is discussed in more detail in Sections 4.3.7.3 and 4.6.2.

*Actually, Kentzer's scheme is one of this group, but we consider it somewhat separately because of its unique features.

SECTION 3

WHAT TO LOOK FOR IN A COMPUTATIONAL PROCEDURE

When confronted with the question, "What should I look for in a computational procedure?" one's spontaneous reply is apt to be "accuracy". In this section we discuss the elements which determine the accuracy of a technique and how we can make preliminary evaluations of a technique prior to testing it. Moretti (1969) has pointed out the importance of considering the computational procedures used at boundary points as well as at interior points in evaluating a numerical technique. That point is certainly valid, but it does not mean that we cannot examine and evaluate separately the components of a technique,* but rather that in evaluating a computer code and predictions it will yield it is necessary to consider the contributions of all components of the technique, including calculation procedures used at computational boundaries as well as those used at interior points. Furthermore, though many of the subsequent arguments have much broader validity, the discussion is directed toward computational procedures at solid wall boundary points of supersonic, inviscid flows where interior points are computed with MacCormack's scheme. Unless otherwise stated, we will be considering two dimensional, steady flow. Some discussion of unsteady and three dimensional flow calculations is given in Section 4.6.2.

Obviously, a good computation procedure must be able to convey numerically information incorporated in the physical/mathematical problem which is being solved. That is why the method of characteristics is such a good procedure for hyperbolic problems in two independent variables. That is also why implicit integration procedures, though they possess nice stability characteristics, are not, in general, nearly as well suited to hyperbolic problems as are explicit procedures. The implicit procedures numerically transmit signals in directions quite different from those directions that the partial differential equations say signals ought to travel (the characteristic directions). In supersonic inviscid flow, we know that the signals are transmitted along characteristics. This does not mean that we must use the method of characteristics to compute such a flow, but that any chosen method ought to maintain, in some fashion, that basic mechanism of transmitting signals. Implicit schemes do not do this. The predictor-corrector scheme of MacCormack evidentally does. So what does this tell us about numerical procedures for computing solid boundary points in supersonic, inviscid flow?

---

*Which is exactly what we are doing in this study.

In the first place, there are two sources of information which must be accounted for: the interior flow and its influence on the boundary, and the boundary geometry. We must account for the effect of each individually as well as their mutual interaction. That is why we can expect a simple, completely explicit, integration procedure to be quite poor. Although it does have adequate mechanisms to account for the development of the interior flow near the wall, it has no mechanism to account for, during a step, the interaction between the wall geometry and the interior flow. Since that interaction is precisely what determines the wall pressure, we do not expect accurate results from such a scheme.

Recently some investigators (c.f. Kentzer, Thomas, et al.), have attempted to overcome this shortcoming of explicit integration schemes by combining the wall boundary condition (normal velocity component $\equiv 0$) into one of the partial differential equations being integrated. The idea has merit, but, as we shall see in Section 4, the resulting accuracy depends very crucially on which equation (or equations) is chosen and how the boundary condition is invoked.

Others (Kentzer, Barnwell) have suggested that accuracy can be improved by putting the partial differential equations in special forms prior to integrating them along the wall. The idea here is that the ability of the equations to transmit information well depends not only on the way the differential equation is approximate by a difference equation but also on the form of the differential equation. The overall validity of this assertion is clear, but we expect to often find it difficult to predict a priori the relative merits of different ways of writing the equations. However, in general one can probably expect improved accuracy if the form of writing the equations somehow gives preference to directions in which signals are transmitted (i.e., characteristic directions).

This brings us to another interesting point, the idea of second order one-sided derivatives and implications with respect to domain of influence and domain of dependence of a point. Consider a supersonic flow going from left to right with a computational grid as shown in the following sketch. The solution is known at station i and it is to be determined at i + 1.

Sketch 3
Computational Grid

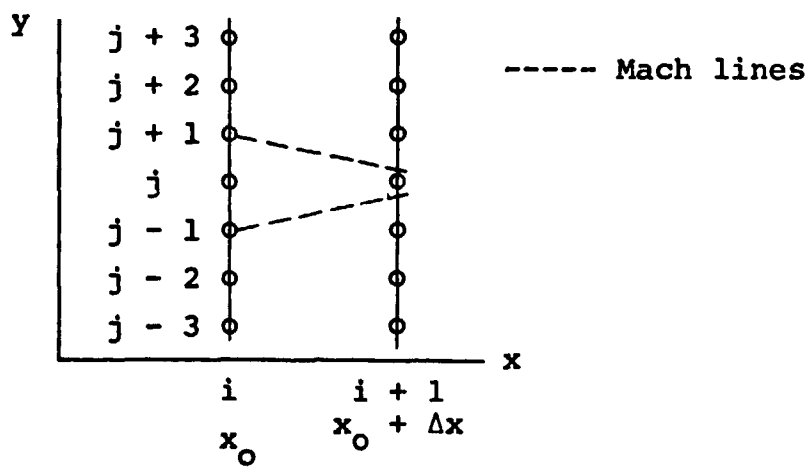

We focus our attention on the problem of determining the solution at (i + 1,j) by an explicit scheme. In a standard, second order explicit scheme (e.g., Lax Wendroff, MacCormack) the solution at (i + 1,j) will depend only on data at the three points (i,j + 1), (i,j), and (i,j - 1), which is compatable with the laws of propagation of signals and domains of influence and dependence. Now, suppose that instead of using those three points, we use the points (i,j), (i,j + 1), and (i,j + 2). Then, though we would be using second order accurate y derivatives, it is obvious that we are using information to determine (i + 1,j) which comes from outside its domain of dependence. (Note location of Mach lines in above sketch.) Obviously, we can think of the three point one-sided derivative as, in a sense, extrapolating the solution from (i,j + 1) and (i,j) to (i,j - 1) but we should not expect as high accuracy from the second procedure as from the first, and we should not be surprised if such a procedure is unstable.

With these thoughts in mind, we can anticipate pretty well the characteristics of a calculation procedure even before testing it. We just need to answer the following question: Does the computational scheme have numerical mechanisms to account for the physical interactions which we know are present? If it does, then it should be one of the better schemes. If not, in the absence of fortuitous blessings, we expect it to be in the ranks of the poorer schemes. These observations are not original, but they are important. Their validity is strikingly illustrated by the results given in Section 4.

SECTION 4

COMPARATIVE RESULTS FOR TWO SAMPLE PROBLEMS

4.1 GENERAL COMMENTS AND DESCRIPTION OF THE SAMPLE PROBLEMS

Now that we have reviewed the general attributes a good computational procedure should have and looked at the characteristics of individual categories of procedures, it is time to compare the predictive abilities of the various procedures. The objective of the test problems is not to be exhaustive, nor is it to test the various methods in situations favorable to certain ones. Rather, it is to test each case in situations which are not necessarily favorable but which are representative of what is required of a technique in every day working codes. To do this we will consider two sample problems, a simple expansion and a simple compression, both for two dimensional, supersonic flow (see sketch 4).

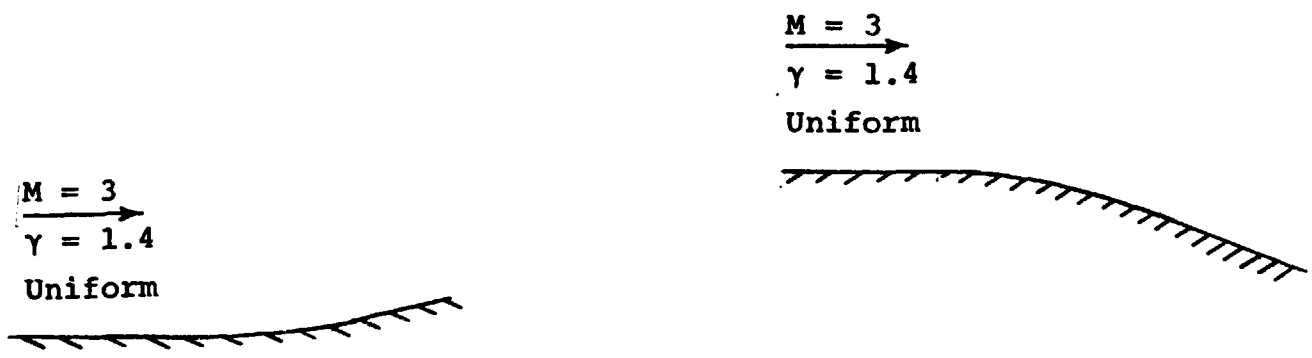

a) simple compression b) simple expansion

Sketch 4 Schematic of Sample Problem

Expansions and compressions are, of course, the heart of supersonic flow fields, and these two sample problems will serve as valid tests of the relative merits of the various procedures. Furthermore, although these flows are comparatively simple, computationally they are quite challenging, as we shall soon see. Finally, they enable us to make the comparison against a valid standard since we can obtain the exact solution along the wall boundary.

In order to present the results in as useful and clear a manner as possible, this section is arranged as follows: First (Section 4.2) we outline the overall computational procedure, with some special attention paid to the boundary point computation. Of particular interest here are the comments relating to the use or non-use of the known surface entropy and total enthalpy. Next (Section 4.3)

we discuss the details of the surface boundary point computational procedures being tested. This is an important section since often small differences in a computational procedure can sometimes significantly affect the result.* Also in that section we introduce working abbreviations for the calculation procedures. The results for the simple compression are presented and discussed in Section 4.4, those for the expansion in Section 4.5. Additional comments and observations (Section 4.6) include a discussion of implications for three dimensional and time dependent flows, special comments vis à vis the envelope shock and its effect for the compression problem, and some discussion of the accuracy of the solution in the interior region.

4.2 GENERAL OUTLINE OF THE COMPUTATIONAL PROCEDURE

4.2.1 Basic Equations and Finite Difference Grid

We are considering an ideal gas with constant specific heat ratio, γ. The general flow direction is from left to right. The geometry for the two sample cases is shown in sketch 5. Initially, for $x \leq 0.0$, the flow is uniform and

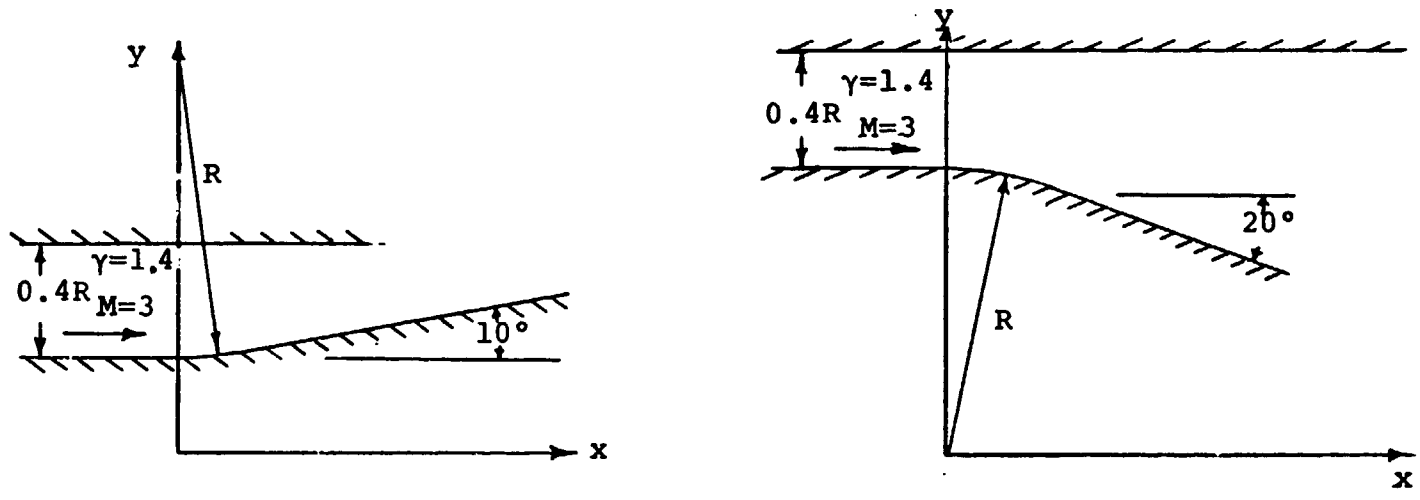

a) compression b) expansion

Sketch 5 Detailed Schematic of Sample Problems

parallel to the x axis, with M = 3. An initial data line of 21 points stretches from the lower wall to the upper wall, the latter always being horizontal.

*In particular, note the discussions of standard predictor-corrector procedures, Thomas' procedures, and Kentzer's procedure and the applicable results.

The basic equations for the steady two-dimensional flow of an ideal gas (isentropic flow, constant isentropic exponent) are

$$\text{continuity:} \quad (\rho u)_x + (\rho v)_y = 0 \tag{1}$$

$$\text{1st momentum:} \quad \rho u u_x + \rho v u_y + p_x = 0 \tag{2}$$

$$\text{2nd momentum:} \quad \rho u v_x + \rho v v_y + p_y = 0 \tag{3}$$

$$\text{entropy:} \quad u S_x + v S_y = 0 \tag{4}$$

$$\text{state:} \quad S = \ln p/p_o - \gamma \ln \rho/\rho_o = P - \gamma R \tag{5}$$

For steady isentropic flow,

$$u\rho_x + v\rho_y = \frac{1}{a^2}\,(up_x + vp_y) \tag{6}$$

with $a^2 = \gamma p/\rho$. Combining (6) and (1) gives the continuity equation in terms of derivatives of pressure and velocity components.

$$\rho u_x + \rho v_y + \frac{1}{a^2}\,(up_x + vp_y) = 0 \tag{7}$$

In order that mesh points always fall on the lower wall, the physical domain is mapped onto a computational domain as shown in the following sketch.*

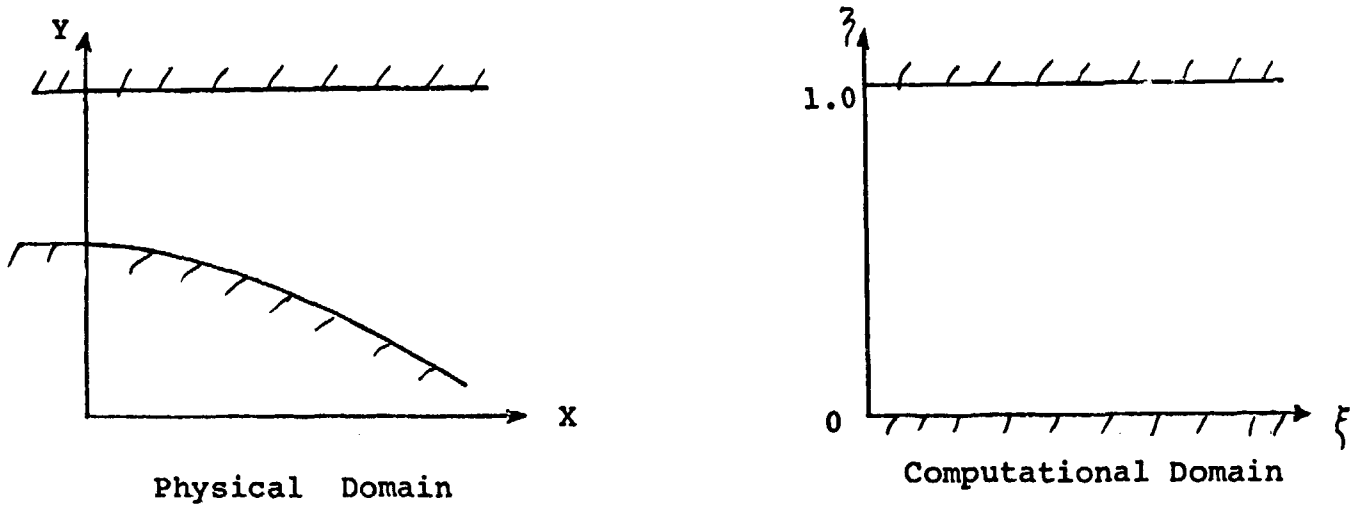

Sketch 6 Physical and Computational Planes

*The computation is terminated before the effect of the upper wall can be felt.

The transformation is

$$\xi = x$$

$$\eta = \frac{y - B}{T - B} = \frac{y - B}{\delta}$$

where the lower and upper walls are described by $y = B(x)$ and $y = T(x)$ respectively and where $\delta(x) = T(x) = B(x)$. Then, the equations of motion become

$$P_\xi + \left\{ cP_\eta + \frac{1}{u^2 - a^2}\left[\gamma(uv_\eta - vu_\eta) + uvP_\eta\right]\right\}/\delta = 0 \tag{8}$$

$$u_\xi + \left\{ cu_\eta + \frac{1}{u^2 - a^2}\left[uvu_\eta - a^2\left(v_\eta + \frac{v}{\gamma} P_\eta\right)\right]\right\}/\delta = 0 \tag{9}$$

$$v_\xi + \left[\left(c + \frac{v}{u}\right)v_\eta + \frac{a^2}{\gamma u} P_\eta\right]/\delta = 0 \tag{10}$$

$$S_\xi + \left(c + \frac{v}{u}\right)S_\eta/\delta = 0 \tag{11}$$

Equations 8 and 9 are both linear (but linearly independent) combinations of Equations 1 and 2; thus they both contain information about the transport of x momentum as well as conservation of mass. Equations 10 and 11 are, respectively Equations 3 and 4 transformed direction to (ξ, η) variables where

$$\left.\begin{aligned} P &= \ln p/p_t \\ R &= \ln \rho/\rho_t \\ S &= P - \gamma R \\ a^2 &= \frac{\gamma P}{\rho} \\ c &= \eta(T_x - B_x) - B_x \end{aligned}\right\} \tag{12}$$

For later use, we note that

$$\left.\begin{aligned} \frac{v}{u} &= \tan\theta \\ q^2 &= u^2 + v^2 \\ h &= \frac{\gamma}{\gamma - 1}\frac{p}{\rho} \\ H &= h + \frac{q^2}{2} \end{aligned}\right\} \qquad (13)$$

4.2.2 Interior Points

At interior points, the equations will be integrated following the scheme of MacCormack as applied to equations in non-divergence form. MacCormack's is a predictor corrector scheme which is easily described by looking at the equation

$$f_\xi + f_\eta = 0 \qquad (14)$$

Then, letting i be the ξ index and j the η index, to obtain the solution at a point (i + 1, j) using data known at a preceding ξ station (i, all j) we proceed

predictor

$$\bar{f}(i+1, j) = f(i, j) - \Delta\xi\left[\frac{f(i, j+1) - f(i, j)}{\Delta\eta}\right] \qquad (15a)$$

corrector

$$f(i+1, j) = \frac{1}{2}\left\{f(i, j) + \bar{f}(i+1, j) - \Delta\xi\left[\frac{\bar{f}(i+1, j) - \bar{f}(i+1, j-1)}{\Delta\eta}\right]\right\} \qquad (15b)$$

For further details about the method, see the two papers by MacCormack.

4.2.3 Lower Wall Boundary Points

Along the surface streamline there is a certain degree of flexibility since the entropy and total enthalpy are known. In almost all the calculations we will use that information, as well as the known body slope, in order to solve as few partial differential equations as possible. Thus, usually we will be solving only one differential equation along the wall, and that one will be an equation for pressure. In other instances (e.g., Thomas' scheme) the basic scheme requires that more than one differential equation be integrated along

the wall. In such instances we can expect errors in surfact entropy and/or total enthalpy to develop. We proceed in this manner because of our two-fold purpose: i) to compare the relative merits of various computation procedures currently in use, and ii) to evaluate the best results that can be achieved within a particular class of schemes. For instance, take the simple explicit integration procedures. We could integrate all four differential equations, continuity, x and y momentum, and entropy. Or we could integrate one equation, say for pressure, and use the three relations for entropy, total enthalpy, and wall slope to calculate the density and two velocity components. If the differential equation to be integrated is chosen optimally, we expect the second approach to yield better results since we are solving three of the four equations exactly.

4.3 DETAILS OF THE COMPUTATION PROCEDURES USED AT SURFACE BOUNDARY POINTS

4.3.1 General Comments

The details of the various surface boundary condition calculation procedures are given in this section. In all, we will consider 25 different procedures, some of which are variations on various themes.

We use simple notation. In the finite difference grid, a point is denoted by two indices, (i,j), where i is the index which increases in the ξ (abscissa) direction and j the index which increases in the η (ordinate) direction. At the initial station, i = 1. In order to invoke reflection type boundary conditions, the j index for lower surface mesh points is j = 2; thus j = 1 is reserved for the row of "image" points needed when reflection type calculations are being used.

The various procedures are given abbreviations which permit a concise and descriptive graphical presentation of the results of Sections 4.4 and 4.5.

In many of the schemes, we simply integrate Equation 8 to obtain the change in surface pressure between stations i and i + 1. In such cases, we have

$$P_{i+1,2} = P_{i,2} + \quad (RHS) \tag{16}$$

where RHS is some representation of the term

$$RHS = -\left\{cP_\eta + \frac{1}{u^2 - u^2}\left[\gamma(uv_\eta - vu_\eta) + uvP_\eta\right]\right\}/\delta \tag{17}$$

It is assumed that the reader is familiar enough with standard notation to know that, for instance, in a simple explicit scheme with two-point one-sided η derivatives, we would have

$$cP_\eta = (B_x)_{i,2}\left[\frac{P_{i,3} - P_{i,2}}{\Delta\eta}\right]$$

$$uv_\eta = u_{i,2}\left[\frac{v_{i,3} - v_{i,2}}{\Delta\eta}\right] \qquad (18)$$

etc.

In order to calculate the surface boundary point at (i + 1,2) from known data at (i,j), $j \geq 2$, we assume the following to be known:

i) The complete solution at every mesh point at station i, [i.e., for all (i,j), $j \geq 2$]

and, if necessary,

ii) The complete solution of the predictor and corrector steps at all <u>interior</u> points at station i + 1 [i.e., for all (i + 1,j), $j \geq 3$]

4.3.2 Reflection (<u>Image Point Procedures</u>)

Reflection procedures are probably used more than any other single class of calculation procedures. We have considered six variations on the basic theme.

R-1* <u>Reflection in the computational plane</u>

All data at boundary points computed as at interior points. Velocity component normal to th wall not set = 0. To compute station i + 1 from data at station i, set

$$P_{i,1} = P_{i,3}$$

$$u_{i,1} = u_{i,3}$$

$$v_{i,1} = -v_{i,3} \qquad (19)$$

$$S_{i,1} = S_{i,3}$$

*Here R-1 is the abbreviation we will use for the first reflection scheme, R-2 for the second reflection scheme, etc.

R-2 Reflection in Physical Plane

All data at boundary points computed as at interior points. Effect is to set, at station i, the velocity component normal to the wall = 0 at the wall.

$$P_{i,1} = P_{i,3}$$

$$S_{i,1} = S_{i,3}$$

$$u_{i,1} = u_{i,3}(\cos^2\theta_{i,2} - \sin\theta_{i,2}) + 2v_{i,3}\sin\theta_{i,2}\cos\theta_{i,2}$$

$$v_{i,1} = v_{i,3}(\sin^2\theta_{i,2} - \cos^2\theta_{i,2}) + 2u_{i,3}\sin\theta_{i,2}\cos\theta_{i,2}$$

where $\theta_{i,2}$ is the angle the tangent to the wall makes to the horizontal. (See sketch below.)

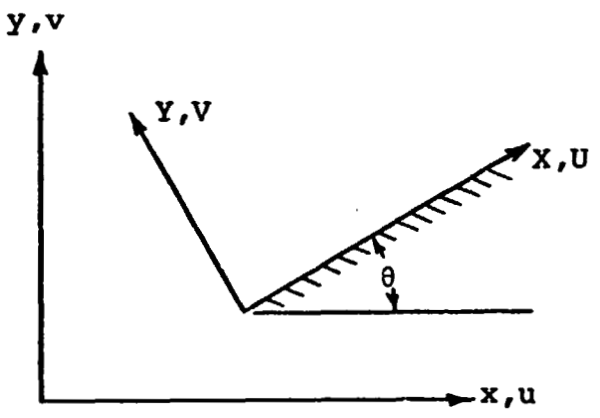

$$U_{i,1} = U_{i,3}$$

$$V_{i,1} = -V_{i,3}$$

R-3,R-4 Reflection in Physical Plane

Same as R-2 for pressure, but known entropy, total enthalpy, and surface slope used to calculate, from $P_{i+1,2}$, the values of $\rho_{i+1,2}$, $u_{i+1,2}$, and $v_{i+1,2}$. Thus, we have from Equations 12 and 13

$$S_{i+1,2} = S_{i,2} \rightarrow \rho_{i+1,2} \rightarrow h_{i+1,2}$$

$$H_{i+1,2} = H_{i,2} \rightarrow q_{i+1,2} = \sqrt{2(H_{i+1,2} - h_{i+1,2})}$$

$$v^2_{i+1,2} + u^2_{i+1,2} = q^2_{i+1,2} \; ; \qquad (21)$$

(concluded)

$$(v/u)_{i+1,2} = \tan \theta_{i+1,2})$$

The difference between R-3 and R-4 is that Equations (21) are imposed only after the corrector steps in R-3 and after both predictor and corrector steps in R-4.

R-5 Kutler - Scheme 1

This is one of two reflection schemes used by P. Kutler (1972). P, ρ, and u are reflected evenly, v is extrapolated. All data at boundary points computed as at interior points.

$$P_{i,1} = P_{i,3}$$

$$R_{i,1} = R_{i,3}$$

$$u_{i,1} = u_{i,3} \qquad (22)$$

$$v_{i,1} = 2v_{i,2} - v_{i,3}$$

$$v_{i,2} = u_{i,2} \tan \theta_{i,2}$$

Apply v = u tan θ after both predictor and correctc

R-6 Kutler - Scheme 2

Kutler's second scheme is the same as R-4, except only the pressure is obtained by integrating a PDE (in this case, Equation 8). ρ, u, and v are obtained from S, H and θ. See R-3.

R-6A Same as R-6 except impose surface boundary condition only after corrector step, not after predictor step.

R-7 Extrapolation

All data at the image point are obtained by linear extrapolation from the interior. Thus

$$P_{i,1} = 2P_{i,2} - P_{i,3}$$

$$R_{i,1} = 2R_{i,2} - R_{i,3}$$

$$u_{i,1} = 2u_{i,2} - u_{i,3}$$

$$v_{i,1} = 2v_{i,2} - v_{i,3} \qquad (23)$$

Pressure is obtained by integrating Equation 8 with MacCormack's scheme. ρ, u, v are obtained from the known S, H, and θ.

4.3.3 Simple Explicit Integration Procedures - One-Sided Derivatives

E-2 Equation 8 solved explicitly for $P_{i+1,2}$ (Simple Euler Scheme) using simple two-point, one-sided η derivatives. ρ, u, v obtained from known S, H, θ

$$\left(\text{e.g., } P_\eta = \left(P_{i,3} - P_{i,2}\right)/\Delta\eta\right) \qquad (24)$$

E-3 Same as E-2 except 3 point η derivatives

$$\left(\text{e.g., } P_\eta = \left(-3P_{i,2} + 4P_{i,3} - P_{i,4}\right)/2\Delta\eta\right) \qquad (25)$$

4.3.4 Simple Implicit Integration Procedure - One Sided Deriviatives

I-2 Same as E-2 except η derivatives computed implicitly as, for example,

$$P_\eta = (P_{i+1,3} - P_{i+1,2})/\Delta\eta \qquad (26)$$

Thus, it is necessary to iterate on the solution at (i+1,2). Iterate until relative change in pressure between two successive iterates is less than 0.0001.

I-3 Same as I-2 except 3 point one-sided η derivatives

$$\left(\text{e.g., } P_\eta = \left(-3P_{i+1,2} + 4P_{i+1,3} - P_{i+1,4}\right)/2\Delta\eta\right) \qquad (27)$$

4.3.5 Standard (and not-so-Standard) MacCormack-like Predictor-Corrector Procedures

MacCormack's scheme is a noncentered predictor-corrector scheme in which, say, a forward η difference is used in the predictor and a backward η difference

is used in the corrector. Now, let's determine how we should apply this approach at solid boundaries.

Consider the equation

$$f_x + f_y = 0$$

Suppose that we know the solution at station i and we wish to continue it to i + 1. All points (i + 1,j), $j \geq 3$ can be easily calculated by the standard MacCormack scheme. We are interested in the point (i + 1,2).

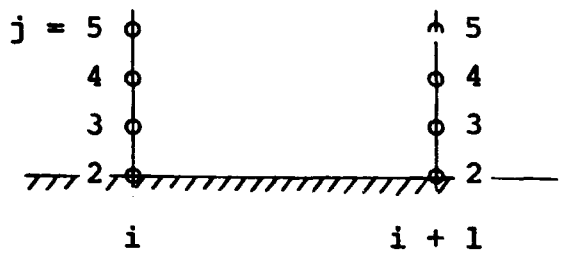

Sketch 4

The simplest approach would be to just use one-sided inward differences on both the predictor and corrector steps. Then, in MacCormack's notation, we have a scheme we call PC-2-2.

PC-2-2

Predictor:

$$\bar{f}(i + 1,2) = f(i,2) - \Delta x \left[\frac{f(i,3) - f(i,2)}{\Delta y}\right] \tag{28a}$$

Corrector:

$$f(i + 1,2) = \frac{1}{2}\left\{ f(i,2) + \bar{f}(i + 1,2) - \Delta x \left[\frac{\bar{f}(i + 1,3) - \bar{f}(i + 1,2)}{\Delta y}\right]\right\} \tag{28b}$$

where $\bar{f}(i + 1,2)$ is the regular predictor value at that interior point. For obvious reasons, we do not expect this result to be very accurate, irrespective of how the boundary condition has been incorporated into the differential equation.

The obvious next step is to use second order accurate one-sided y derivatives. Then we have scheme PC-3-3.

PC-3-3

Predictor:

$$\bar{f}(i + 1,2) = f(i,2) - \Delta x \left[\frac{-3f(i,2) + 4f(i,3) - f(i,4)}{2\Delta y}\right] \tag{29a}$$

Corrector:

$$f(i + 1,2) = \frac{1}{2}\left\{f(i,2) + \bar{f}(i + 1,2) - \Delta x \left[\frac{-3\bar{f}(i + 1,2) + 4\bar{f}(i + 1,3) - \bar{f}(i + 1,4)}{2\Delta y}\right]\right\} \tag{29b}$$

One <u>might</u> expect scheme PC-3-3 to be better than scheme PC-2-2.

To carry the investigation somewhat further, let's look at the MacCormack Scheme at an interior point. It is (in one form):

Basic Scheme

Predictor:

$$\bar{f}(i+1,j) = f(i,j) - \Delta x \left[\frac{f(i,j) - f(i,j-1)}{2\Delta y} \right]$$

Corrector:

$$f(i+1,j) = \frac{1}{2} \left\{ f(i,j) + \bar{f}(i+1,j) - \Delta x \left[\frac{\bar{f}(i+1,j+1) - \bar{f}(i+1,j)}{\Delta y} \right] \right\}$$

Comparing the basic scheme with schemes PC-2-2 and PC-3-3, we note that the corrector for scheme PC-2-2 is identical to the basic corrector. One might then reason that it is sensible to use the 'more accurate' predictor of scheme PC-3-3 with the corrector of scheme PC-2-2 in trying to construct a calculation scheme at the wall consistent with that used at interior points. Thus, we have a third scheme: PC-3-2.

PC-3-2

Predictor:

$$\bar{f}(i+1,2) = f(i,2) - \Delta x \left[\frac{-3f(i,2) + 4f(i,3) - f(i,4)}{2\Delta y} \right] \qquad (31a)$$

Corrector:

$$f(i+1,2) = \frac{1}{2} \left\{ f(i,2) + \bar{f}(i+1,2) - \Delta x \left[\frac{\bar{f}(i+1,3) - \bar{f}(i+1,2)}{\Delta y} \right] \right\} \qquad (31b)$$

In scheme PC-3-2, the predictor is an attempt to somehow simulate at the boundary the basic predictor step.

Now it is clear, or at least seems to be, how to construct a completely consistent scheme. Referring to sketch 7, what is needed is a formula for replacing the term

$$\frac{f(i,j) - f(i,j-1)}{\Delta y} \qquad (32)$$

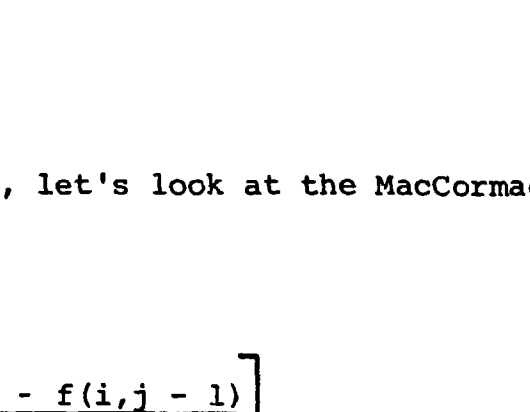

Sketch 7

in the basic predictor step with a comparable term involving f(i,j), f(i,j + 1),

and f(i,j + 2). But what is (32)? It is just the derivative of f with respect to y at the midpoint between (i,j - 1) and (i,j). So, to determine the term to replace (32), let's look at the usual one dimensional difference line segment (sketch 8). The correspondence between points in sketches 7 and 8 is

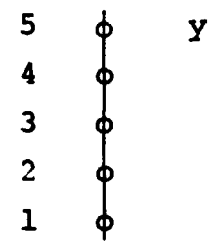

Sketch 8

Sketch 7		Sketch 8
j + 2	⟷	5
j + 1	⟷	4
j	⟷	3
j - 1	⟷	2
j - 2	⟷	1

Term (32) is essentially, as far as sketch 8 is concerned

$$f'_{23} = \frac{f_3 - f_2}{\Delta y}, \tag{33}$$

the second order derivative of f with respect to y at the midpoint between points 2 and 3. So, all that is necessary is to represent f'_{23} to the same accuracy as (33), but using points 3, 4, and 5. Following the usual procedure, we have

$$f_3 = f_{23} + f'_{23}\left(\frac{\Delta y}{2}\right) + \frac{1}{2} f''_{23}\left(\frac{\Delta y}{2}\right)^2$$

$$f_4 = f_{23} + f'_{23}\left(\frac{3}{2}\Delta y\right) + \frac{1}{2} f''_{23}\left(\frac{3}{2}\Delta y\right)^2 \tag{34}$$

$$f_5 = f_{23} + f'_{23}\left(\frac{5}{2}\Delta y\right) + \frac{1}{2} f''_{23}\left(\frac{5}{2}\Delta y\right)^2$$

Eliminating f_{23} and f''_{23} from these three equations yields the desired equation for f'_{23} in terms of f_3, f_4, f_5.

$$f'_{23} = \frac{-2f_3 + 3f_4 - f_5}{\Delta y} \tag{35}$$

(Compare this with the usual three point, one-sided second order derivative used above in PC-3-3). Thus, we construct PCN-3-2, which we expect is the predictor corrector scheme for the boundary most consistent with MacCormack's scheme at interior points.

PCN-3-2

Predictor:

$$\bar{f}(i+1,2) = f(i,2) - \Delta x \left[\frac{-2f(i,2) + 3f(i,3) - f(i,4)}{\Delta y}\right] \tag{36a}$$

Corrector:

$$f(i+1,2) = \frac{1}{2}\left\{f(i,2) + \bar{f}(i+1,2) - \Delta x \left[\frac{\bar{f}(i+1,3) - \bar{f}(i+1,2)}{\Delta y}\right]\right\} \tag{36b}$$

All four of these predictor corrector schemes have been tested. As we shall see in Sections 4.4 and 4.5, the results are somewhat surprising and quite enlightening. In all four of these "standard" predictor-corrector schemes, the known surface entropy, total enthalpy, and slope were used to calculate surface density and velocity components from the computed pressure in both predictor and corrector steps. Thus Equation 8 is the only partial differential equation integrated along the surface.

4.3.6 Method of Characteristics

MOC - Method of Characteristics

Interpolations and solution made in physical plane. Data at the * point obtained by linear interpolation between (i,2) and (i,3) (see sketch, following page).

$$\lambda = \frac{uv - a\sqrt{u^2 + v^2 - a^2}}{u^2 - a^2}. \tag{37}$$

$p_{i+1,2}$ computed from campatibility equation

$$\frac{dp}{dx} - b\frac{d\tau}{dx} = 0 \tag{38}$$

in finite difference form

$$p_{i+1,2} = p^* + \bar{b}(\tau_{i+1,2} - \tau^*) \tag{39}$$

λ and b are averaged between * point and (i + 1,2).

$$S_{i+1,2} = S_{i,2} + \rho_{i+1,2} + h_{i+1,2}$$

$$H_{i+1,2} = H_{i,2}$$

$$q_{i+1,2} = \sqrt{2(H_{i+1,2} - h_{i+1,2})} \qquad (40)$$

$$(v/u)_{i+1,2} = \tan \theta_{i+1,2}$$

$$v^2_{i+1,2} + u^2_{i+1,2} = \text{?}^2_{i+1,2}$$

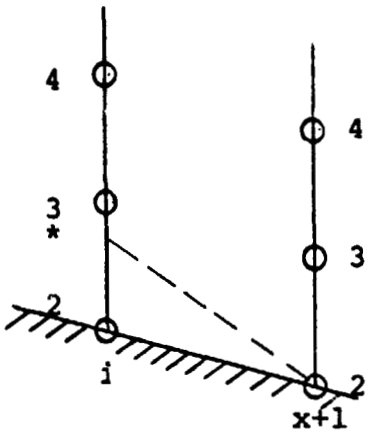

4.3.7 Miscellaneous Procedures

In this category we have those methods which do not fit into any of the preceding categories. Though a diverse melange, this group is the one where we expect the potentially greatest return as far as accuracy vs. complexity are concerned.

4.3.7.1 Kentzer's Method*

Pressure from the characteristic-like partial differential equation

$$\frac{\partial p}{\partial x} = - \lambda^- \frac{\partial p}{\partial y} + b \left(\frac{\partial \tau}{\partial x} + \lambda^- \frac{\partial \tau}{\partial y} \right) \qquad (41)$$

where

$$\frac{\partial}{\partial y} = \frac{1}{\delta} \frac{\partial}{\partial \eta} \qquad (42)$$

The η derivatives are two-point, one-sided derivatives explicit in x. That is, to go from i to i + 1,

$$\frac{\partial p}{\partial y} = \frac{1}{\delta_i} \frac{(p_{i,3} - p_{i,2})}{\Delta \eta} \qquad (43)$$

$$\frac{\partial \tau}{\partial x} = \frac{\tan \theta_{i+1} - \tan \theta_i}{\Delta x} \qquad (44)$$

etc. $\bar{\lambda}$ and b are evaluated at (i,2). Then

*For a predictor-corrector variation of this scheme, see Section 4.3.7.5.

$$S_{i+1,2} = S_{i,2}$$

$$H_{i+1,2} = H_{i,2} \tag{45}$$

$\rho_{i+1,2}$, $u_{i+1,2}$, $v_{i+1,2}$ are computed from $\theta_{i+1,2}$

4.3.7.2 Thomas' Procedure (see Thomas and Thomas, et al.)

The basic idea is to replace one momentum equation with the boundary condition of zero velocity component normal to the lower wall. This is done by replacing the (x,y) velocity components, (u,v), with components $(\bar{U},\bar{V})$ parallel to and normal to the wall. Since $\bar{V}$ is everywhere normal to the wall, $\bar{V} \equiv 0$. Also,

$$\bar{U} = u \cos\theta + v \sin\theta \tag{46}$$

$$\bar{U}_\xi = \bar{U}_x - \frac{c}{\delta}\bar{U}_\eta \tag{47}$$

$$\bar{U}_\xi = u_x \cos\theta + v_x \sin\theta - (u \sin\theta - v \cos\theta)\theta_x$$

where

$$u_x = u_\xi - \frac{c}{\delta} u_\eta$$

$$v_x = v_\xi - \frac{c}{\delta} v_\eta \tag{48}$$

Equation (47) for $\bar{U}$ is integrated along with Equation (8) for pressure, as outlined by Thomas and by Thomas, et al. $\theta_x = d\theta/dx$ is known from the specified velocity distribution. $\bar{V} \equiv 0$, and $p = p(x,s)$ complete the integration along the lower wall, since

$$u = \bar{U}\cos\theta - \bar{V}\sin\theta$$

$$v = \bar{U}\sin\theta + \bar{V}\cos\theta \tag{49}$$

We try two versions of this scheme, identified as Thomas-2 and Thomas-3.

Thomas-2 - Equations 47 and 8 are integrated using two-point one-sided η derivatives computed explicitly in the ξ coordinate

Thomas-3 - Same as Thomas-3 except standard three-point one-sided η derivatives are used.

4.3.7.3 Combined Equations

The analysis used by Thomas employs the specified variation of $\theta(x)$ in computing the velocity changes by integrating the streamwise momentum equation. No use is made of the known variation of $\theta(x)$ in integrating the equation for pressure, nor is there any direct coupling between the continuity equation and one or both of the momentum euqations. We know that the primary physical force determining surface pressure variation is momentum exchange away from the wall, and it is natural to consider combining the pressure equation (Equation 8) with one or more of the momentum equations and with the specified variation of $\theta(x)$. This is, of course, what is done in the method of characteristics and Kentzer's method.

We have investigated two such additional combinations of the differential equations and surface boundary conditions. They are identified by the prefix CE, meaning Combined Equations.

CE-1 Inspection of Equations (3) and (7) leads to one obvious possibility. Multiply (7) by -v and add to (3) to get

$$\rho(uv_x - vu_x) + \left(1 - \frac{v^2}{a^2}\right)p_y - \frac{uv}{a^2}\,p_x = 0$$

Noting that the streamline slope is given by

$$\tau = \frac{v}{u} \tag{51}$$

and

$$u^2\tau_x = uv_x - vu_x \tag{52}$$

we get

$$\rho u^2\tau_x + \left(1 - \frac{v^2}{a^2}\right)p_y - \frac{uv}{a^2}\,p_x = 0 \tag{53}$$

This becomes, after converting to (ξ,η) and P,

$$P_\xi = \frac{\gamma}{\tau}\left(\tau_\xi + \frac{c}{\delta}\,\tau_\eta\right) - \frac{1}{\delta}\left(C - \frac{a^2}{u^2\tau} + \tau\right)P_\eta \tag{54}$$

where τ_ξ can be computed directly from the specified wall geometry. A quick inspection of Equation 54 gives considerable cause for worry, since τ appears twice in the denominator, and τ can be zero. This reflects the fact that Equation 54 embodies only the continuity equation and the normal momentum equation for determining the induced streamwise pressure gradient. The most important equation for determining that pressure gradient, the streamwise

momentum equation, was not used in obtaining Equation 54. Nevertheless, a calculation was made for the simple expansion problem utilizing Equation 54. The results were quite poor, as was expected, the pressure being low by more than an order of magnitude in the first step. That large error is directly attributable to numerical inaccuracies resulting from the τ in the denominator.

Four Other CE Schemes

Following the same basic spirit discussed above, both momentum equations and the continuity equation are combined, and the specified variation of $\theta(x)$ is used to simplify the resulting equation and to give the direct coupling between changes in wall inclination and the streamwise pressure gradient. Equation 7 is multiplied by -u and added Equation 2 to get

$$- \rho u^2 \tau_y - \frac{uv}{a^2} p_y + \left(1 - \frac{u^2}{a^2}\right) p_x = 0 \tag{55}$$

Equations 55 and 53 are added to yield

$$\left(1 - \frac{u^2 + uv}{a^2}\right) p_x + \left(1 - \frac{v^2 + uv}{a^2}\right) p_y + \rho u^2 (\tau_x - \tau_y) = 0 \tag{56}$$

Converting to (ξ,η) and P we get

$$P_\xi = \frac{-\left[\tau_\xi + \frac{c-1}{\delta} \tau_\eta\right]\left(\frac{\gamma u^2}{a^2}\right) - \frac{1}{\delta}\left[2 - \frac{(u^2 + uv)c + v^2 + uv}{a^2}\right] P_\eta}{1 - \frac{u^2 + uv}{u^2}} \tag{57}$$

which is a well behaved, simple partial differential equation which can be very easily integrated.

We have integrated Equation (57) in four different ways which we identify as CE-2, CE-3, CE-PC-2-2, and CE-PC-3-2.

CE-2 Equation (57) is integrated in a straight forward explicit Euler type scheme with two-point, one-sided η derivatives computed at station i. Thus,

$$P(i + 1,2) = P(\xi + \Delta\xi,2) = P(i,2) + \Delta\xi P_{\xi} \tag{58}$$

where P_{ξ} is given by (57) and the η derivatives are computed as, for example,

$$P_{\eta} = \frac{P(i,3) - P(i,2)}{\Delta\eta} \tag{59}$$

CE-3 The same as CE-2 except three-point one-sided η derivatives are used, e.g.,

$$P_{\eta} = \frac{-3P(i,2) + 4P(i,3) - P(i,4)}{2\Delta\eta} \tag{60}$$

CE-PC-2-2

This is a predictor-corrector type solution of Equation (57) after the fashion of MacCormack. First equation (57) is integrated as in CE-2 to get the predictor value, $\bar{P}(i + 1,2)$. Then we get the η derivatives in (57) by differencing (one-sided differences) the results of the predictor step at station $(i + 1)$. Then we combine the initial value, the predictor value, and the corrector as in MacCormack's scheme

$$P(i + 1,2) = \frac{1}{2}\left\{P(i,2) + \bar{P}(i + 1,2) + \Delta\xi \cdot RHS\right\} \tag{61}$$

where RHS is the right hand side of (57) with η derivatives and coefficients computed from the predictor solution at $(i + 1)$. Two-point one-sided η derivatives are used in both the predictor and the corrector steps.

CE-PC-3-2

The same as CE-PC-2-2 except three-point one-sided η derivatives used in predictor steps. (Two point η derivatives still used for corrector steps.)

4.3.7.4 Euler Predictor, Simple Wave Corrector

EP-SWC Second order (and higher) accurate numerical procedures for integrating the equations at interior points obviously incorporate the

mathematical/physical signal propagation phenomena so well characterized by the theory of characteristics. The predictor/corrector procedures (c.f. MacCormack's Scheme) can be thought of as, in essence, computing the solutions for two simple waves, the solutions of which are summed to yield the complete solution.* At the wall, it is not possible to do a regular predictor-corrector, since there is no flow on one side of the wall.** The wall boundary condition replaces "the information feeding in from the other side". The problem is to devise an integration scheme incorporating these phenomena.

Consider the simplest finite difference scheme for integrating the continuity and both momentum equations (p, u, v are dependent variables). This scheme was utilized for the continuity equation in scheme E-2. By comparing $\theta° = v/u$ at $x = x_o + \Delta x$ with the known surface inclination, we can evaluate the error in the integration. Now, we can superimpose on the solution a simple wave (compression or expansion) to "turn the flow" so that v/u will be correct. Corresponding to such a simple wave is a pressure increment, Δp, which is to be added to the pressure there. This procedure can be thought of as a predictor-corrector procedure with the corrector a simple wave. In the calculation, the corresponding pressure increment was computed from Equation 174 of NACA Report 1135 for expansions through small angles, $\Delta\nu$. Terms through $(\Delta\nu)^2$ were used, so the equation is also valid for compression waves. The expression is

$$\frac{p_2}{p_1} = 1 - \frac{\gamma M_1^2}{\sqrt{M_1^2 - 1}}(\Delta\nu) + \gamma M_1^2 \frac{(\gamma + 1)M_1^4 - 4(M_1^2 - 1)}{4(M_1^2 - 1)^2}(\Delta\nu)^2 \qquad (62)$$

$\Delta\nu$ is positive for an expansion and negative for a compression. In the reported calculations, the predictor step was computed according to scheme E-2, except that all four of Equations (8-11) were integrated in the predictor step (using two-point one-sided η derivatives). Then, the pressure change to correct v/u was computed from Equation (62). Finally, ρ, u, and v were computed from p and the known surface S, H, and streamline slope.

---

*While this is not rigorously correct, the argument is an aid in helping to understand the important elements of computational procedures.

**We omit reflection techniques from consideration here. For further comments on these procedures, see Section 2.

4.3.7.5 Kentzer's Scheme: Predictor-Corrector Version

Moretti (1971) has used a predictor-corrector version of Kentzer's scheme. First equations (5) and (6) are transformed to the computational plane. Thus

$$\frac{\partial p}{\partial x} + \lambda \frac{\partial p}{\partial y} = b\left(\frac{\partial \tau}{\partial x} + \lambda \frac{\partial \tau}{\partial y}\right) \tag{5}$$

becomes

$$\frac{\partial p}{\partial \xi} + \frac{c + \lambda}{\delta} \frac{\partial p}{\partial \eta} = b\left(\frac{\partial \tau}{\partial \xi} + \frac{c + \lambda}{\delta} \frac{\partial \tau}{\partial \eta}\right) \tag{63}$$

On the lower wall, $c = -b_x = -\frac{v}{u}$, so we have

$$\frac{\partial p}{\partial \xi} + \Lambda \frac{\partial p}{\partial \eta} = b\left(\frac{\partial \tau}{\partial \xi} + \Lambda \frac{\partial \tau}{\partial \eta}\right) \tag{64}$$

where

$$\Lambda = \frac{1}{\delta}\left(-\frac{v}{u} + \lambda\right) \text{ along the lower wall}$$

Now

$$b = \frac{\rho u^2}{\sqrt{M^2 - 1}} \quad \text{and} \quad \frac{\partial \tau}{\partial \eta} = \frac{\partial \frac{v}{u}}{\partial \eta} = \frac{1}{u^2}\left(uv_\eta - vu_\eta\right) \tag{65}$$

so that

$$\frac{\partial p}{\partial \xi} = -\Lambda \frac{\partial p}{\partial \eta} + \frac{\rho u^2}{\sqrt{M^2 - 1}} \frac{\partial \tau}{\partial \xi} + \frac{\rho \Lambda}{\sqrt{M^2 - 1}}\left(uv_\eta - vu_\eta\right) \tag{66}$$

or

$$\frac{\partial P}{\partial \xi} = -\Lambda \frac{\partial p}{\partial \eta} + \frac{\rho u^2}{\sqrt{M^2 - 1}} \frac{\partial \tau}{\partial \xi} + \frac{\gamma \Lambda}{a^2 \sqrt{M^2 - 1}}\left(uv_\eta - vu_\eta\right) \tag{67}$$

In version of Kentzer's scheme, equation (67) is used in a MacCormack-like predictor-corrector calculation. Thus,

$$\bar{P}(i + 1,2) = P(i,2) + P_\xi(i,2)\Delta\xi \qquad \text{a)}$$

and

$$P(i + 1,2) = \frac{1}{2}\left\{P(i,2) + \bar{P}(i + 1,2) + P_\xi(i + 1,2)\Delta\xi\right\} \qquad \text{b)} \tag{68}$$

The η derivatives at i and i + 1 are two-point one-sided derivatives between the initial conditions at (i,2) and (i,3) and the predictor solution at (i + 1,2) and (i + 1,3) respectively. In the current calculation, the term $\partial\tau/\partial\xi$ was computed exactly, whereas in the results using Kentzer's procedure it was computed by taking a two point difference $\left(\text{i.e., } \partial\tau/\partial\xi = [\tau(i + 1,2) - \tau(i,2)]/\Delta\xi\right)$.

4.4 SIMPLE COMPRESSION - RESULTS AND DISCUSSION

Our interest here is the comparative ability of the various procedures to predict the pressure distribution on the surface of the simple compression. The predicted pressures are compared with each other and with the exact solution on Figures 1a-1h. The initial data (pressure and density) were specified accurate to four significant figures. Pertinent considerations vis à vis the envelope shock which forms are discussed in Section 4.6.1.1; it might be fruitful to quickly skim that discussion prior to studying the results reported in this section.

The results for the reflection schemes R-1, R-2, R-3, and R-4 are shown on Figure 1a and for R-5, R-6, R-6A and R-7 on Figure 1b. Some interesting observations can be quickly noted. Simple reflection in the computational plane (R-1) is disastrous, and not surprisingly so since there is no mechanism at all for introducing into the flow field the fact that the surface streamline must follow the wall whose slope is changing. Comparing schemes R-2 and R-3, both of which use reflection in the physical plane, we see an example of the value of utilizing as much information as is available. The only difference between the two runs is that R-2 solves the Euler equations for all four variables, p, S, u, v, while R-3 solves for p only with a differential equation, obtaining S, u, and v from the known surface entropy, total enthalpy, and streamline slope. The comparison between R-3 and R-4 is also quite interesting. The only difference between these two runs is that in R-4 the known surface S, H, θ are used in obtaining the predictor solution as well as the corrector solution, while in R-3 the predictor solution solves all four partial differential equations for p, S, u, v, the known surface S, H, θ only being used in obtaining ρ, u, and v from p in the corrector step. We see that R-4 is much quicker to respond to changes in curvature, but that it also tends to exhibit larger overshoots. This characteristics seems to hold for other reflection schemes as well, at least for the compression. Kutler's two schemes yield essentially comparable results. There is no distinct improvement of the prediction of scheme R-6 over R-5. Again, R-6a, which utilizes known surface S, H, and θ only after the corrector step, lags R-6 where the surface slope changes, but exhibits far less overshoot on the ramp section. Procedure R-7, which obtains all the data at the image point by linear extrapolation from the interior,* has much larger overshoot than either R-5 or R-6, the corresponding runs with Kutler's procedures.

*Recall that R-5 and R-6 (Kutler's two schemes) obtain v by linear extrapolation and p, ρ, and u by simple reflection in the computational plane.

We can summarize the results of the reflection schemes as follows:

1) Reflection in the physical plane is superior to reflection in the computational plane.

ii) It is preferable to obtain p by integrating a differential equation and ρ, u, v from known S, H, and θ.

iii) Schemes which are most responsive to changes in surface curvature (note - not slope) (e.g., R-4, R-5, R-6, R-7) tend to exhibit larger overshoots than schemes which are not so sensitive to changes in surface curvature (e.g., R-3, R-6a).

iv) None of the reflection schemes tested yields particularly good results.

The results of the two simple explicit (E-2 and E-3) and the two simple implicit (I-2 and I-3) schemes also show some interesting behavior (Figure 1-C). First note that the predictions of both E-3 and I-3 using three point one-sided second order accurate derivatives are much worse than the corresponding predictions of schemes E-2 and I-2 which use two-point one-sided first order accurate derivatives. This is an illustration of a point that is sometimes missed. Just because one uses higher order difference expressions it does not mean that the solution is more accurate. In fact, we know that three point derivatives violate the law of forbidden signals, and we know further that supersonic flow fields can have derivatives which are discontinuous in certain directions, namely normal to the Mach lines. Therefore, we not only should not be surprised by these results, we should expect them. Looking now at the two "lower order" schemes, E-2 and I-2, note that the implicit scheme (I-2) gives better results than the explicit scheme (E-2) even though I-2 also, in a sense, violates the law of forbidden signals. However, it does tie in the changes in the interior with changes in the surface slope during one step, and its violation is "dispersive" rather than "dissipative". Thus, though neither procedure is very accurate, the implicit schemes, compared to the simple explicit schemes, have a better mechanism for coupling the interior flow solution with the specified boundary condition. Finally, it should be noted that the explicit schemes are more prone to stability problems. Though the results of scheme E-3 do not really look unstable, it is possible that the run is marginally stable or unstable. Because of what we know about the law of forbidden signals, it would not be at all surprising if scheme E-3 has poorer stability limits. Thomas (AIAA 71-596) asserts as much with respect to his scheme (see the discussion below) using three point η derivatives.

The results for the standard predictor corrector schemes are shown in Figure 1-d. In all four runs shown there, the pressure was calculated by integrating Equation (8) with a MacCormack-like predictor-corrector scheme, except that both predictor and corrector results were computed with one-sided η derivatives.

In both the predictor and corrector steps, the known surface entropy, total enthal enthalpy and slope were used to obtain the surface density and velocity components. None of the schemes is consistently superior. While scheme PC-2-2 (two-point predictor/two-point corrector) responds to the initial expansion better than PC-3-3, the latter, surprisingly, has a much lower initial overshoot on the straight section. Both have about equivalent (but poor) ability to "home-in" on the correct solution along the straight section. A somewhat unexpected result is the poor predictive ability of scheme PCN-3-2, the scheme which is meant to be as consistent as possible with MacCormack's predictor-corrector scheme. The conclusion which one apparently must draw is that any attempt to deduce an "extended" (past the surface streamline) flow field solution is not likely to be very successful. On the basis of these results, it is apparent that standard predictor-corrector schemes do not show much promise.

The results of the method of characteristics calculation (MOC) are shown in Figure 1e, along with the results of the new predictor-corrector scheme (EP-SWC) which utilizes a simple explicit Euler predictor followed by a simple expansion or compression wave corrector. Both techniques yield quite accurate solutions, the maximum relative error in surface pressure being 0.28% for the method of characteristics calculation and 0.10% for the EP-SWC calculation (see discussion on errors below). These small errors are achieved in calculations where the surface pressure is changing as much as 26% in one step!

The results for both versions of Kentzer's method, Thomas-2 and CE-2 are shown together on Figure 1f since these four methods all use a partial differential equation formed by combining one or more of Euler's equations with the surface boundary condition. All four calculations employed two-point, one-sided η derivatives. Kentzer's basic procedure and Moretti's predictor-corrector version both predict the solution very well, the maximum relative errors being 0.56% and 0.33% respectively. This is indeed amazing since Kentzer's scheme integrates the compatability equation as a simple partial differential equation along the streamline (not along the characteristic)! The results of these four calculations strikingly show the importance of how the differential equations and the boundary conditions are combined. Thomas essentially just made certain that his system of equations was complete and not redundant. In procedure CE-2 we have taken care to couple the equations in a form which accounts, as well as possible,* for the interaction between the interior flow field and the solid wall boundary. The superiority of CE-2 over Thomas-2 is quite clear.

The results of the two schemes Thomas 3 and CE-3** runs are shown in Figure 1g. Obviously CE-3 is superior. In fact, Thomas-3 may be exhibiting some of the poor stability characteristics alluded to by Thomas (AIAA-71-596).

---

*Within the constraints of the overall solution procedure and the requirement that we want to integrate the equation as a simple partial differential equation

**The same as Thomas-2 and CE-2 except for three point one-sided η derivatives.

The results of the predictor corrector versions (CF-PC-2-2 and CE-PC-3-2) of the combined equations schemes (CE-2 and CE-3) are shown in Figure 1h. These results are fairly good, scheme CE-PC-2-2 being slightly better than CE-PC-3-2. Both are better than CE-2 on the curved section, but not as good as CE-2 on the straight section. Both are far better than Thomas-2, Thomas-3, and CE-3. On this problem, none of the others is competitive with Kentzer's scheme.

In order to better illustrate the comparative accuracy of the different procedures, on Figures 2a, 2b, and 2c we have plotted the relative error in computed surface pressure for representative schemes from each category. Recall that the initial data was specified to four significant figures, so relative errors less than .0002 must be considered fortuitous. Furthermore, it is important to look at the overall accuracy of a scheme; isolated points of significantly higher than average accuracy are also fortuitous. Using the method of characteristics as a standard, it seems reasonable to rate the schemes as follows:

Typical Relative Error in % $\frac{p - p_{exact}}{p_{exact}} \times 100$	Rating
$\leq 0.5\%$	very good to excellent
0.5% to 1%	good
1% to 10%	fair
$\geq 10\%$	unacceptable

We see that (Fig. 2a), for this problem, the method of characteristics, Kentzer's method (both versions), and the new simple Euler predictor-simple wave corrector scheme (EP-SWC) all rate in the very good to excellent category with errors mostly less than 0.3% and the average error less than 0.1%. It is interesting to note that all four methods appear to settle on an error trend for $x/R > 0.3$, though Kentzer's method is a little slow in homing-in on the trend. The simple standard predictor corrector (PC-2-2) and reflection in the physical plane (R-4) yield results which are poor on the compression turn and the first part of the straight segment, but which improve considerably for $x/R > 0.4$.

Simple explicit integration (scheme E-2) must be rated poor, while simple implicit integration (scheme I-2) is in the fair to poor range (Figure 2b).

Of the remaining schemes in the combined equations class,* Thomas' scheme with two-point derivatives (Thomas-2) is quite poor for predicting surface pressure, scheme CE-2 (Euler integration) yeidls fair results, and the predictor corrector scheme CE-PC-2-2, though slightly better on the average than CE-2, is also in the fair category.

*Recall that Kentzers method is also in this class.

Since it has yielded such good results, it is interesting to look at the new EP-SWC scheme calculations in a little more detail. In Figure 3 we have plotted the results of both the predictor and the corrector calculations. We see that in the first interval the predictor has no idea that the boundary slope is changing, so the entire change in the solution along the surface streamline is taken up by the simple wave corrector step. Subsequently, the non-uniform flow above the wall carries with it information about the changing wall slope, and the predictor contributes a large part of the change until the straight segment is reached. For the first interval thereafter the predictor acts as though the surface slope were going to continue to increase, and the corrector brings in again (as in each step) the interaction between the surface and the interior flow. Finally, for $0.242 \leq x/R \leq 0.34$, the predictor computes an expansion which must be corrected with a simple wave compression.

It is also interesting to note that in Moretti's predictor-corrector version of Kentzer's scheme, except for one interval, the contribution of the corrector is quite small. On the curved section the change from predictor to corrector is between 0.13% and 0.85% while the solution is changing between 14% and 26% in one interval. It is only in the interval where the surface curvature is discontinuous that the corrector contributes a major portion of the change. In that interval the change between predictor and corrector is 8.3%. Thus, the strength of Kentzer's approach appears to primarily reside in the form of the differential equation, rather than refinements in the differencing procedure.

4.5 SIMPLE EXPANSION - RESULTS AND DISCUSSION

The simple expansion is the second of this pair of elemental problems used to test these computational procedures. The initial mesh spacing and flow conditions are the same as for the compression.

The predictions of the various reflection schemes are compared with the exact solution in Figure 2a and 2b. Again, simple reflection in the computational plane is disastrous. These results differ somewhat from those for the compression in the following respects:

i) Scheme R-2, reflection in the physical plane with p, S, u, v all computed by integrating Euler's equations, shows less ability to home-in on the solution on the straight segment.

ii) Scheme R-4 is again superior to R-3 on the curved surface, but it is now equal to R-3 on the straight segment.

iii) The percent overshoot of R-3 is higher (19.1% vs 8.4% for the compression).

iv) Compared to R-3 and R-4, Kutler's schemes R-5 and R-6 do better than they did on the compression.

v) R-7 again shows comparatively large overshoot.

The results of the two simple explicit (E-2 and E-3) and two simple implicit (I-2 and I-3) schemes (Figure 4c) are a bit different than they were for the simple compression. On this problem there is not clear superiority of two point η derivatives compared to three point derivatives. In fact, overall probably I-3 is a little superior to I-2 and E-3 to E-2. Both E-3 and I-3 respond quicker than the corresponding E-2 and I-2 to the initial curvature change and to the change where the straight segment begins, but again E-3 and I-3 exhibit greater overshoot on the straight segment. As for the compression, none of these schemes yield good results.

The four standard predictor-corrector schemes yield comparable results (Figure 4d). Again, overall PC-2-2 seems to be somewhat better than the others, primarily because of its superior ability to home-in on the solution on the straight segment. Again, none of these results are acceptable, with errors as high as 26% for scheme PC-3-3.

The method of characteristics (MOC) and the new simple-Euler-predictor/simple-wave-corrector (EP-SWC) schemes yield excellent results (Figure 4c). The maximum relative errors are 0.58% for the method of characteristics and 0.43% for the EP-SWC scheme. This high accuracy is achieved when the exact solution changes as much as 22% in one step!

The results of Thomas procedure and of the basic combined equations approach with Euler integration (CE-2), both using two-point one-sided η derivatives, are compared with Kentzer's predictions and the exact solution on Figure 4f. Again we see that scheme CE-2 yields far better predictions for surface pressure than does the Thomas-2 scheme, and Kentzer's methods are still the best. Kentzer's basic procedure, while still pretty good, does not do as well on the expansion (Fig. 4f) pansion (Figure 4f) as it did on the compression (Figure 1f). While doing pretty well on the curved section, it has about a 10% overshoot on the straight segment, after which it very quickly homes-in on the correct solution. Even on the curved section, typical errors are considerably higher for the expansion (1-7%, Figure 5a) than they were for the compression (0.8-1.0%, Figure 2a). There is no obvious explanation for the comparatively poorer ability to predict expansions than compressions. On this problem, Moretti's predictor-corrector version model is considerably better than the basic Kentzer scheme. The overshoot is down to 3.4%, and on the curved section the errors are 1/2 to 1 order of magnitude smaller. Again, except in the one interval where the surface curvature is discontinuous, the corrector changes the predictor by less than 1%. Thus, we can attribute some of the differences between Kentzer's basic scheme, as used here, and Moretti's predictor to the different treatment of the derivative of the surface slope (see Section 4.3.7.5). Additional studies of these two approaches and the treatment of the surface slope derivative will be reported in the future.

Schemes CE-3 and Thomas-3, both using three-point one-sided η derivatives, are compared with the exact solution in Figure 4g. The results here for Thomas-3 are considerably better than they were for the compression, but it again shows a strong tendency to overshoot on the straight segment.

Finally, the results of the two corresponding predictor-corrector schemes, CE-PC-2-2 and CE-PC-3-2 are shown on Figure 4h. Scheme CE-PC-3-2 is slightly better than CE-PC-2-2, and on this problem both are better than any of the other schemes in this category,* except Kentzer's scheme.

The relative errors of some of the schemes are compared with each other in Figures 5a, 5b, and 5c. The method of characteristics (MOC) and the new Euler predictor, simple-wave corrector (EP-SWC) scheme are far superior to any of the others, with Kentzer's scheme considerably better than those remaining.

As with the expansion wave, the path of the EP-SWC predictor corrector scheme is given in Figure 6 (see Figure 3 and its discussion).

4.6 FURTHER COMMENTS AND OBSERVATIONS

4.6.1 Accuracy of the Solution at Interior Points

4.6.1.1 Simple Compression - The Envelope Shock

For the compression problem it is important to consider the influence that the envelope shock which will form may have on the results. No provision was taken to treat that shock as a sharp discontinuity, so it is possible that, particularly with those schemes using three-point one-sided differences, the solution at the lower wall is affected by numerical inaccuracies resulting from the shock smearing.

As a first step to evaluate this effect, a full method of characteristics calculation was generated with a code which computes shock waves as sharp discontinuities. The code (referred to as SUPER), detects envelope shocks by the crossing of characteristics of the same family. It is a second order accurate solution since both characteristic slopes and coefficients in the equations are averaged in a solution which iterates each step. In order to obtain mesh point spacing on the lower wall at about the same interval as in the "finite difference" calculation, the mesh points on the initial data line were spaced at distance $\Delta y/R = 0.01$ apart. The calculation proceeds from mesh points on the initial data line ($x = 0.0$) along right-running characteristics, and it was continued until the code halted because the number of points on the characteristic line exceeded 50, the maximum allowed. The last computed right-running characteristic originated at $x/R = 0.0$, $y/R = 1.28$. The surface pressure computed with the full method of characteristics calculation agrees very well with the exact

*Gas dynamic equations combined with surface boundary condition in differential form.

tropic compression solution (Figure 7). The resulting flow field and some interesting additional information are shown in Figure 8. The shock was first detected at x/R = 0.254, at which point a sharp shock solution yielded a pressure ratio of $\bar{p} = p_2/p_1 = 1.129$. In order to determine as closely as possible the actual abscissa of the beginning of the shock, the pressure ratio across the shock was plotted as a function of x/R and the plot was extrapolated back to the abscissa where $\bar{p} = p_2/p_1 = 1.0$ (Figure 9), yielding the initiation of the shock at x/R = 0.24. The right running characteristic passing through that point hits the lower wall at x/R = 0.38. On the last computed right running characteristic, the shock was located at x/R = 0.379, y/R = 1.146, and the shock slope has almost reached its asymptotic value (see Figure 8). Also shown on Figure 8 are the initial finite difference grid for the calculations reported herein, the finite difference grid at x/R = 0.255,* the left running Mach Line which originates at the beginning of the compression turn, and the asymptotic shock angle. Note that, including the lower wall point, there are four mesh points between the lower wall and the shock in the region x/R = 0.25. Further downstream, there will be more points between the shock and the lower wall (see Figure 8).

In a study of one-dimensional time-dependent flows with shock waves computed by shock smearing, Gary compared shock speeds predicted by Lax-Wendroff differencing of the Euler equations in divergence form with predictions using the equations in non-divergence form (as done in this study). He obtained much greater errors in computed shock speed utilizing non-divergence form than when the divergence form was used. Kutler anticipated** similar behavior in the present case, expecting the smeared shock location to differ significantly from the correct value. To investigate this behavior as well as to study the effect of the shock smearing on the present results, the computed pressure profiles at three sections are plotted for Case EP-SWC in Figure 10. In Figure 10a we see that when the shock is just beginning to form (x/R ~ .25) the region of strong pressure gradients as predicted by the finite difference grid somewhat lags that predicted by the full method of characteristics calculation. The finite difference solution overshoots by about 9% the pressure profile on the compression side. At x/R = 0.3664 (Figure 10b) the shock is well established, and the smeared shock is displaced even more from the exact solution, and the pressure overshoot is now about 27%. Because of the mesh point limitation, we have no complete method method of characteristics solution for all y beyond x/R = 0.37. However, since the computed shock angle is very close to the asymptotic value, we can extrapolate it to obtain the shock location at another abscissa, for example for x/R = 0.5234 (Figure 10c). Then it is easy to construct the exact pressure profile and to

*Recall that, at a given x, there are twenty equal intervals between the lower wall and the ordinate y/R = 1.4.

**Private communication.

compare it with the prediction using the finite difference formulation with shock smearing (Figure 10c). Again, we see the displaced shock location and pressure overshoot (still 27%) predicted with shock smearing.

Now, what is the importance of these results vis à vis this study? One might remark, for instance, that if the envelope shock were treated as a sharp discontinuity, the problem of inaccuracies due to displaced shocks and pressure overshoots would disappear. However, that is misleading, for the inaccuracies in boundary point calculations do not primarily originate with the poor shock description. Also, no matter how the shock is treated, we must always live with some errors which will result in the interior calculation even if the boundary solutions are exact. Furthermore, we must face the situation depicted in Figure 10a, where the shock, as a shock, contributes a negligible part of the compression, but where there still is the usual pressure overshoot which occurs even when the equations are cast in divergence form. Thus, it is just as erroneous to replace that smooth compression with a shock as it is to represent the compression through a shock with shock smearing. Even if we attempt to devise a code in which shocks are essentially always treated as sharp discontinuities, we must realize that if the flow is at all complicated, weak secondary compressions and shocks may exist which are not accounted for within the code logic. Our task is to insure that in such situations relatively minor inaccuracies in the interior do not lead to large inaccuracies at boundaries.

Finally the purpose of this study is to evaluate various computation procedures in situations they are expected to handle as a matter of course. All the computations are identical except for the boundary point computations, and the tests have been of situations typical of those faced by everyday working codes.

It is clear that schemes using three-point one-sided derivatives will be much more susceptible to the small or large oscillations shown in Figures 10a-10c. However, the disadvantage of three-point differences goes deeper than that. Even if the interior solutions were exact, these procedures will generally exhibit the comparatively almost undamped overshoot discussed in Section 4.4 and 4.5.

4.6.1.2 Simple Expansion

To further clarify some aspects of the interaction between solutions at boundary points with those at interior points, we consider the simple expansion problem. Since the solution is just a simple Prandtl-Meyer turn, we can calculate the exact solution at any point in the flow field. First we consider one of the better schemes for computing boundary points. The solution using the EP-SWC procedure at boundary points is compared with the full method of characteristics solution and with the exact solution, all at $x/R = 0.2648$, in Figure 11. The agreement is very good between all three, the full method of characteristics

solution showing excellent agreement with the exact simple wave solution. The maximum error at an interior point for the calculation using EP-SWC is about 2 to 2-1/2%, which is somewhat higher than the errors on the boundary point.

Further downstream, the pressure profile has a sharp discontinuity in slope. The results of the EP-SWC calculation are compared with the exact solution at x/R = 0.5095, 0.6654 in Figures 12a and 12b respectively. Note that the agreement in the expansion region is quite good, but that there is a tendency to develop small wiggles near the discontinuity in profile slope. However, as was demonstrated in Sections 4.4 and 4.5, there are schemes for computing boundary points which are insensitive to these small wiggles, and the wiggles need not have a deleterious affect on the boundary calculations.

It is also interesting to compare the pressure profile for a couple of the poorer schemes with the exact solution. The results for schemes CE-PC-2-2 and Thomas-2 at x/R = .43 are shown in Figure 13. Note that the large errors in computed surface pressure do not really have much effect on the interior flow, at least in this case. However, it is important to remember that surface pressure is generally the single most important result of these calculations!

4.6.2 Three Dimensional and Time Dependent Flows

We can expect most of the results and conclusions to carry over to time dependent as well as three dimensional steady flows. The details of some of the procedures will vary, of course, but the general principles we have been discussing and testing are not restricted to two independent variables. The advantage of the new predictor-corrector scheme for three or more independent variables is obvious since the implementation of either Kentzer's scheme or the method of characteristics is quite cumbersome. There is a certain degree of arbitrariness in applying the scheme to three or more independent variables, but comparisons with method of characteristics calculations for shuttle type vehicles have been very favorable (Rakich & Kutler, 1972).

The extension to three dimensional steady flow can be easily sketched. Consider, for example, a cartesian coordinate system (x, y, z) with velocity components (u,v,w) and unit vectors $(\hat{i},\hat{j},\hat{k})$. Let the flow be supersonic in the general direction of the x axis (i.e., u must be supersonic, v and w will generally be subsonic, though they also could be supersonic). If the surface geometry is given by an equation of the form

$$F(x,y,z) = 0 \qquad (63)$$

then the unit normal to the surface is given by

$$\hat{n} = \frac{F_x\hat{i} + F_y\hat{j} + F_z\hat{k}}{\sqrt{F_x^2 + F_y^2 + F_z^2}} = n_1\hat{i} + n_2\hat{j} + n_3\hat{k} \tag{64}$$

Finally, we denote the velocity vector by $\vec{q}$,

$$\vec{q} = u\hat{i} + v\hat{j} + w\hat{k} \tag{65}$$

As in the two dimensional case, we first generate a predictor step solution for p_o, ρ_o, u_o, v_o, w_o using MacCormack's scheme with inward differences. Then, since the boundary condition is that

$$\vec{q} \cdot \hat{n} = 0 \tag{66}$$

along the surface, we find the angle between the predicted velocity vector $\vec{q} = u_o\hat{i} + v_o\hat{j} + w_o\hat{k}$ and the unit normal.

$$\Delta\nu = \sin^{-1}\left[\frac{\vec{q}_o}{|\vec{q}_o|} \cdot \hat{n}\right] \tag{67}$$

Then we impress a simple wave to turn the velocity vector through the angle $\Delta\nu$. Again, associated with that wave is a pressure change given by Equation (62). Next, we find the corrected velocity components from the expression

$$\vec{q}_1 = \vec{q}_o - \vec{q}_o \cdot \hat{n} \tag{68}$$

If we know exactly the surface total enthalpy and entropy at the point, we can find the exact value of the density and velocity modulus corresponding to the corrected pressure, p_1. In such a case, we can make a final small correction to the velocity vector by maintaining the direction given in (68) and scaling its modulus to the known value.

It should be clear that this procedure is not completely rigorous. For one thing, there is no simple wave in three dimensional flow, so the use of equations (67), (62) and (68) is certainly an approximation. How good an approximation it is can only be determined after the fact. Preliminary results for sharp cones and blunted shuttle vehicles at incidence have been very good. This should not be too surprising since one can often treat three dimensional flows as locally two-dimensional with crossflow effects accounted for in an "inhomogeneous" term.

Obviously we could construct the corresponding scheme for unsteady flow computations. In fact, in a sense the corrector is similar to Godunov's method for time dependent flows.

SECTION 5

CONCLUDING REMARKS

It need hardly be mentioned that the range of computational procedures considered in this study is not completely comprehensive. One can, of course, think of quite a number of variations on schemes investigated here, and it is very likely that one could invent a scheme quite different to any of those we have examined. However, this study is complete, as far as procedures are concerned, in that all currently used procedures are probably represented in one of the categories, and the schemes tested are representative of the best results that can be achieved in each category.

The procedures have been compared for an ideal gas at Mach = 3 in two-dimensional flow. The results would be essentially the same for an equilibrium gas. Although we anticipate quantitative differences at other Mach numbers, qualitatively these results should carry over as Mach number varies. Similar comments should apply if the geometry of the test problems were altered.

There are a number of observations to be made about and conclusions to be drawn from the results presented in Sections 4.4 and 4.5. It should be evident that any purely explicit integration procedure not incorporating explicitly the wall geometry changes possesses an inherent lag in that it has no mechanism for introducing into the solution for one step changes in wall geometry occuring during that step. Thus, we can expect such procedures to give poor results any time wall curvature effects are important. On the other hand, we have seen that purely explicit reflection procedures tend to recover fairly quickly once the surface geometry becomes straight.

Higher order one-sided differences do not generally yield better results (c.f., results for schemes E-3, I-3, PC-3-3, Thomas-3, CE-3). They tend to be more quickly responsive to changes in surface slope, but they also show strong tendencies to large, poorly damped oscillations. As already noted, this should not be surprising since the use of three point differences violates the law of forbidden signals.

[illegible] integration procedures have given markedly better results than [illegible] The best procedures are the method of characteristics, the [illegible] predictor simple wave corrector procedure, and the two versions [illegible] Though very competitive on the compression, Kentzer's method [illegible] comparatively on the expansion problem.

The success of the new predictor-corrector procedure (EP-SWC) is probably to be explained as follows: The simple Euler predictor step accounts for the development of the interior flow between the surface and the next point in. The simple wave corrector step then accounts for the interaction of the predictor solution with the surface boundary. We have seen that the scheme, though quite simple, yields very accurate results. It has been extended to three-dimensional steady flow* and the results agree very well with those achieved using the method of characteristics in three dimensions. It requires very little computing time and, because it is so simple, is unlikely to result in numerical problems in difficult situations. While no formal analysis of its accuracy has been made, the results achieved so far indicate that it is accurate to second order in mesh spacing.

Other than the developme t of the new scheme, the most important result of this study is the very striking demonstration of the fact that accuracy depends very critically on the manner in which the equations are solved. This fact is clearly demonstrated by comparing the results of methods E-2, Thomas-2, CE-2 and Kentzer, all of which used two-point one-sided η derivatives. The latter two procedures give considerably better results than the former two. The reason for the differences lies solely in how the equations are written, including whether and how the surface boundary condition is incorporated in the partial differential equation for pressure.

*The scheme outlined in Section 4.5.2 has been incorporated in Kutler's code (Kutler, et al., 1972) and comparisons have been made with a full three-dimensional method of characteristics calculation for a shuttle type vehicle at M = 7, and 5° angle of attack (Rakich and Kutler, 1972).

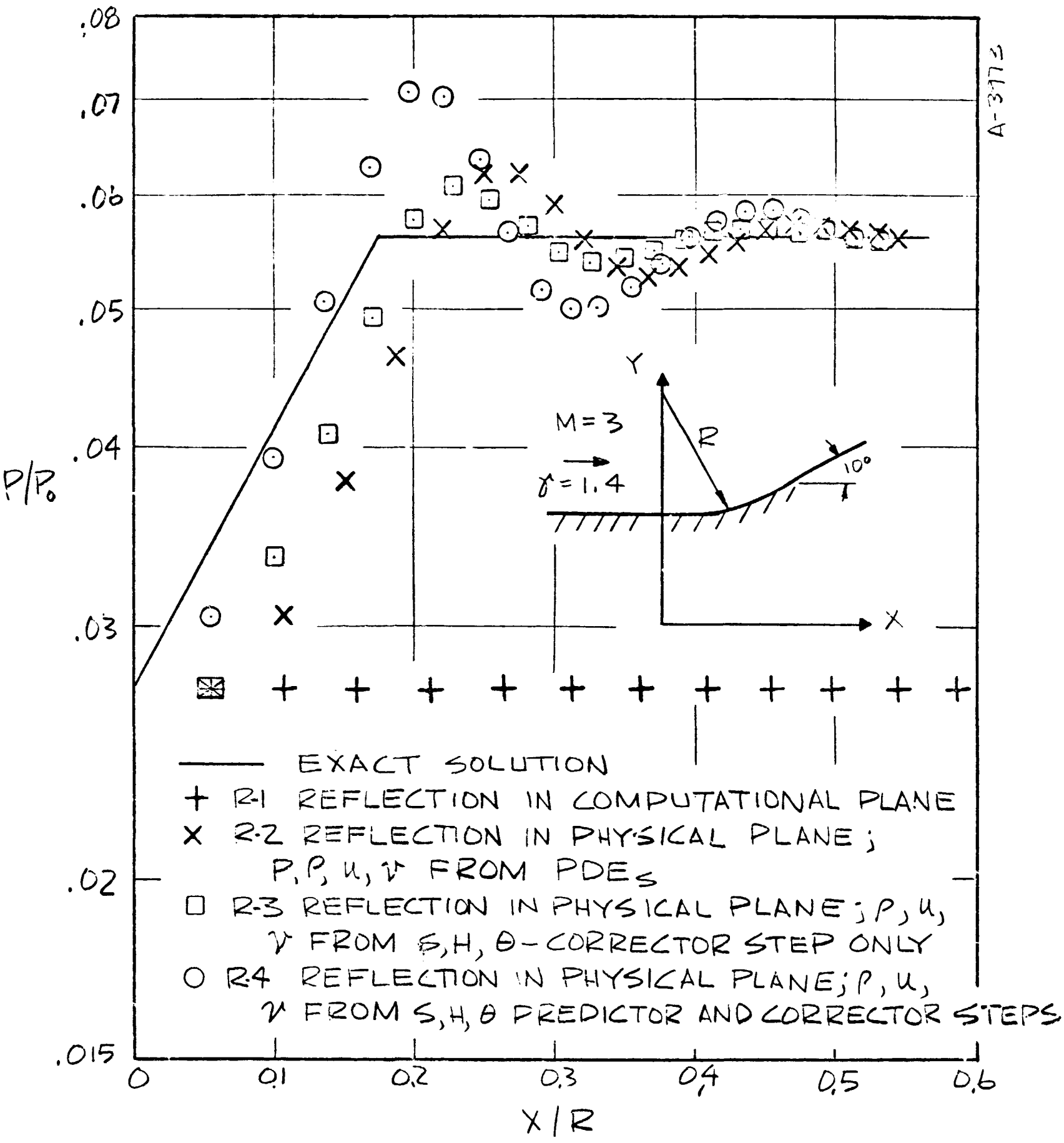

FIGURE 1a FOUR REFLECTION SCHEMES

FIGURE 1 SIMPLE COMPRESSION; COMPARISON OF PREDICTED SURFACES PRESSURES WITH EXACT SOLUTIONS

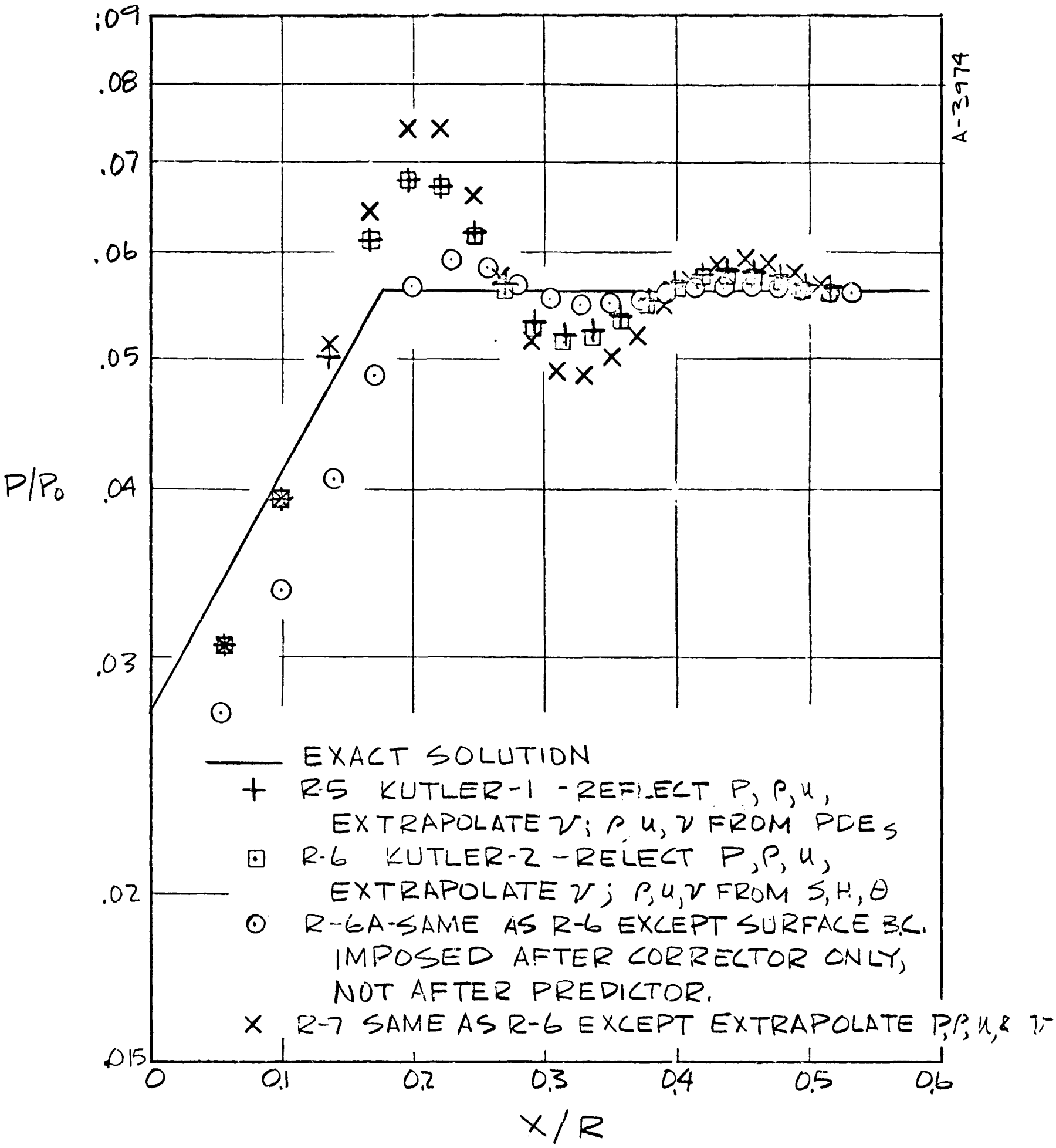

FIGURE 1-b FOUR MORE REFLECTION SCHEMES

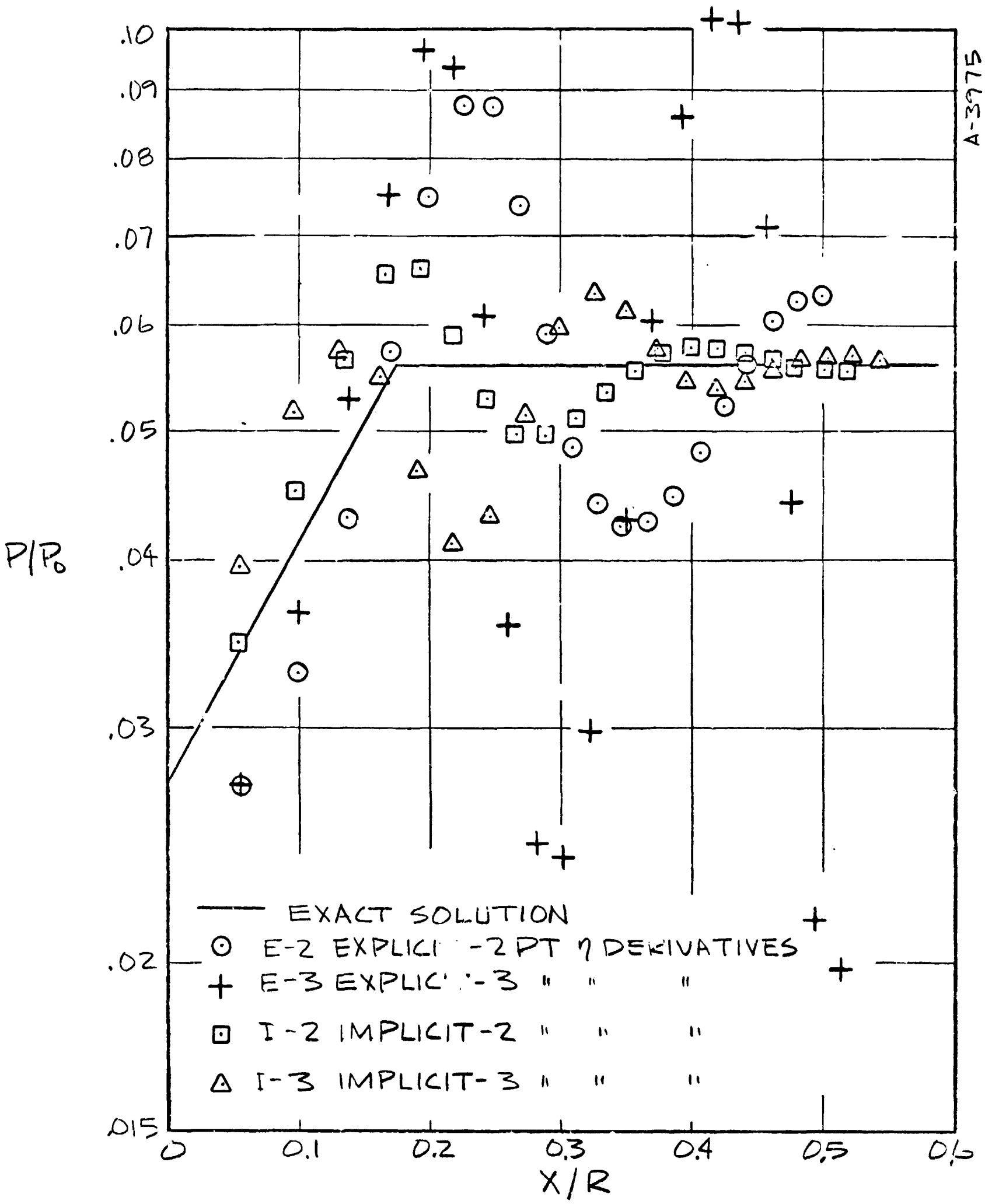

FIGURE 1-C SIMPLE EXPLICIT AND SIMPLE IMPLICIT SCHEMES

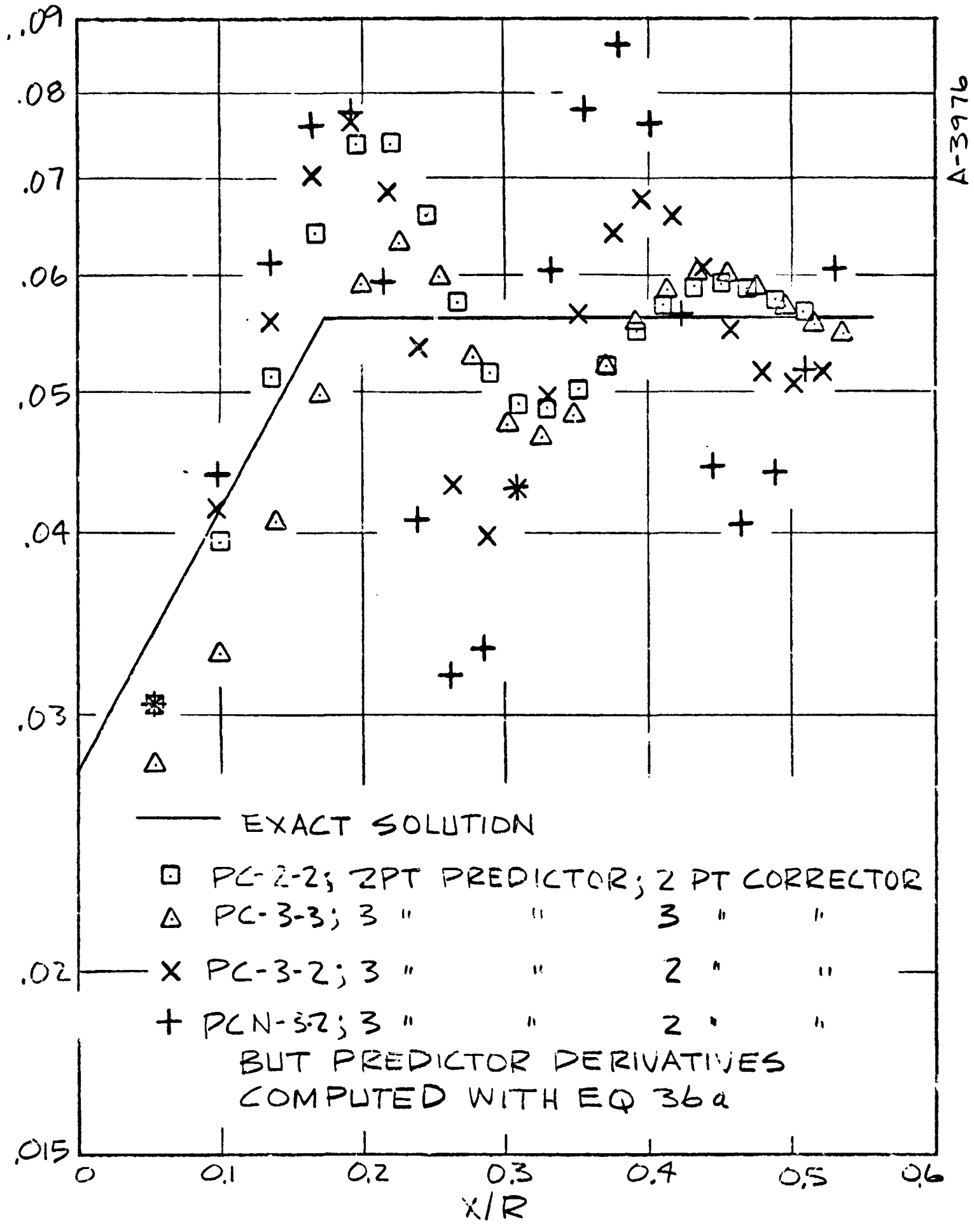

FIGURE 1-d STANDARD PREDICTOR-CORRECTOR SCHEMES

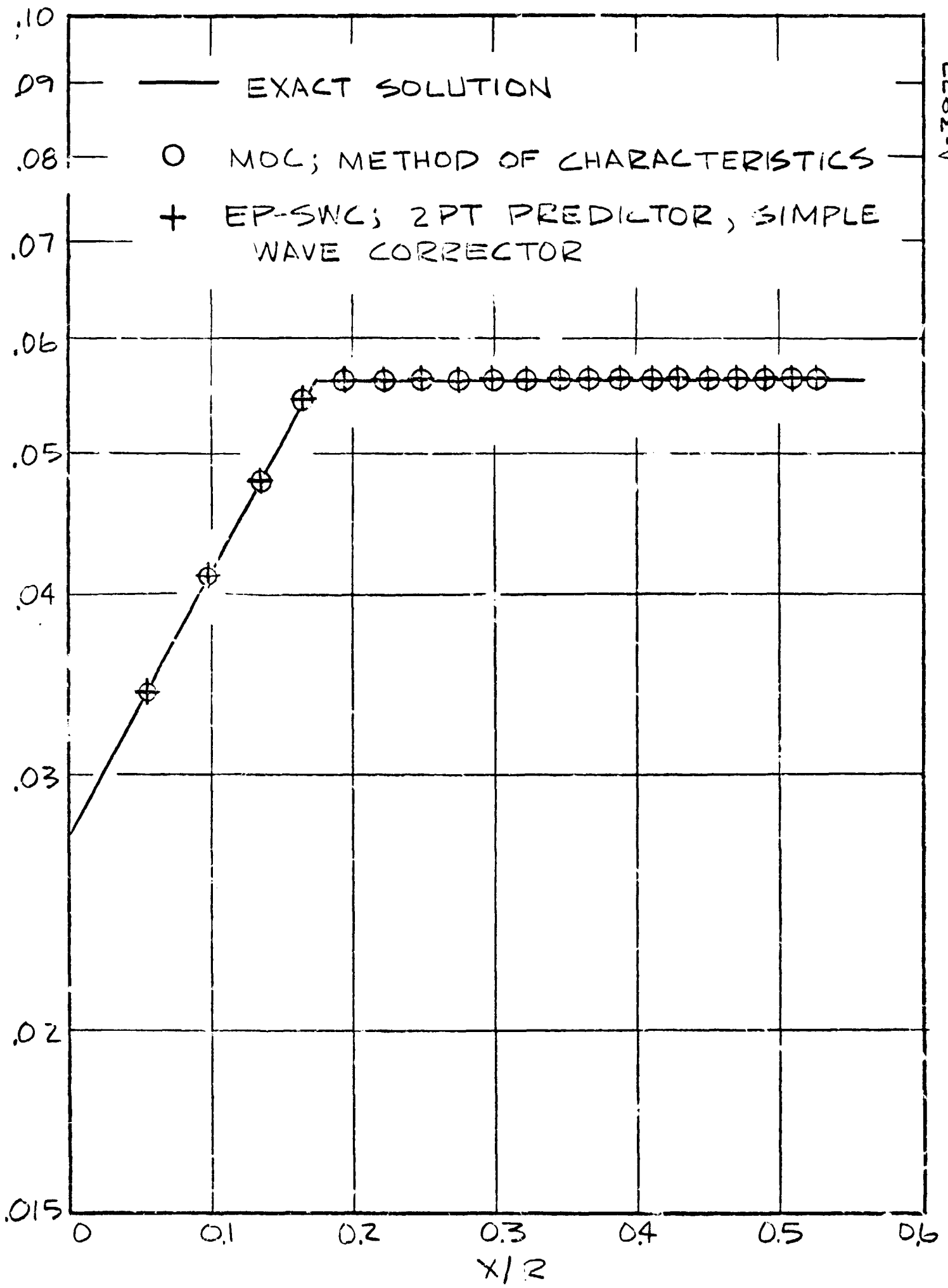

FIGURE 1-e METHOD OF CHARACTERISTICS AND NEW EULER-PREDICTOR/SIMPLE-WAVE-CORRECTOR SCHEME

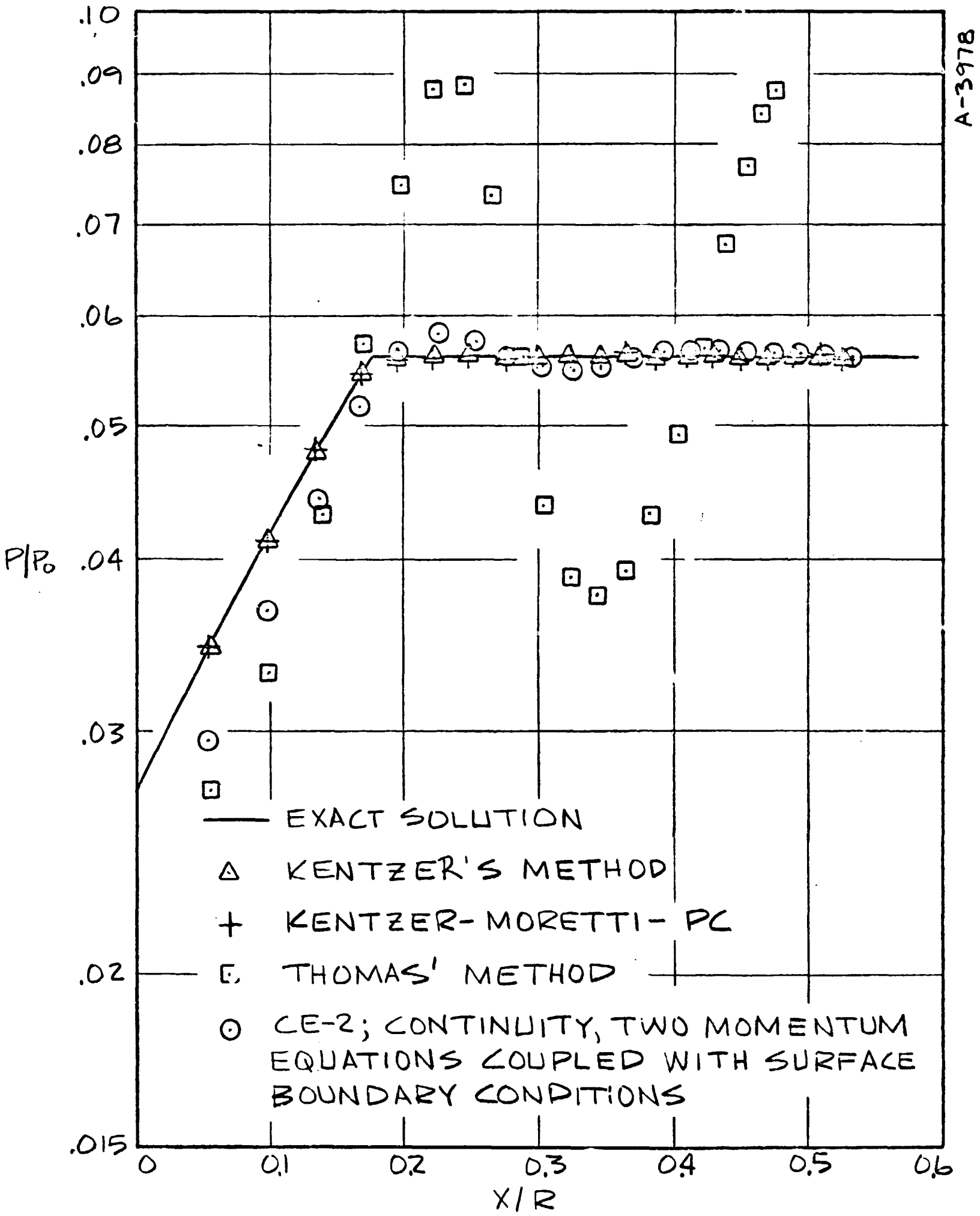

FIGURE 1-f FOUR "COMBINED EQUATIONS" SCHEMES USING TWO-POINT ONE SIDE η DERIVATIVES

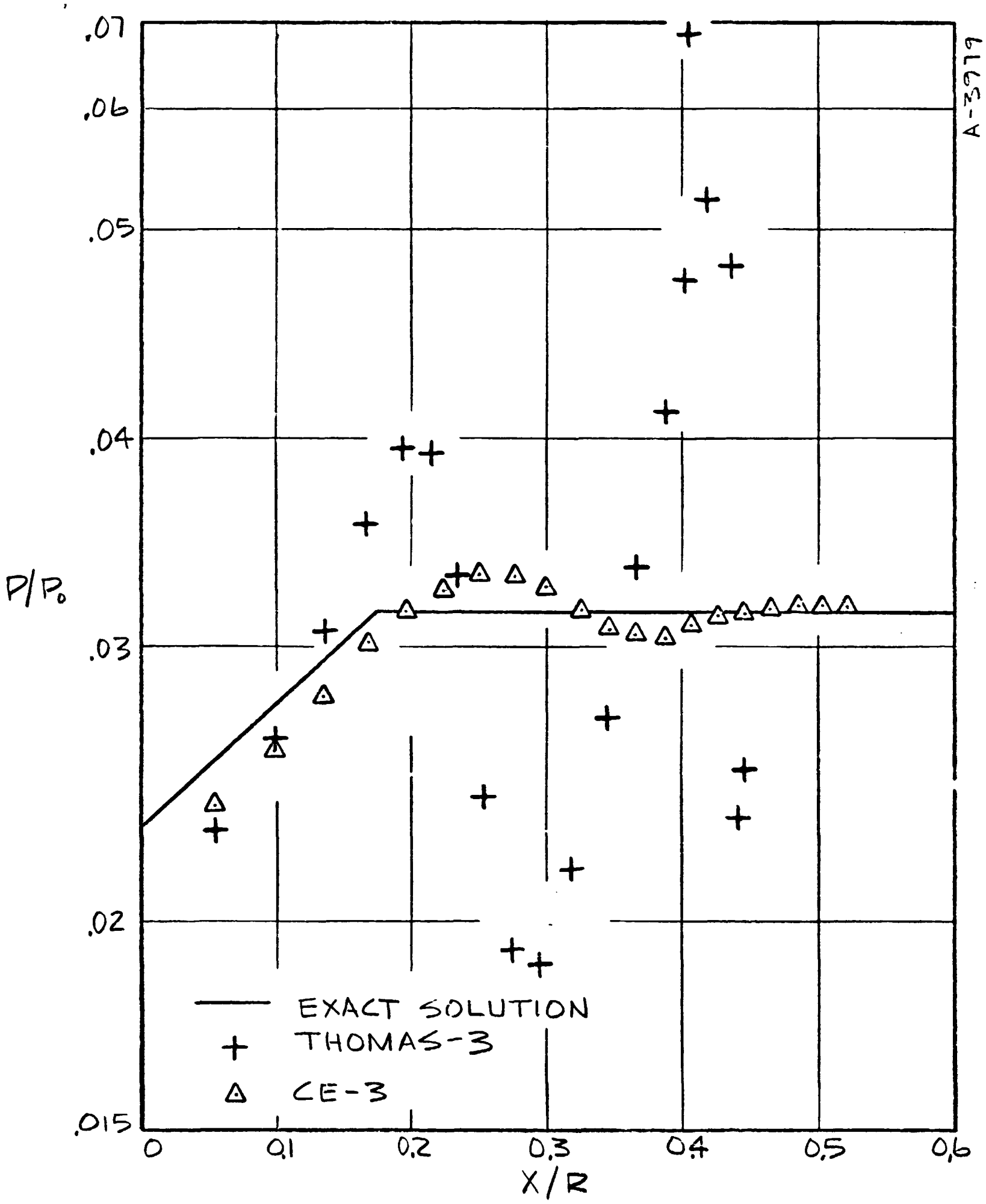

FIGURE 1-g TWO "COMBINED EQUATIONS" SCHEMES USING THREE-POINT ONE-SIDED η DERIVATIVES

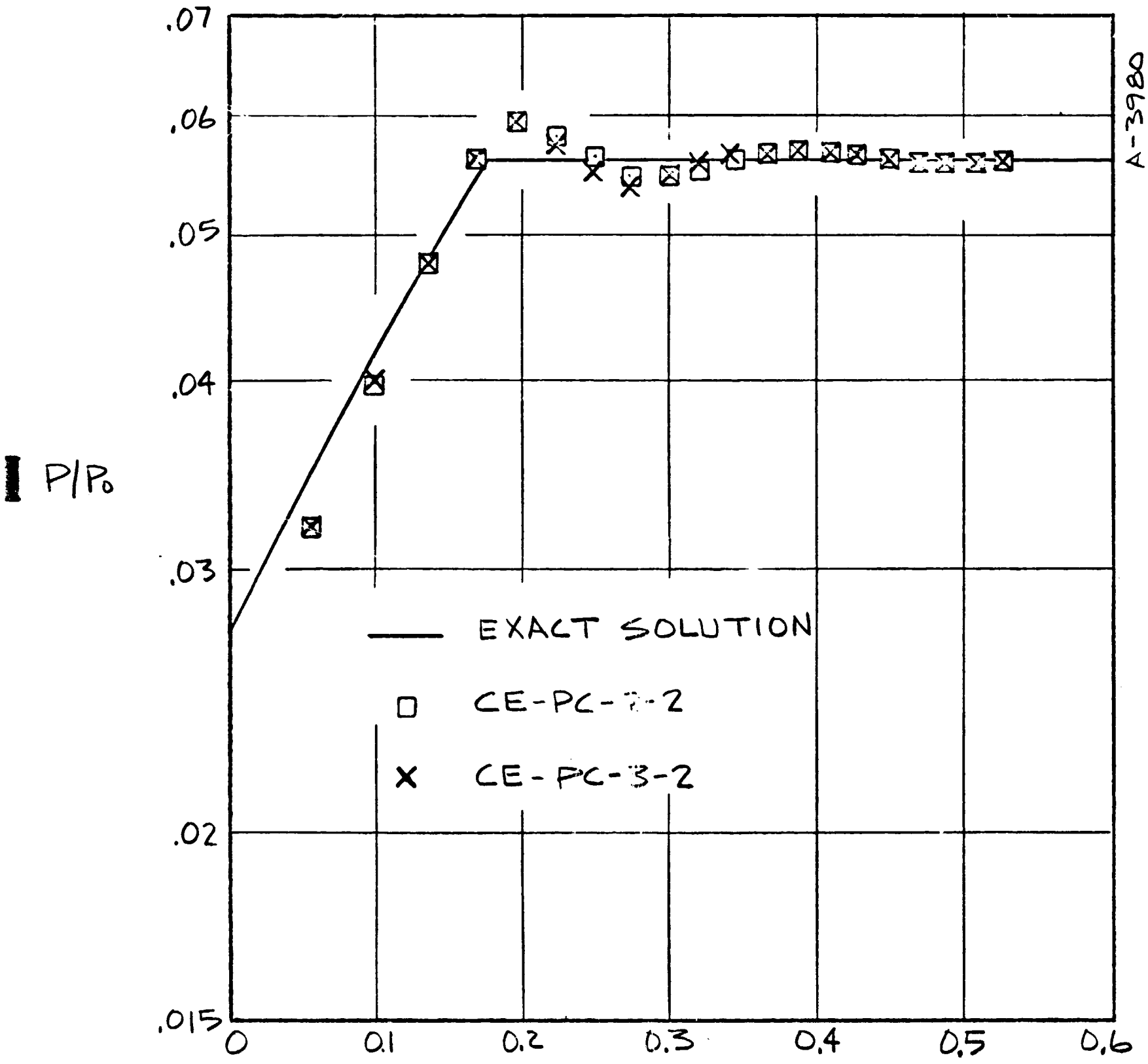

FIGURE 1-h TWO "COMBINED-EQUATIONS" / PREDICTOR-CORRECTOR SCHEMES

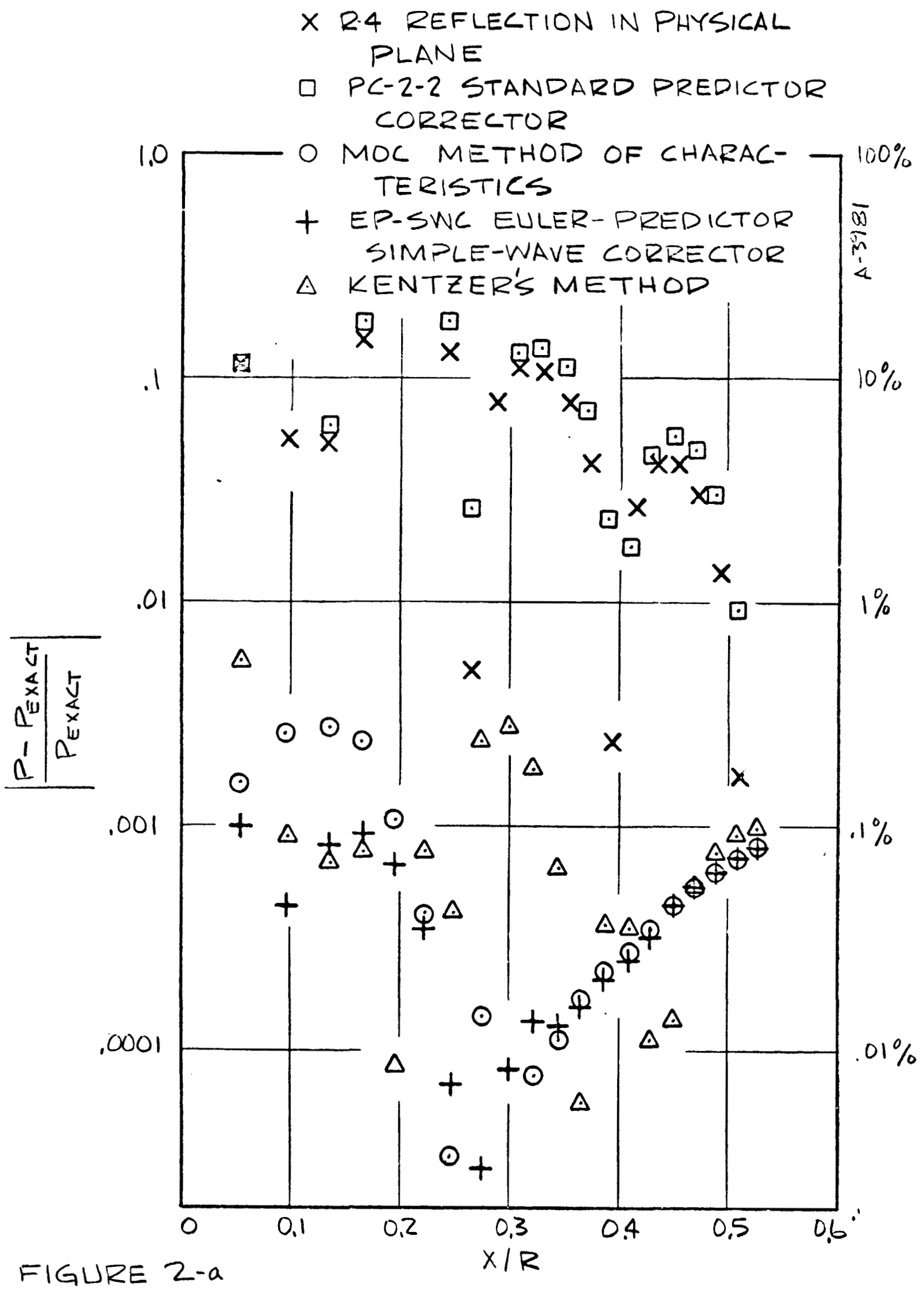

FIGURE 2-a

FIGURE 2 SIMPLE COMPRESSION: COMPARISON OF TYPICAL RELATIVE ERRORS IN SURFACE PRESSURE DISTRIBUTION

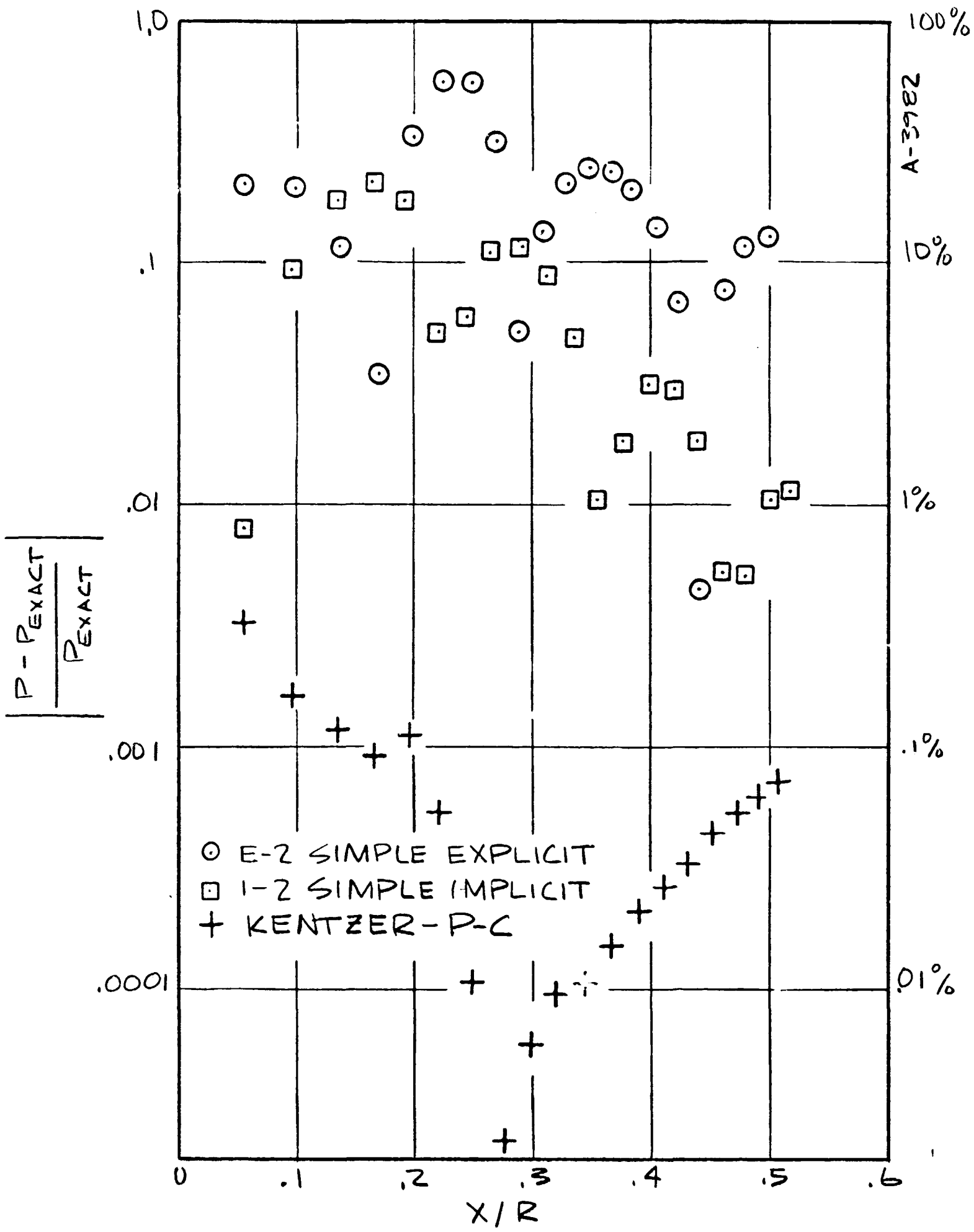

FIGURE 2-b
FIGURE 2 (CONTINUED)

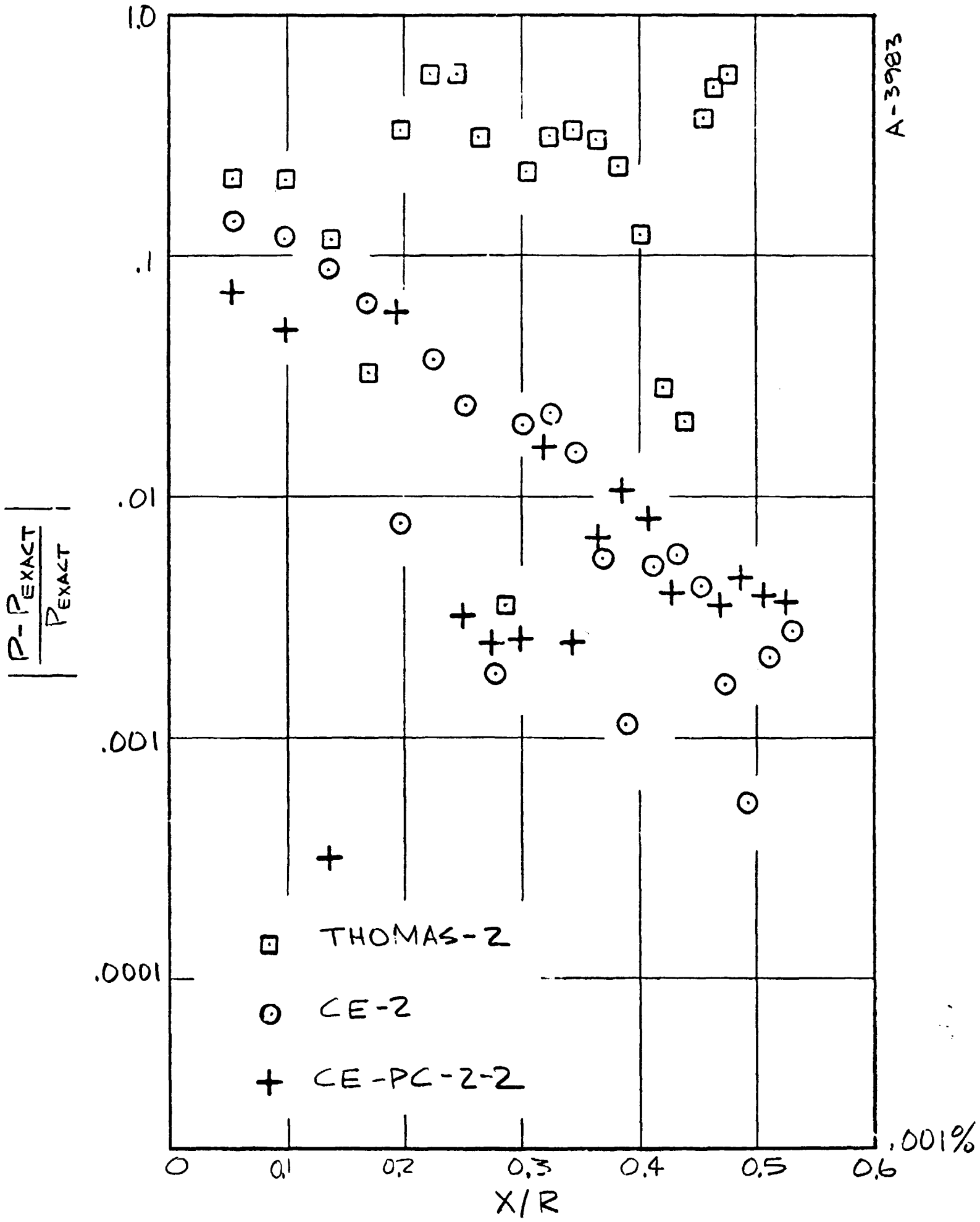

FIGURE 2-C

FIGURE 2 (CONCLUDED)

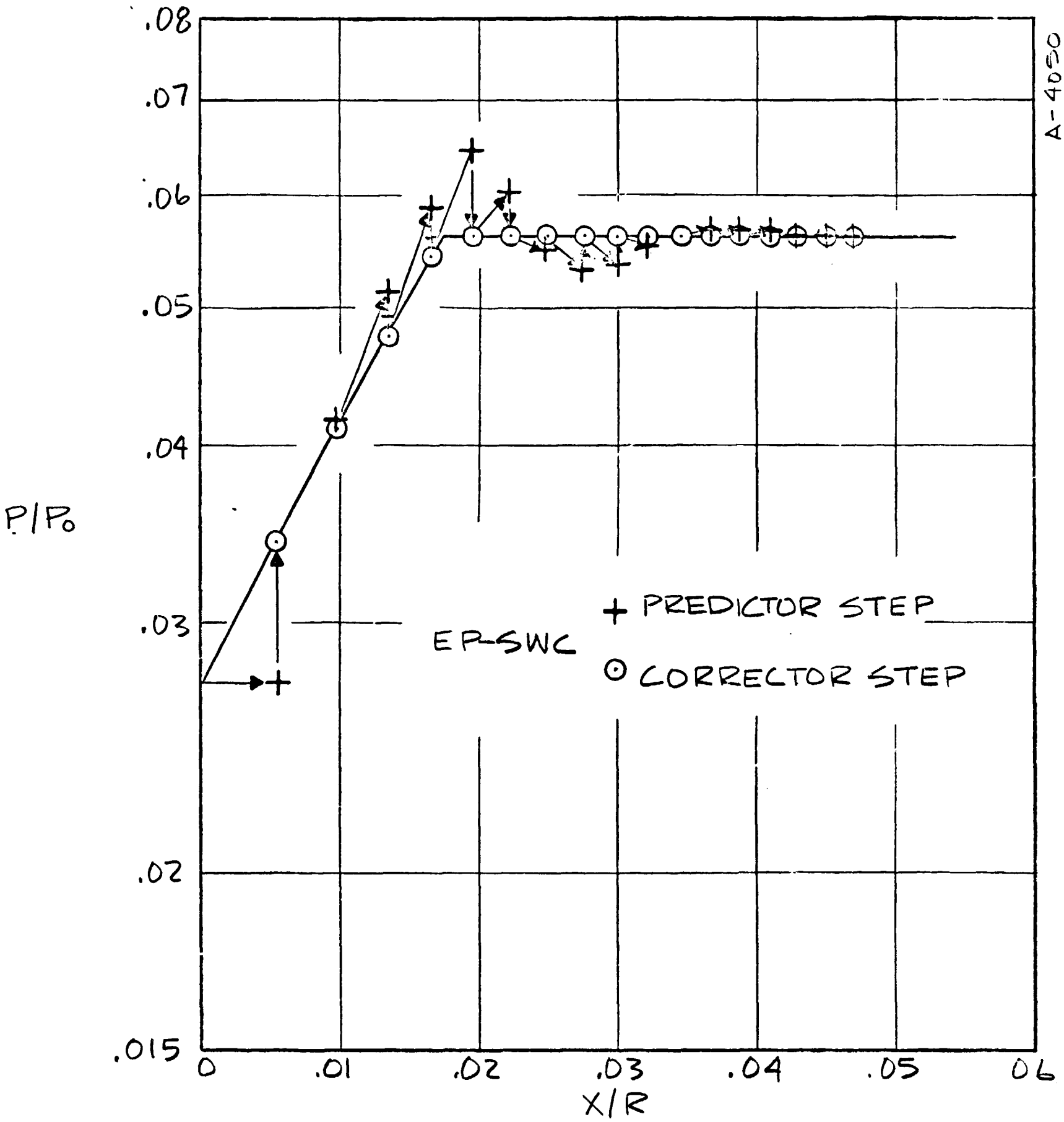

FIGURE 3 THE "PATH" OF THE NEW EULER-PREDICTOR SIMPLE WAVE CORRECTOR (EP-SWC) SCHEME SIMPLE COMPRESSION

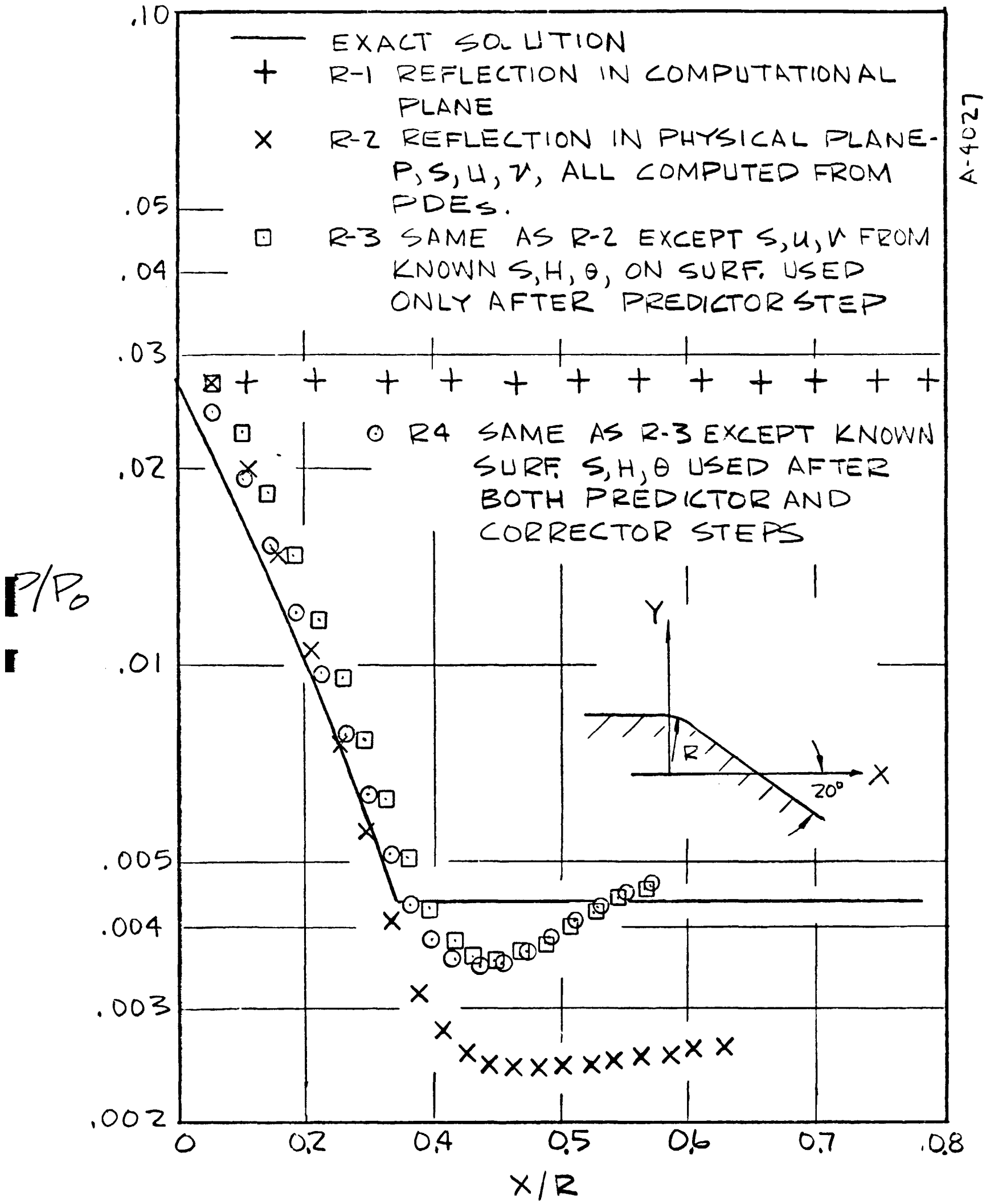

a) FOUR REFLECTION SCHEMES

FIGURE 4 SIMPLE EXPANSION – COMPARISON OF PREDICTED SURFACE PRESSURES WITH EXACT SOLUTION

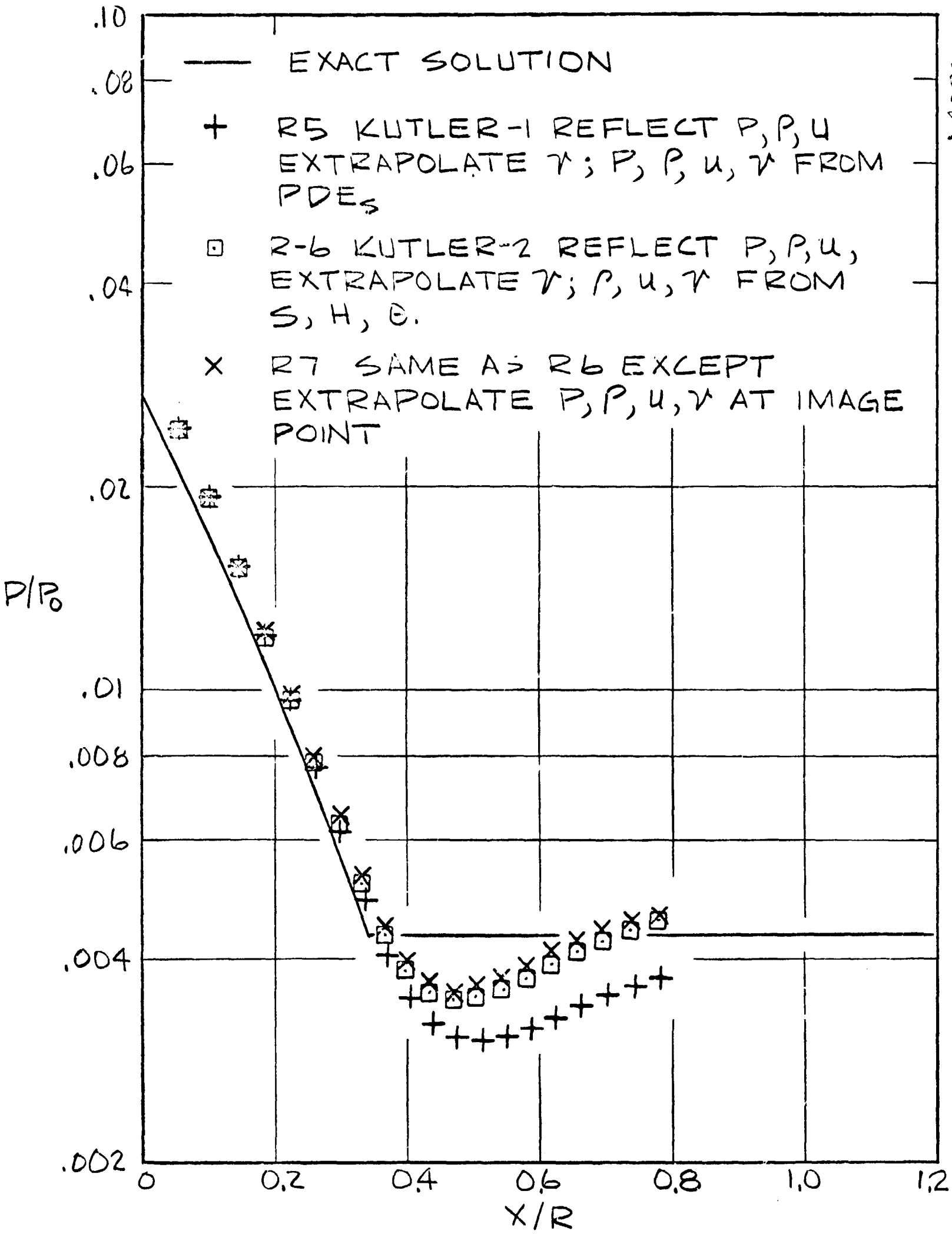

b) THREE REFLECTION SCHEMES

FIGURE 4 (CONTINUED)

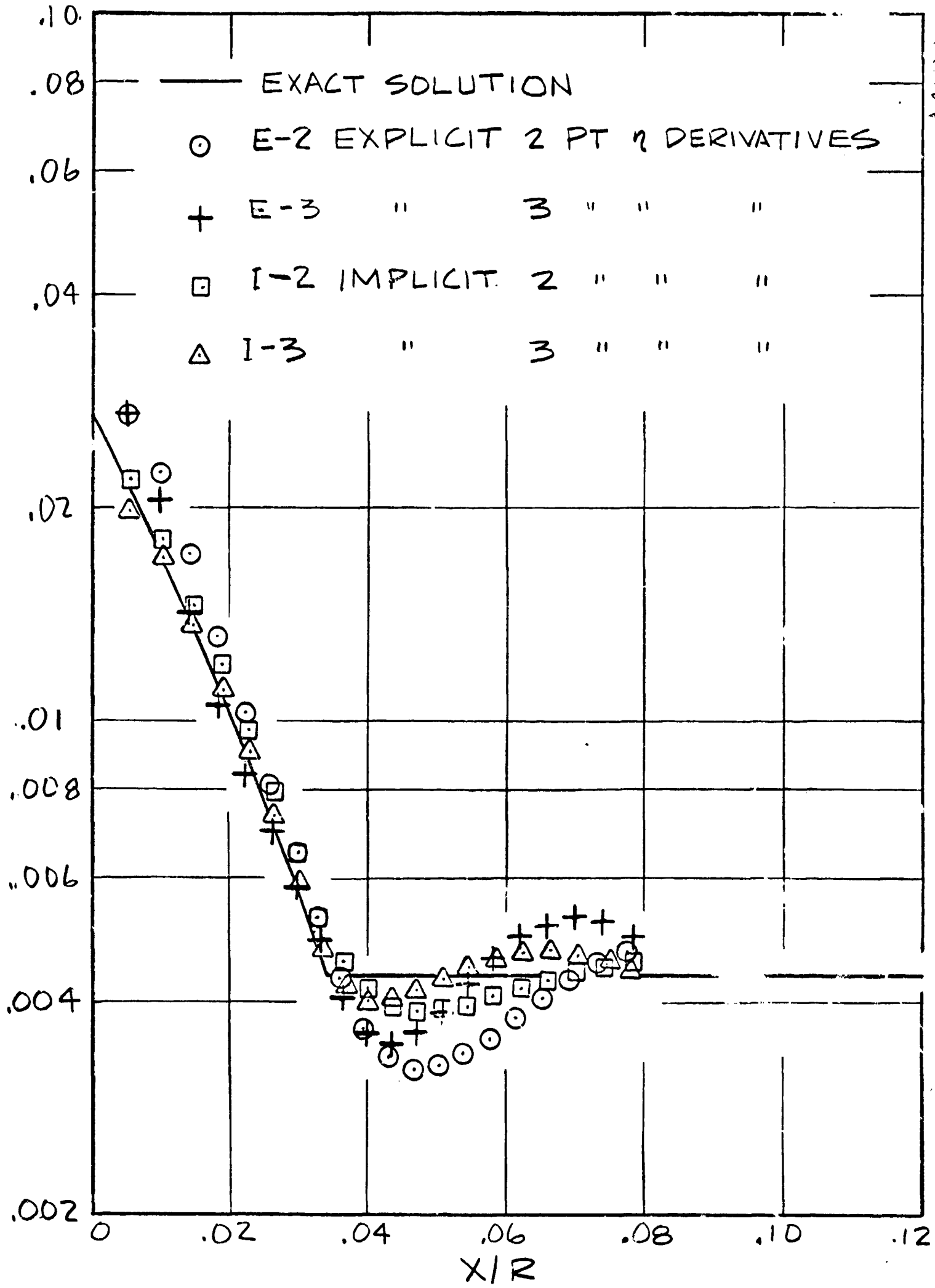

C) SIMPLE EXPLICIT AND SIMPLE IMPLICIT SCHEMES

FIGURE 4 (CONTINUED)

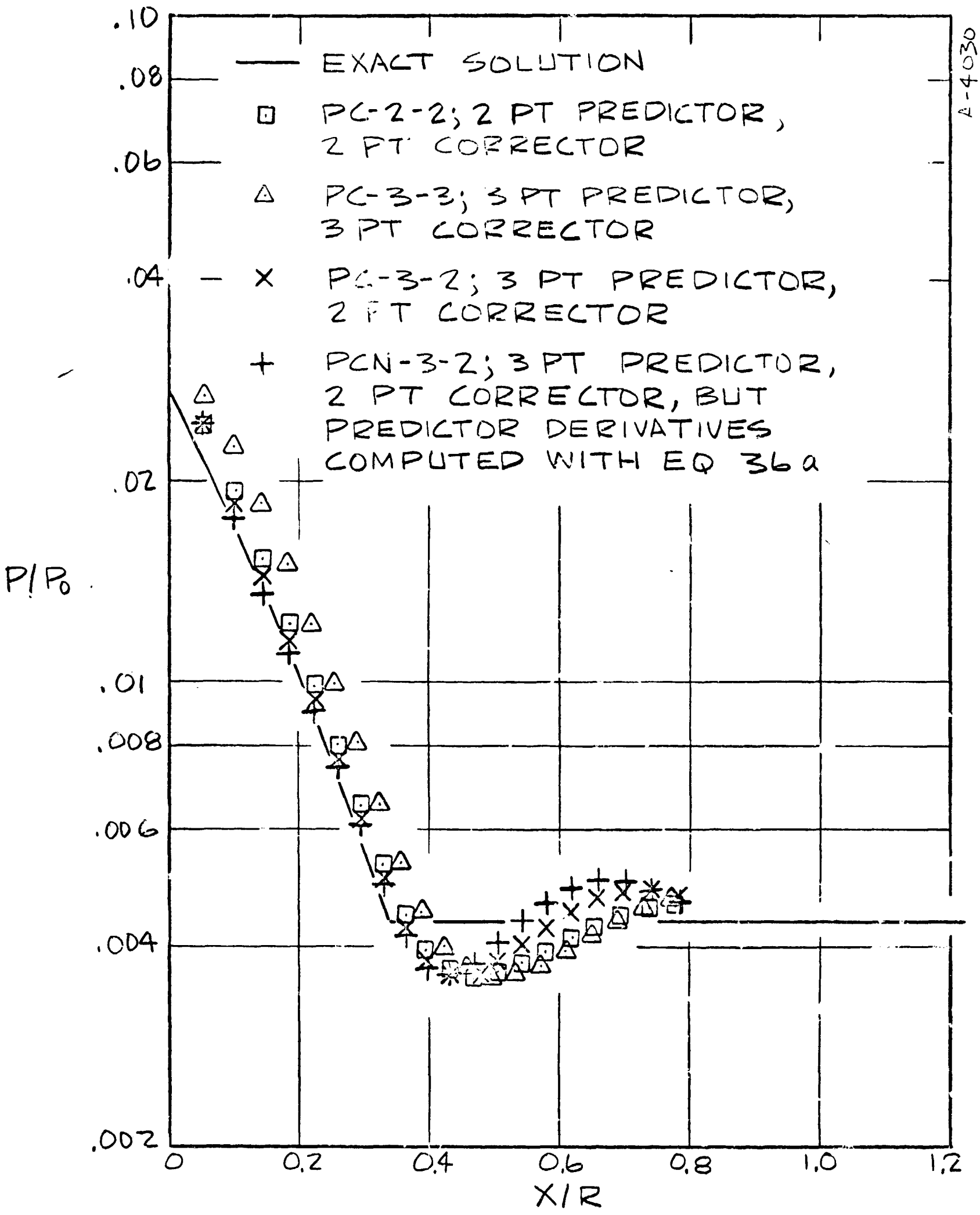

d) STANDARD PREDICTOR-COPRECTOR SCHEMES

FIGURE 4 (CONTINUED)

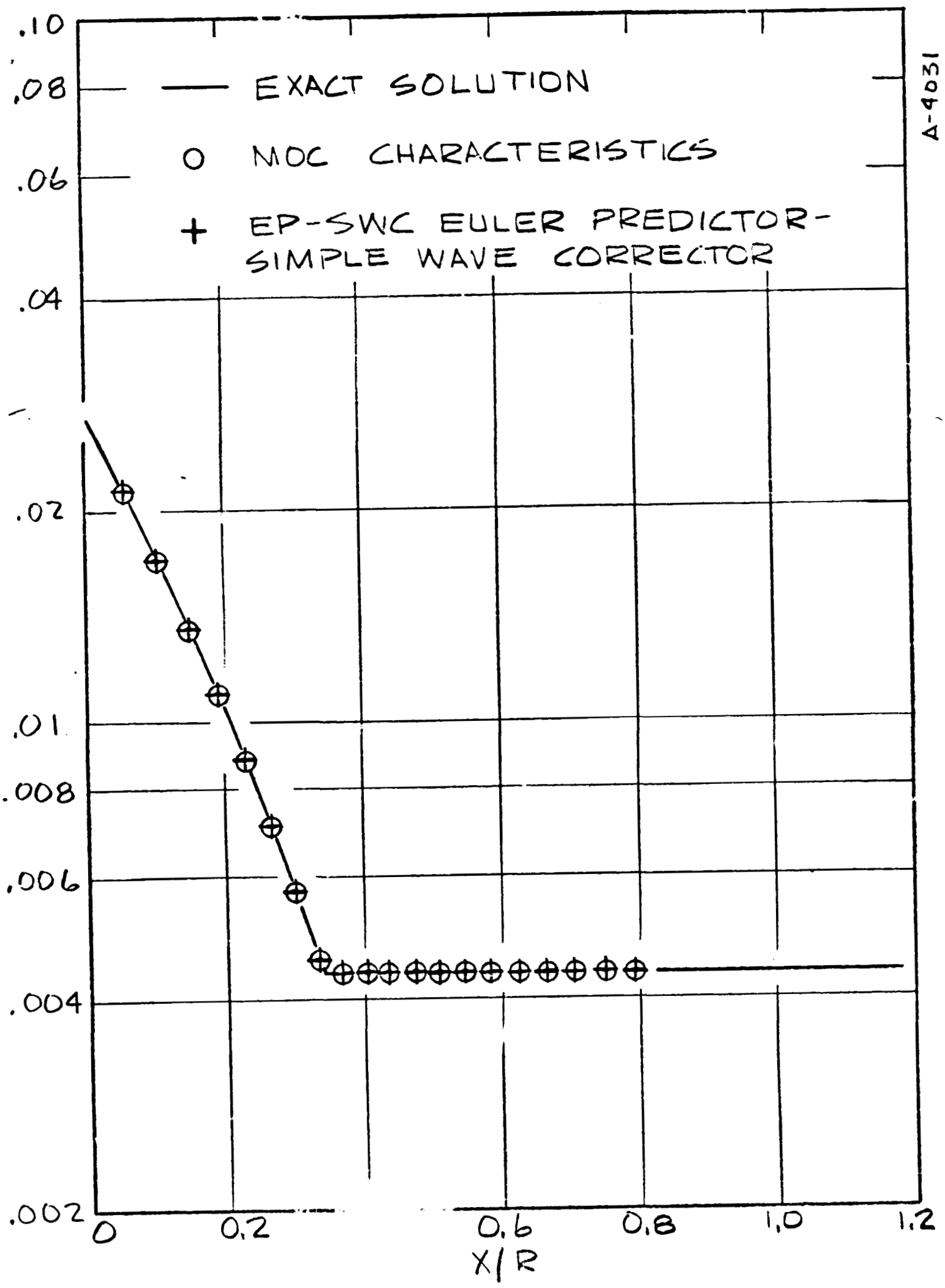

e) METHOD OF CHARACTERISTICS AND NEW EULER-PREDICTOR/SIMPLE-WAVE-CORRECTOR SCHEME

FIGURE 4 (CONTINUED)

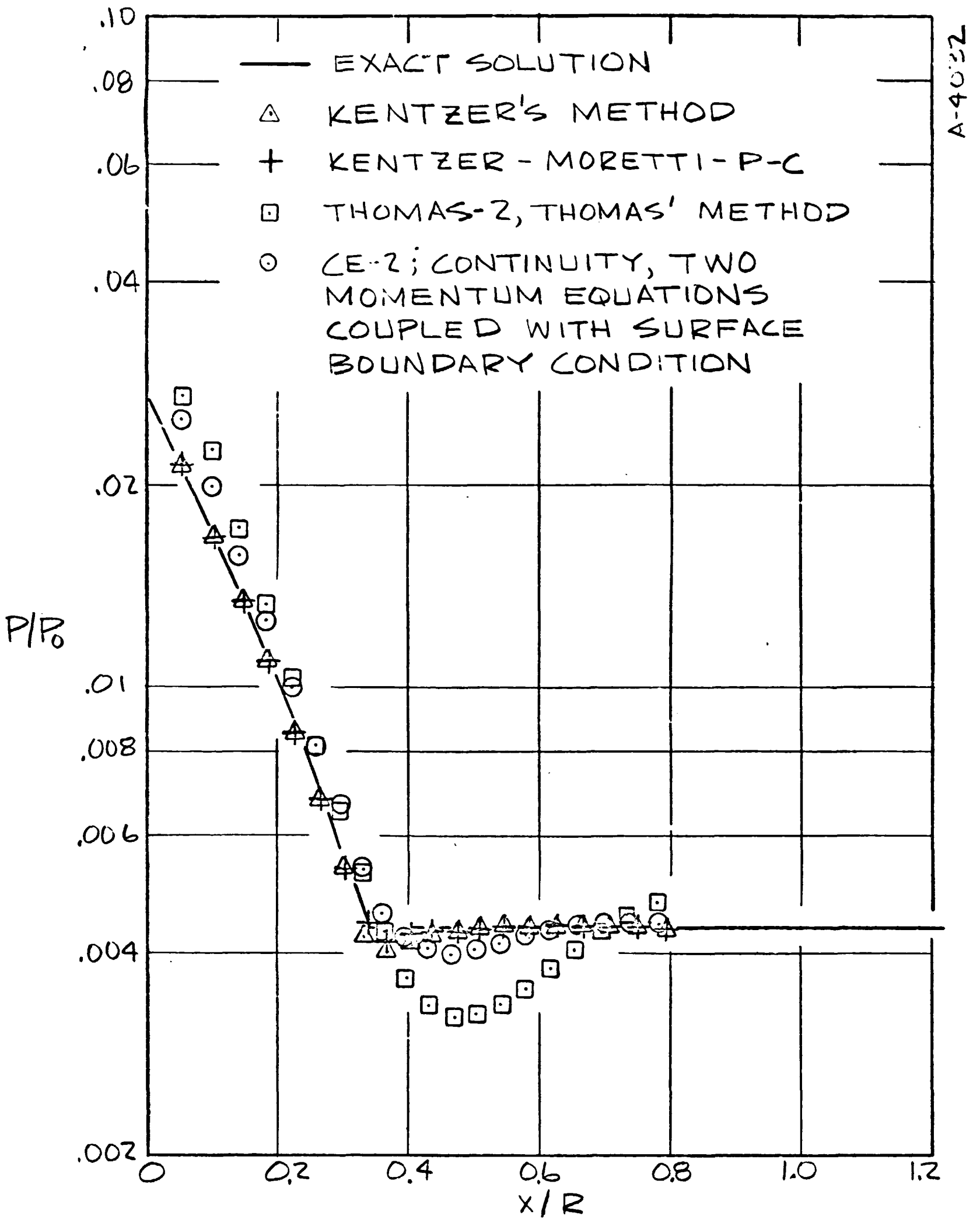

f) FOUR "COMBINED EQUATIONS" SCHEMES USING TWO-POINT ONE-SIDED η DERIVATIVES

FIGURE 4 (CONTINUED)

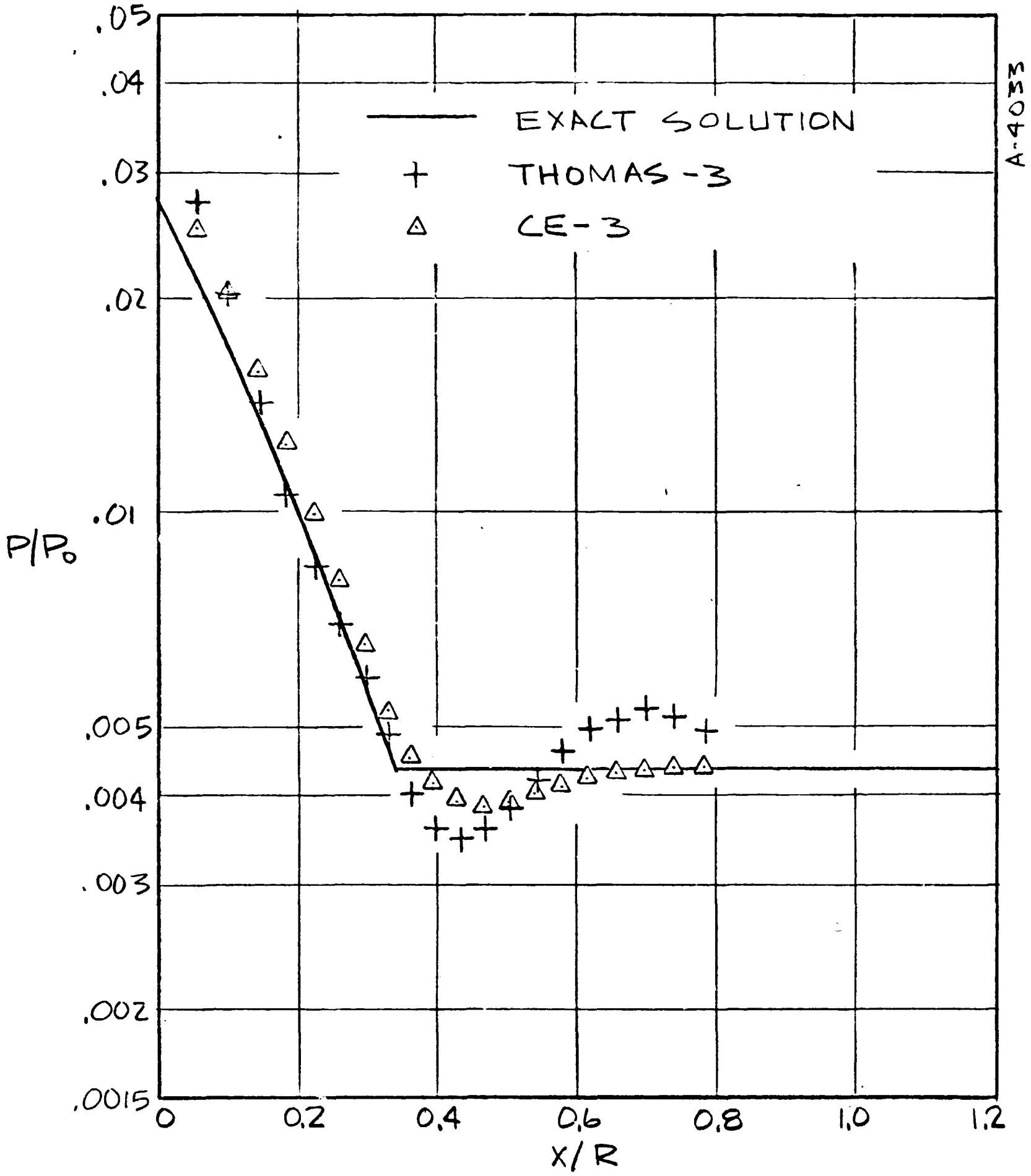

9) TWO "COMBINED EQUATIONS" SCHEMES USING THREE-POINT ONE-SIDED DERIVATIVES

FIGURE 4 (CONTINUED)

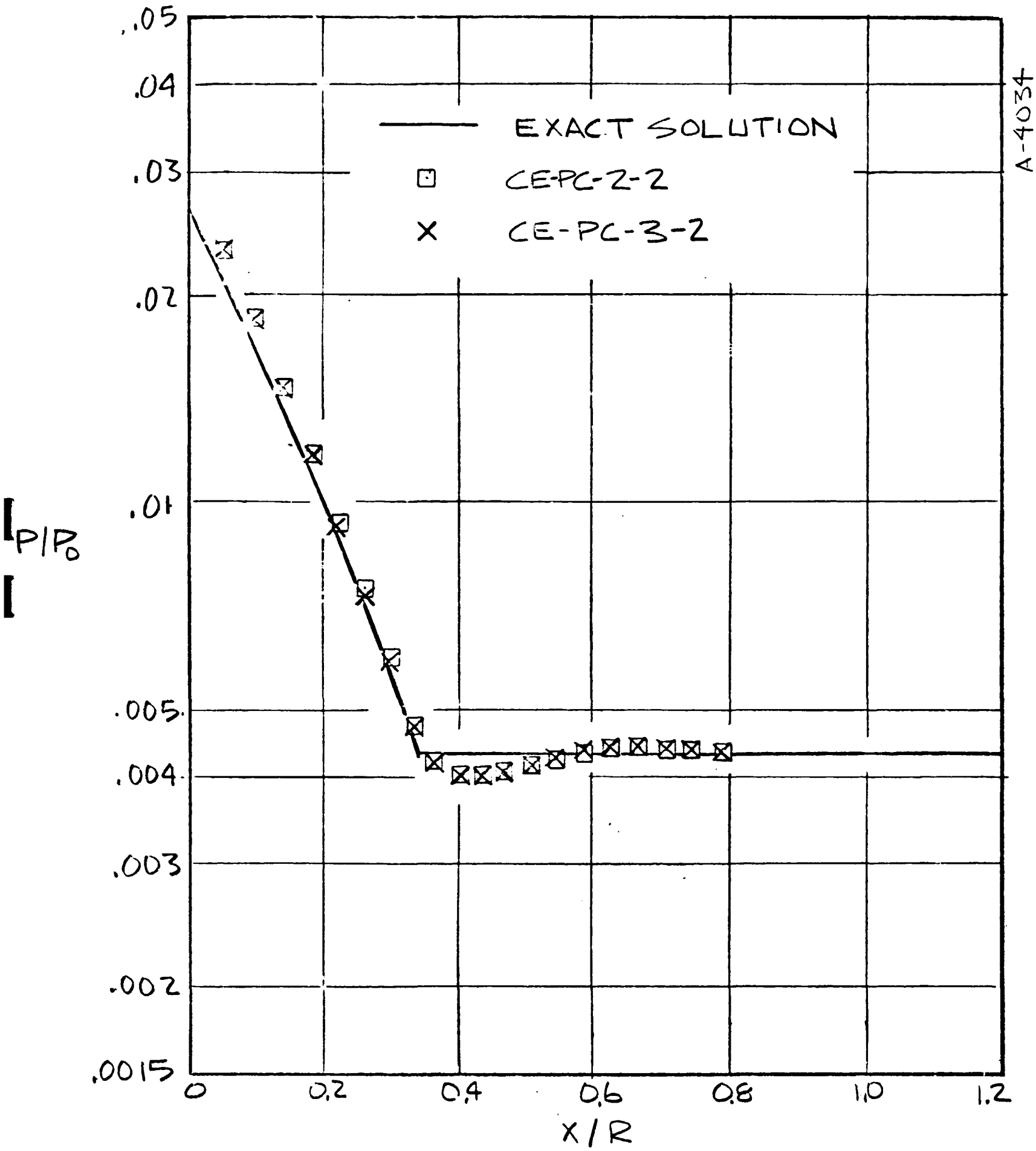

h) TWO "COMBINED EQUATIONS" / PREDICTOR-CORRECTOR SCHEMES

FIGURE 4 (CONTINUED)

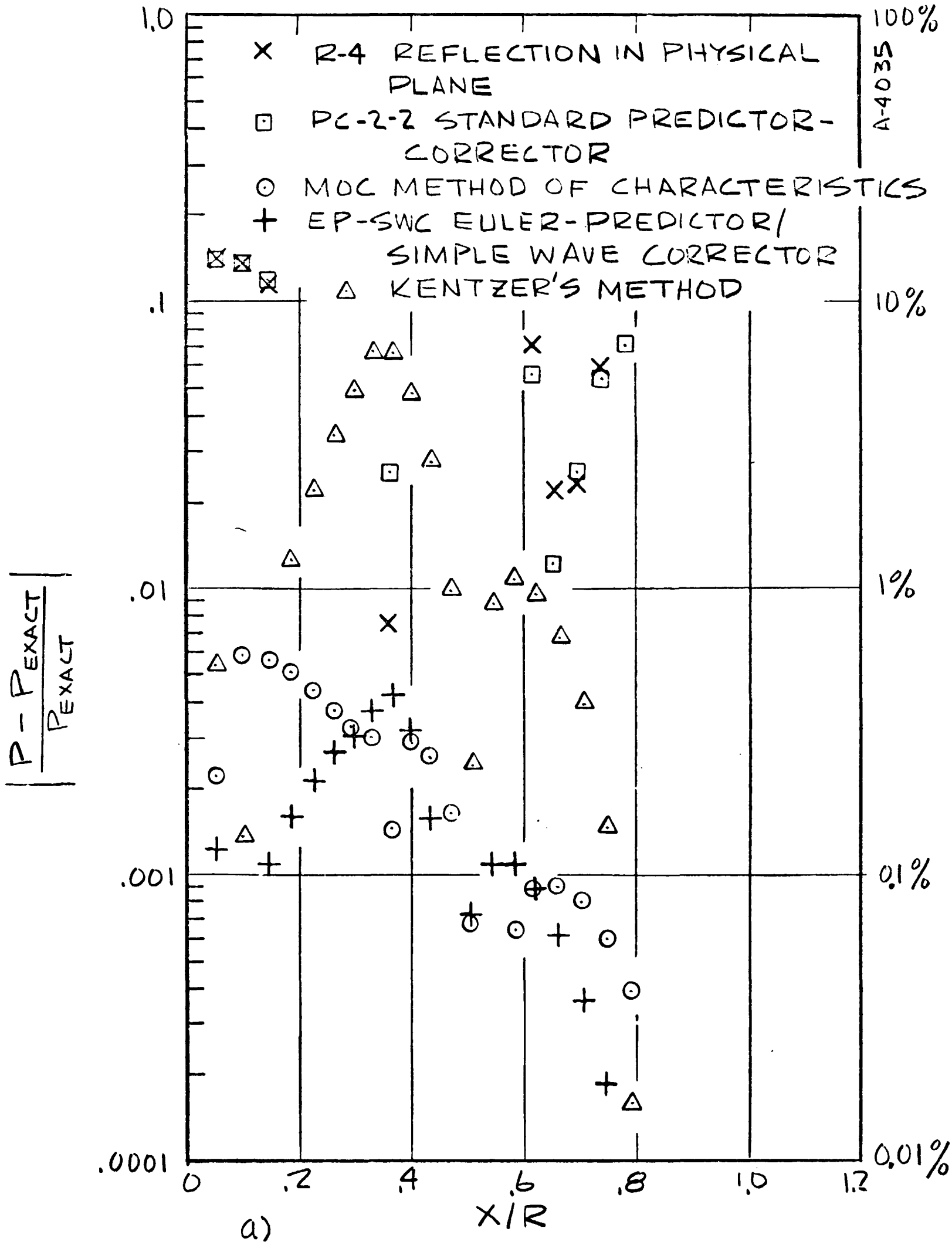

FIGURE 5 SIMPLE EXPANSION - COMPARISON OF TYPICAL RELATIVE ERRORS IN SURFACE PRESSURE DISTRIBUTIONS

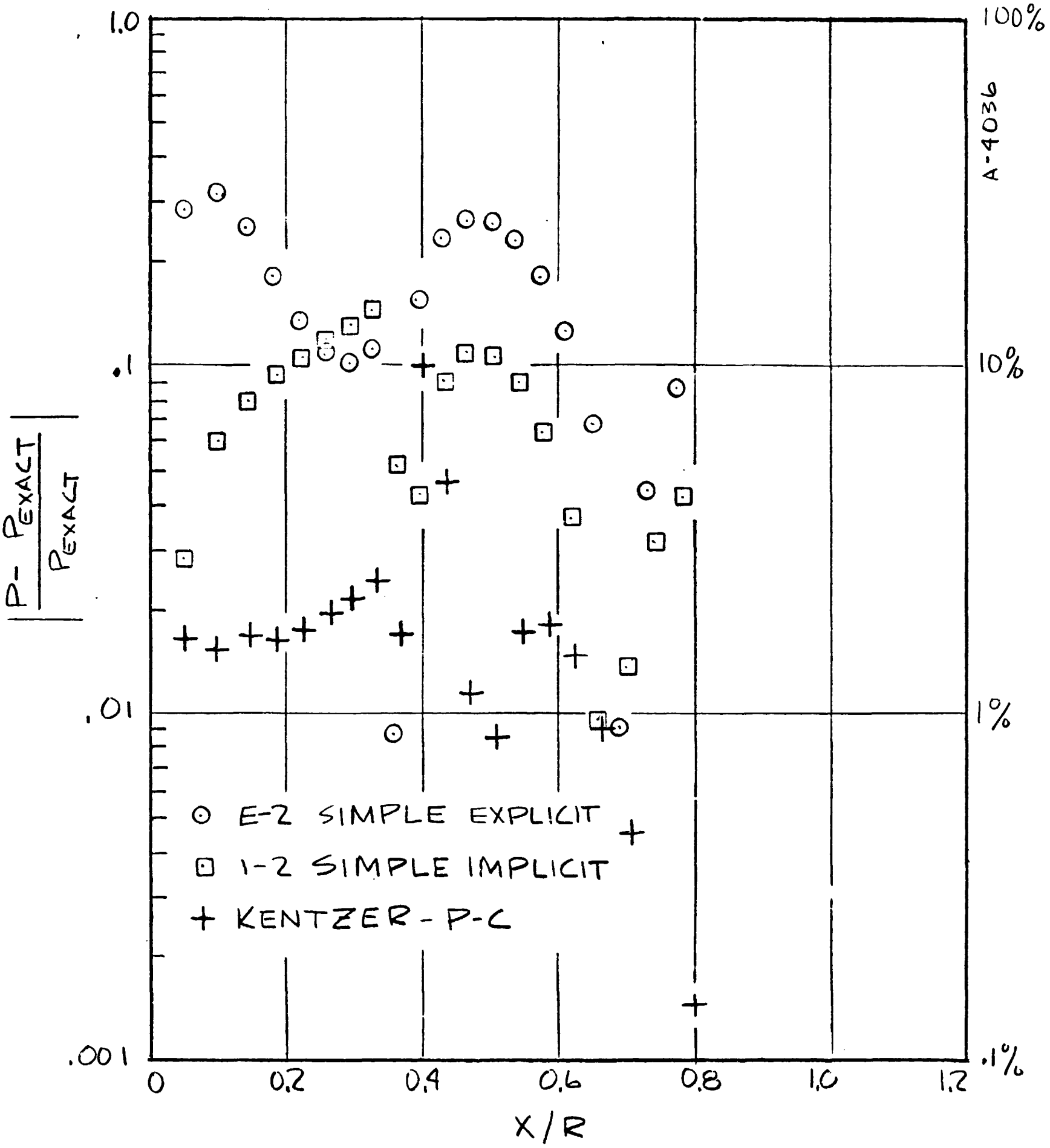

b)

FIGURE 5 (CONTINUED)

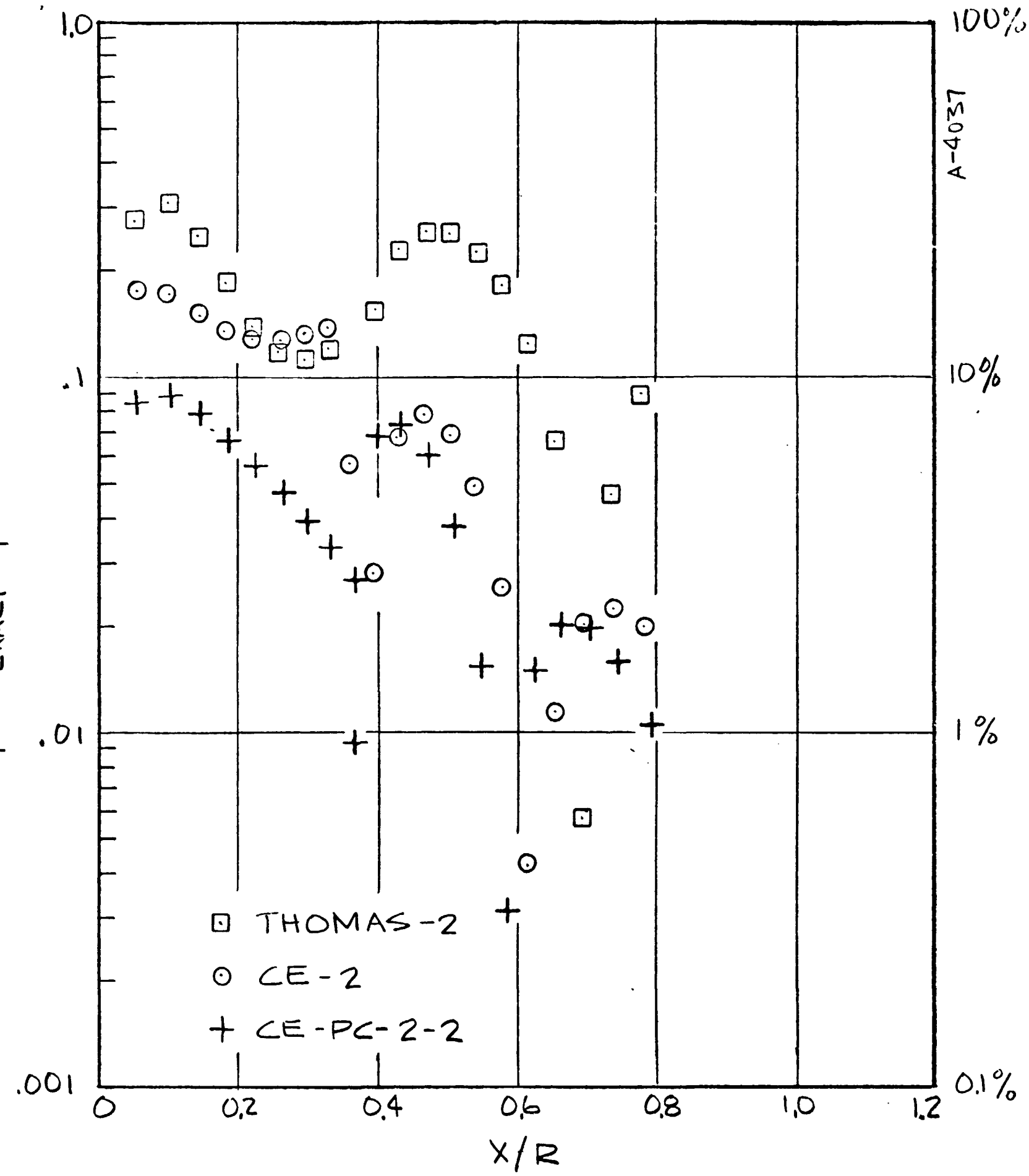

c)

FIGURE 5 (CONCLUDED)

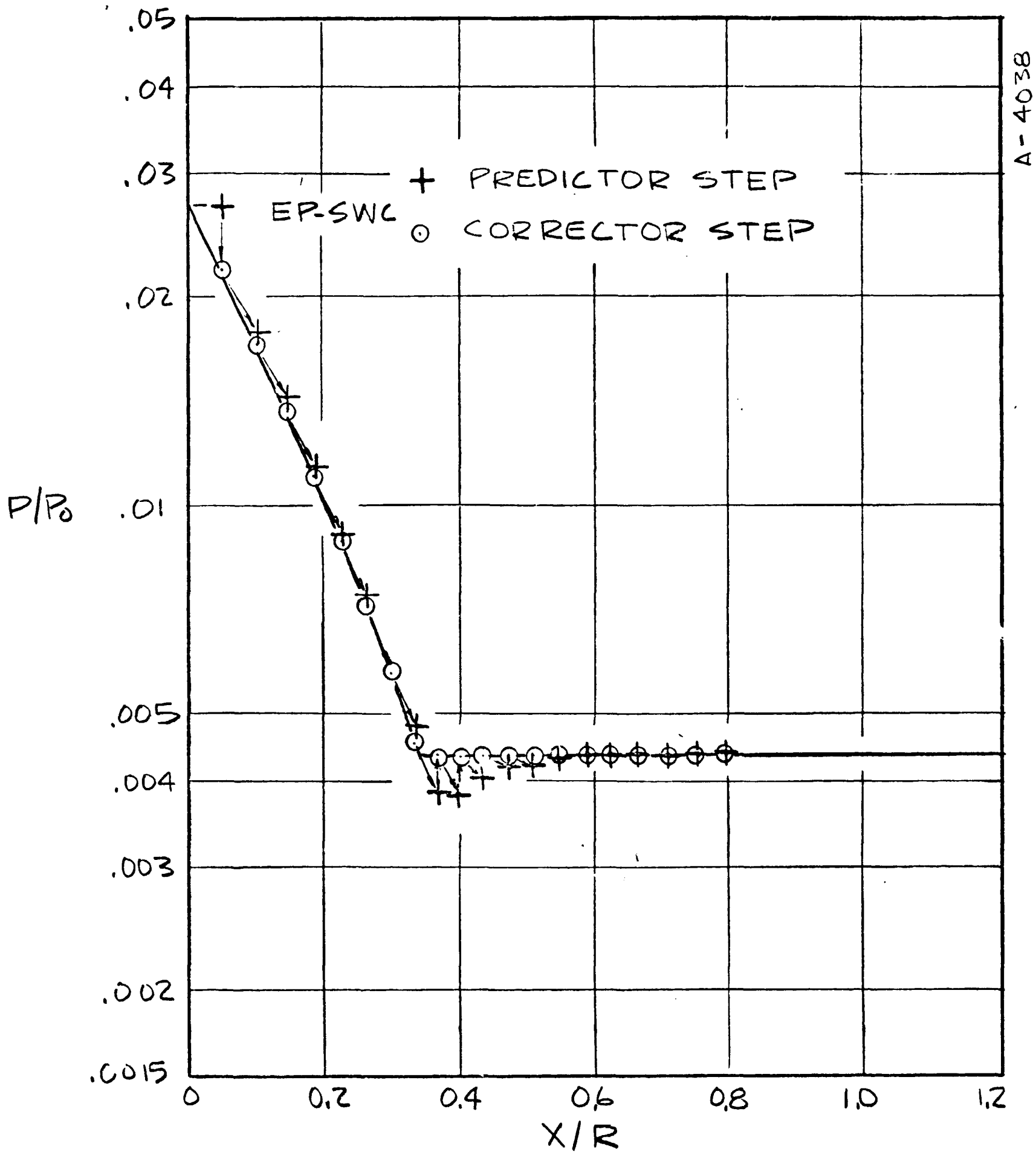

FIGURE 6 THE "PATH" OF THE NEW EULER-PREDICTOR / SIMPLE-WAVE-CORRECTOR (EP-SWC) SCHEME -SIMPLE EXPANSION

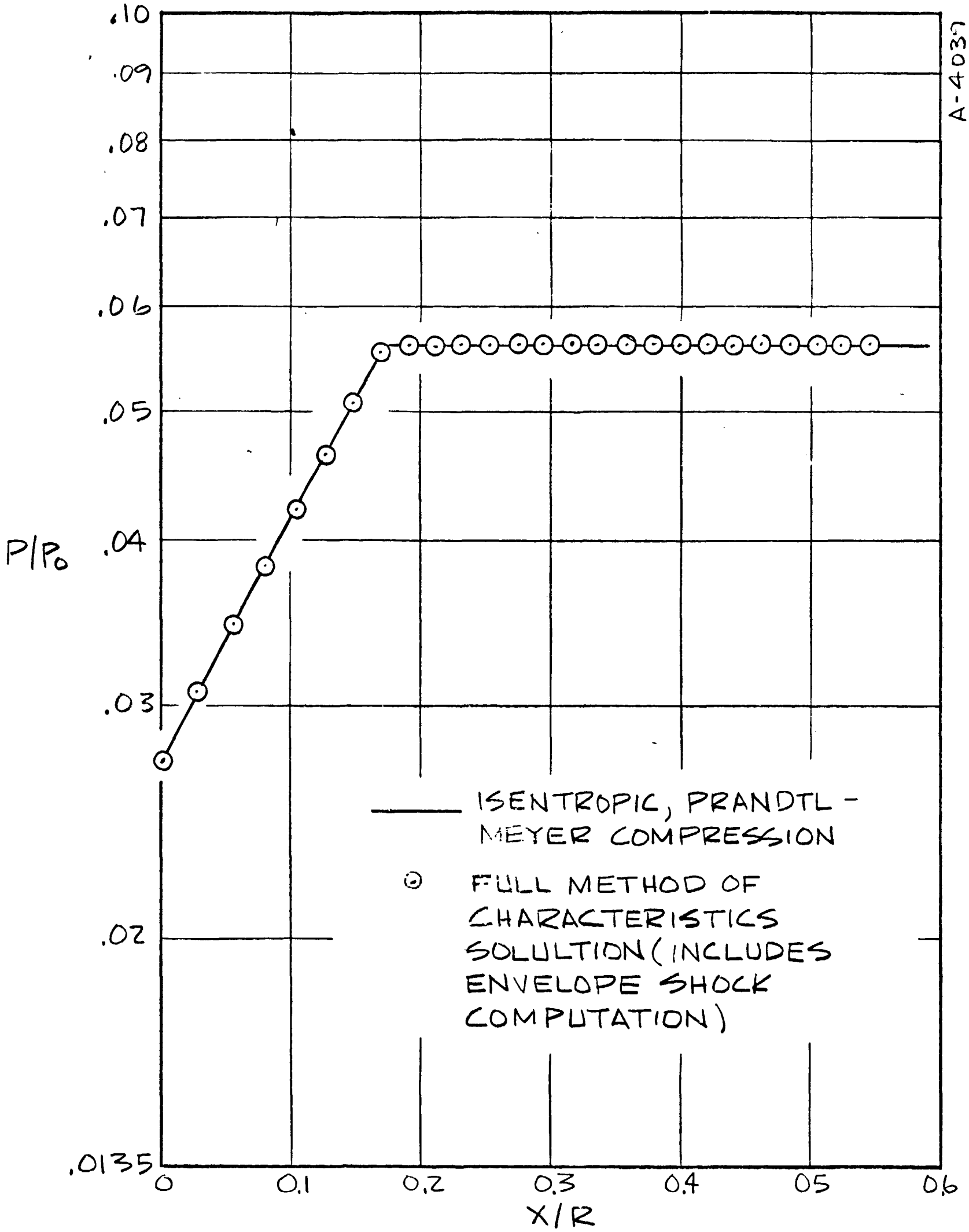

FIGURE 7 COMPARISON OF SURFACE PRESSURE BY FULL METHOD OF CHARACTERISTICS SOLUTION WITH THE ISENTROPIC COMPRESSION SOLUTION

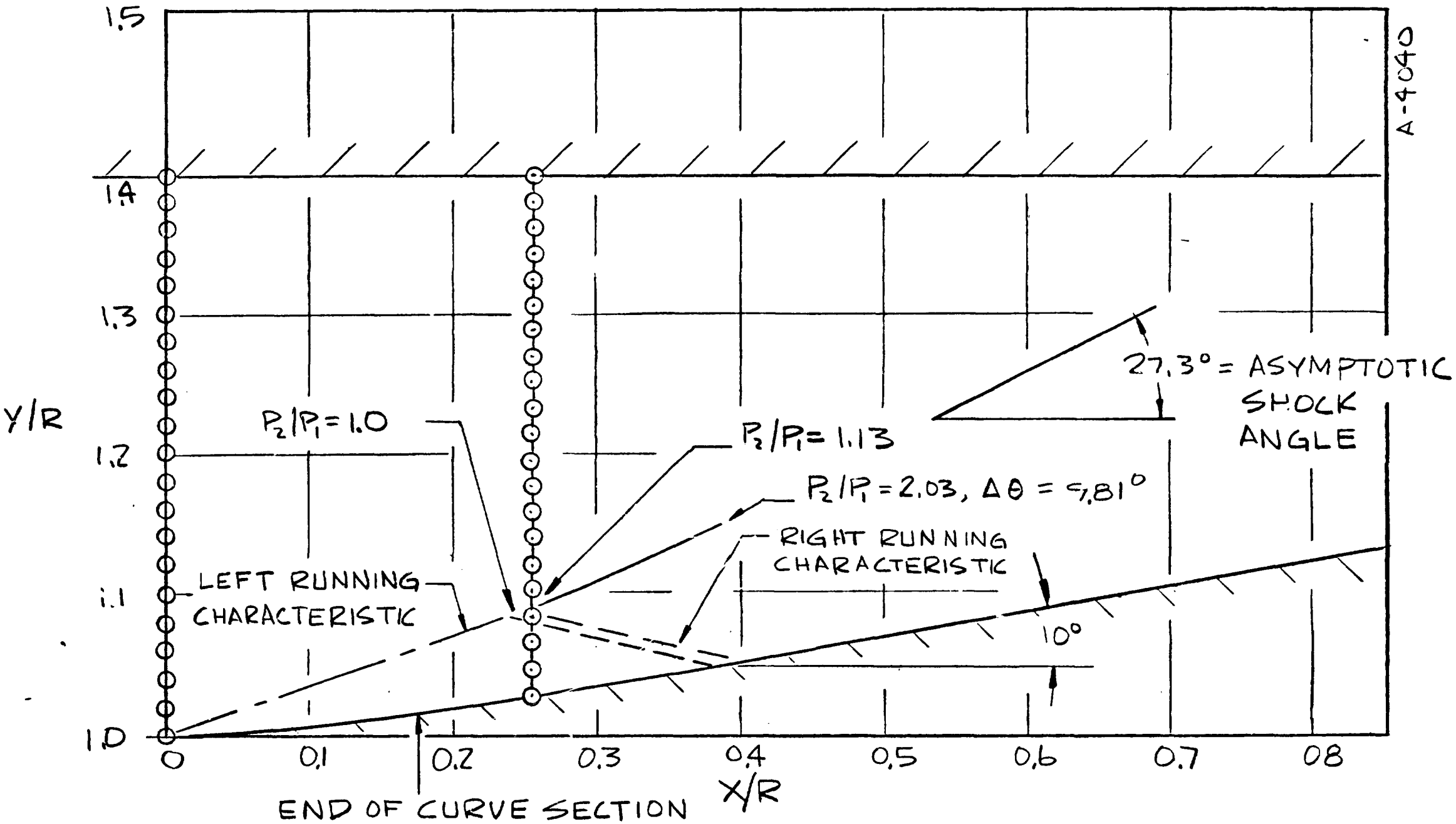

FIGURE 8 COMPUTED FLOW FIELD FOR THE COMPRESSION PROBLEM

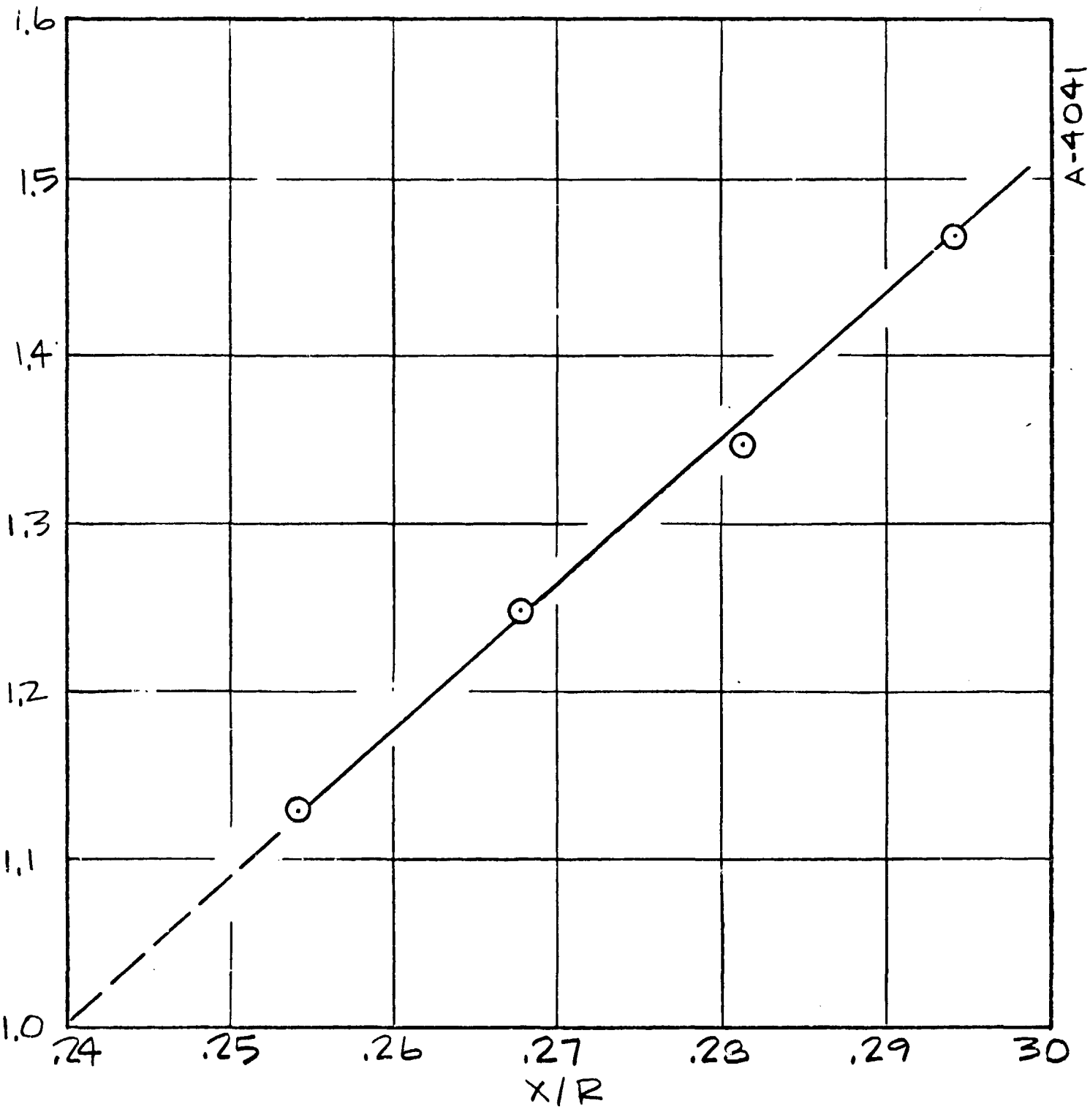

FIGURE 9 STATIC PRESSURE RATIO ACROSS SHOCK VS. SHOCK ABSCISSA (FULL METHOD OF CHARACTERISTICS CALCULTION)

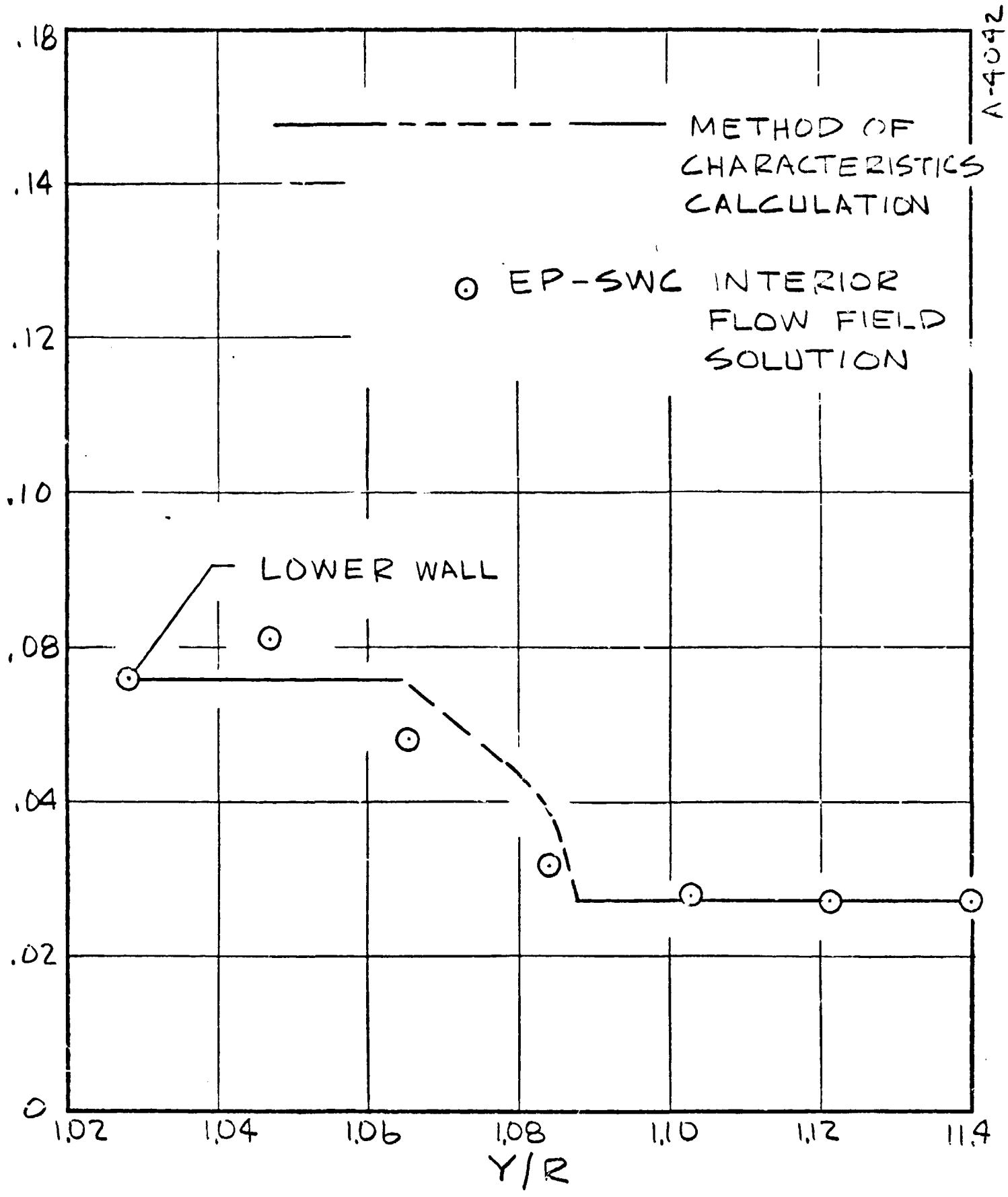

10-a : X/R = .248

FIGURE 10 COMPARISON OF PRESSURE PROFILES COMPUTED BY FULL METHOD OF CHARACTERISTICS CALCULATION WITH THOSE OF FINITE DIFFERENCE SOLUTION USING BOUNDARY CONDITION SCHEME EP-SWC (COMPRESSION PROBLEM)

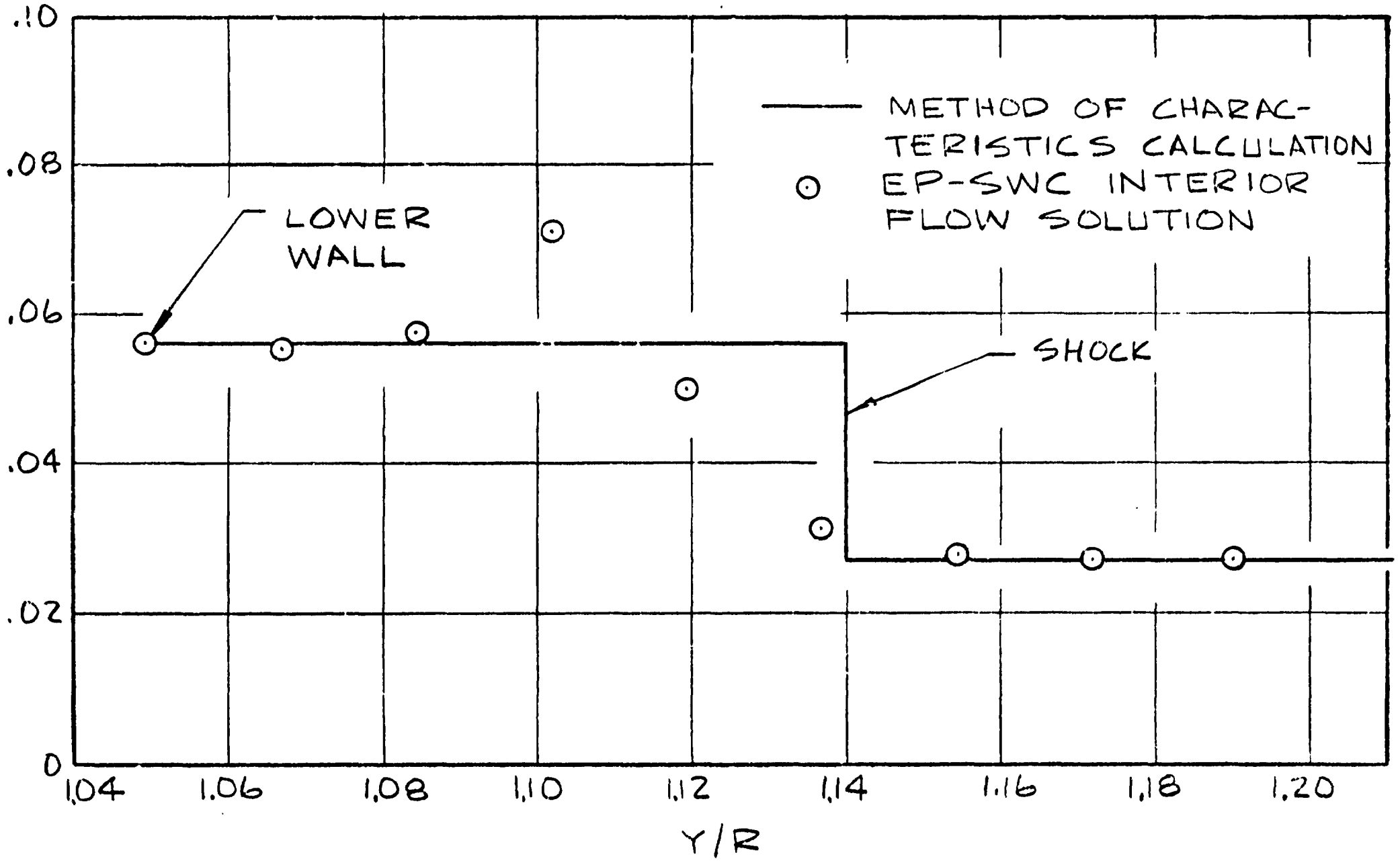

b) $X/R = 0.3664$

FIGURE 10 (CONTINUED)

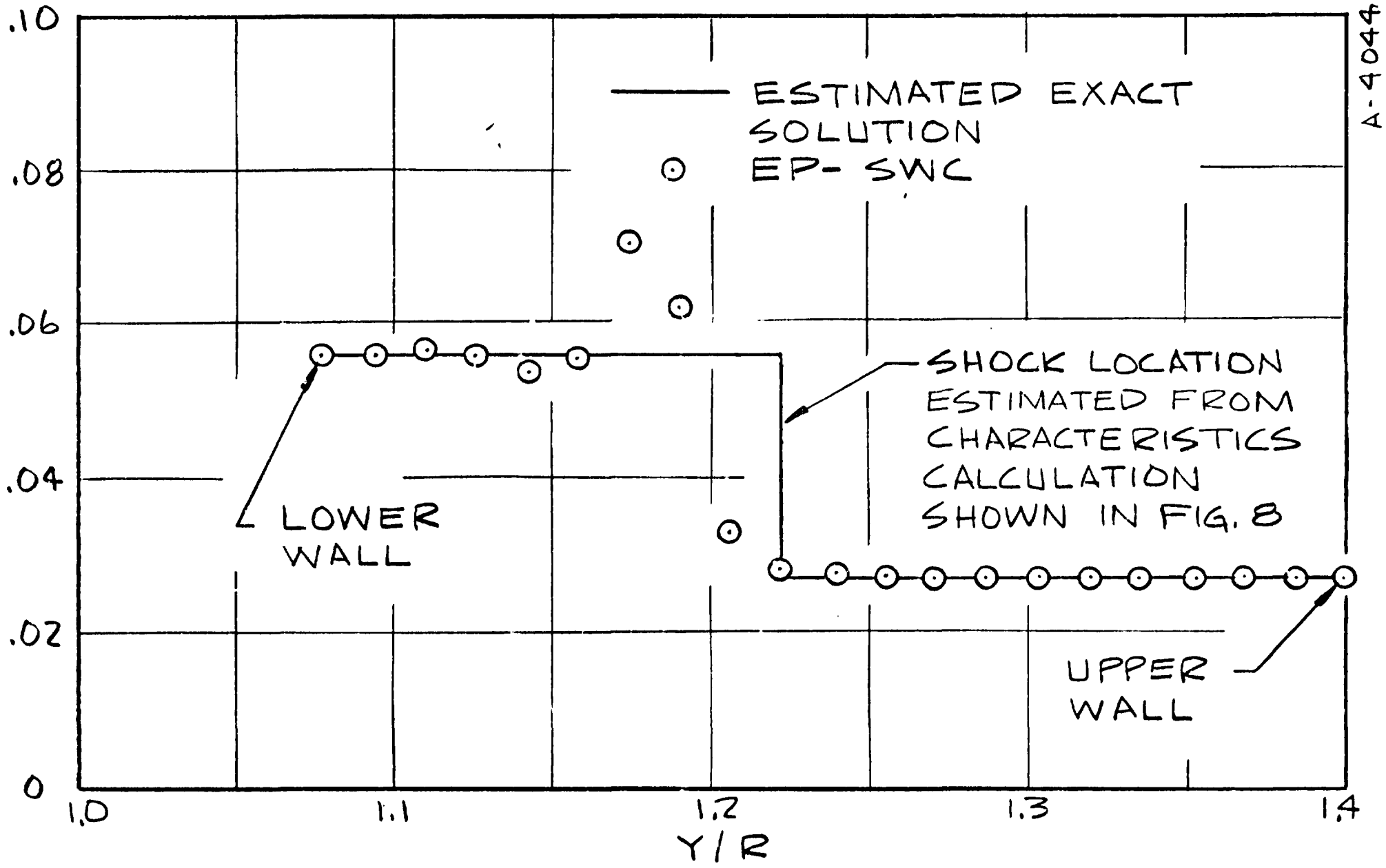

C) X/R = 0.5264

FIGURE 10 (CONCLUDED)

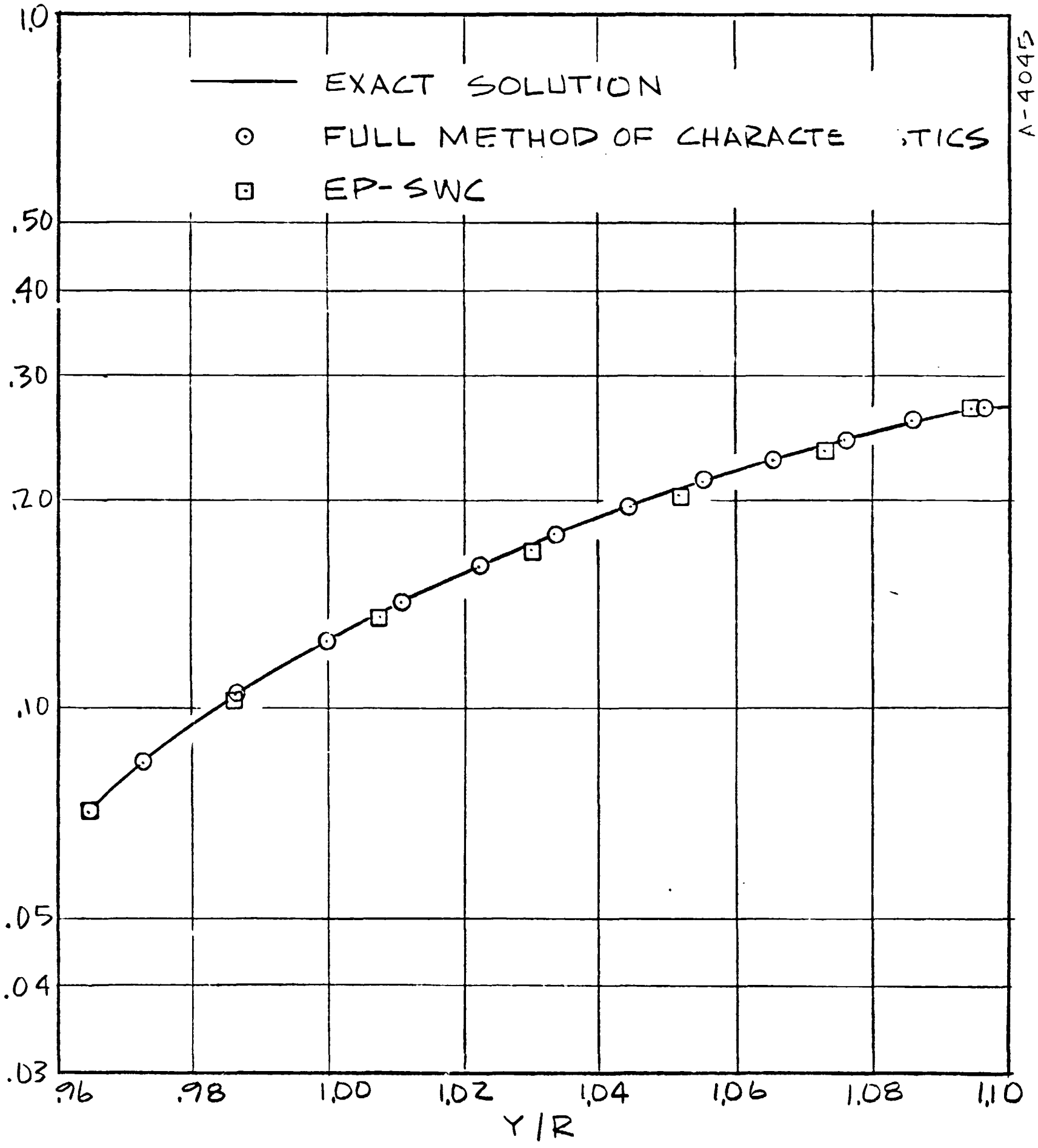

FIGURE 11 SIMPLE EXPANSION WAVE - COMPARISON OF PRESSURE PROFILES

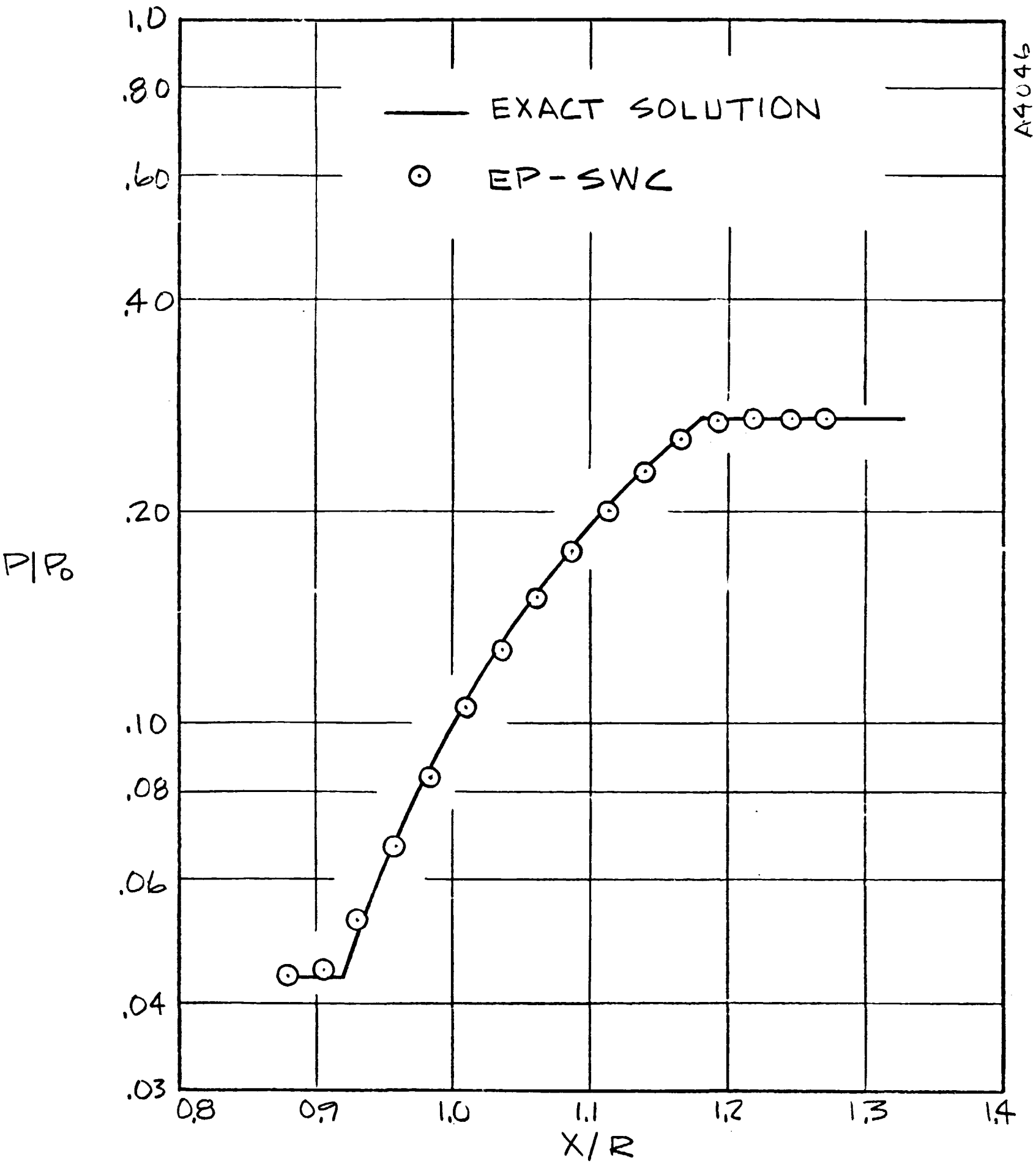

a) X/R = 0.5095

FIGURE 12 SIMPLE EXPANSION - COMPARISON OF RESULTS OF EP-SWC SCHEME WITH EXACT SOLUTION FOR PRESSURE PROFILES

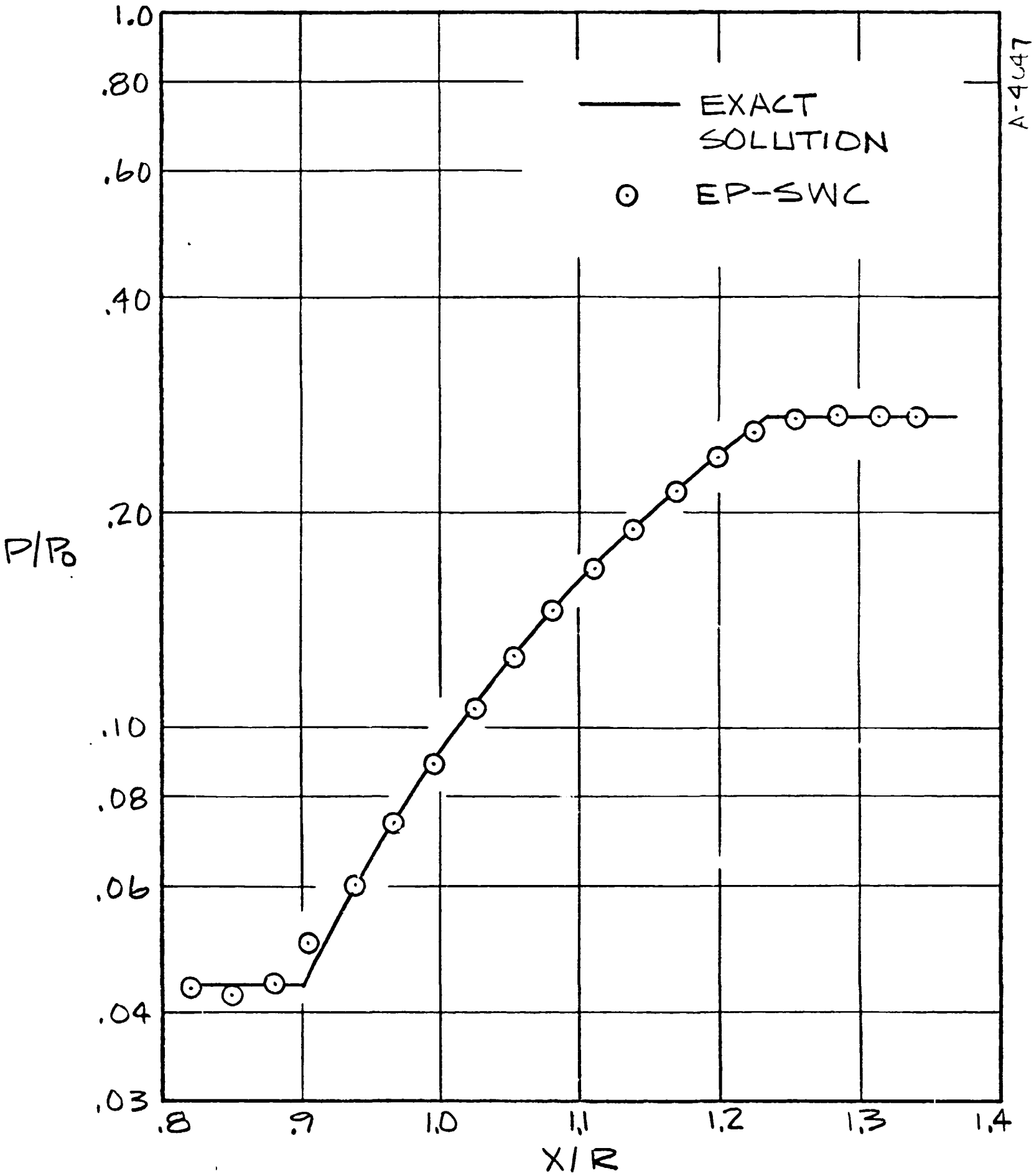

b) X/R = 0.6654

FIGURE 12 (CONCLUDED)

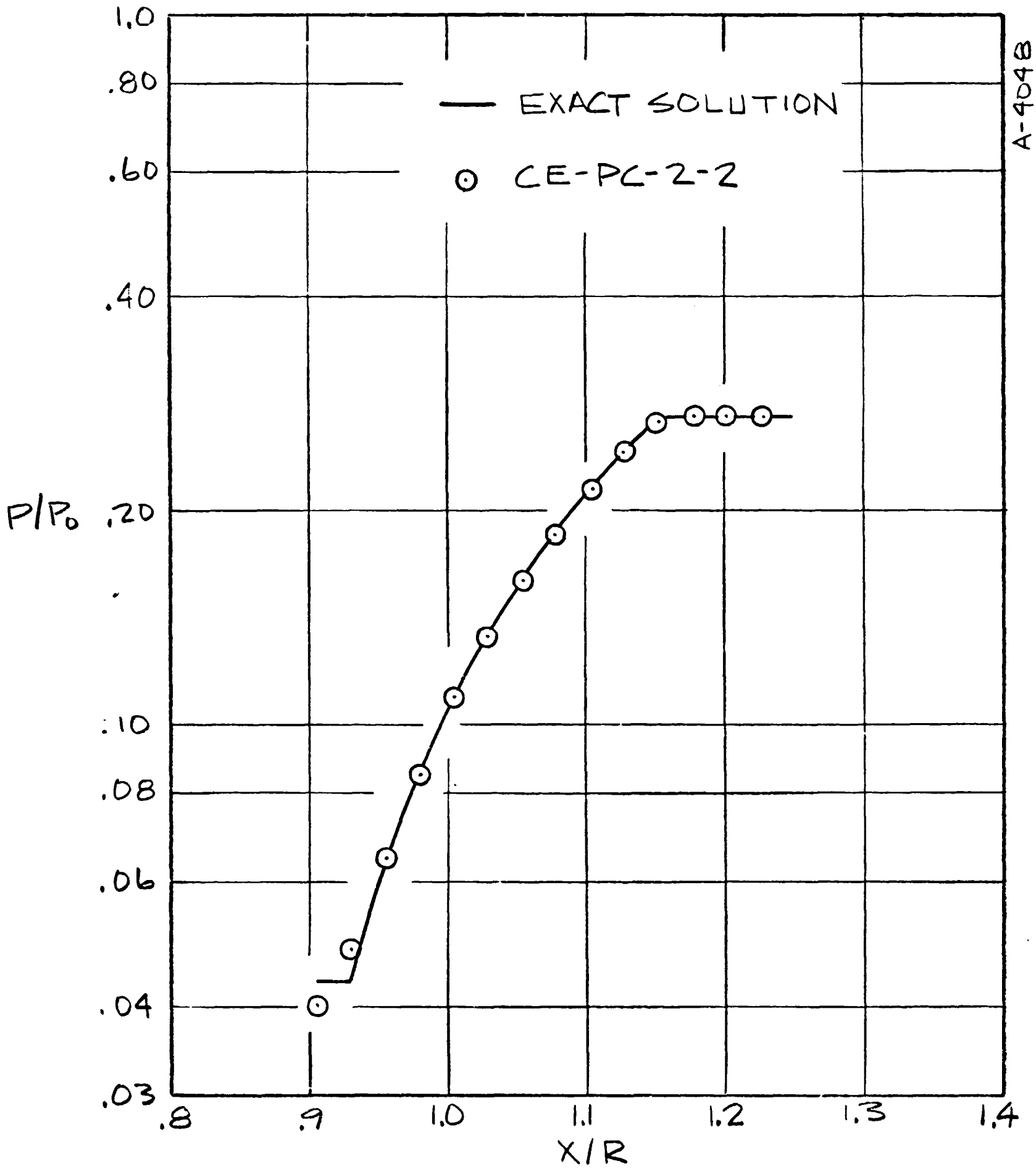

a) SCHEME CE-PC-2-2

FIGURE 13 SIMPLE EXPANSION WAVE - COMPARISON OF PRESSURE PROFILES PREDICTED BY TWO OF THE POORER SCHEMES WITH EXACT SOLUTION

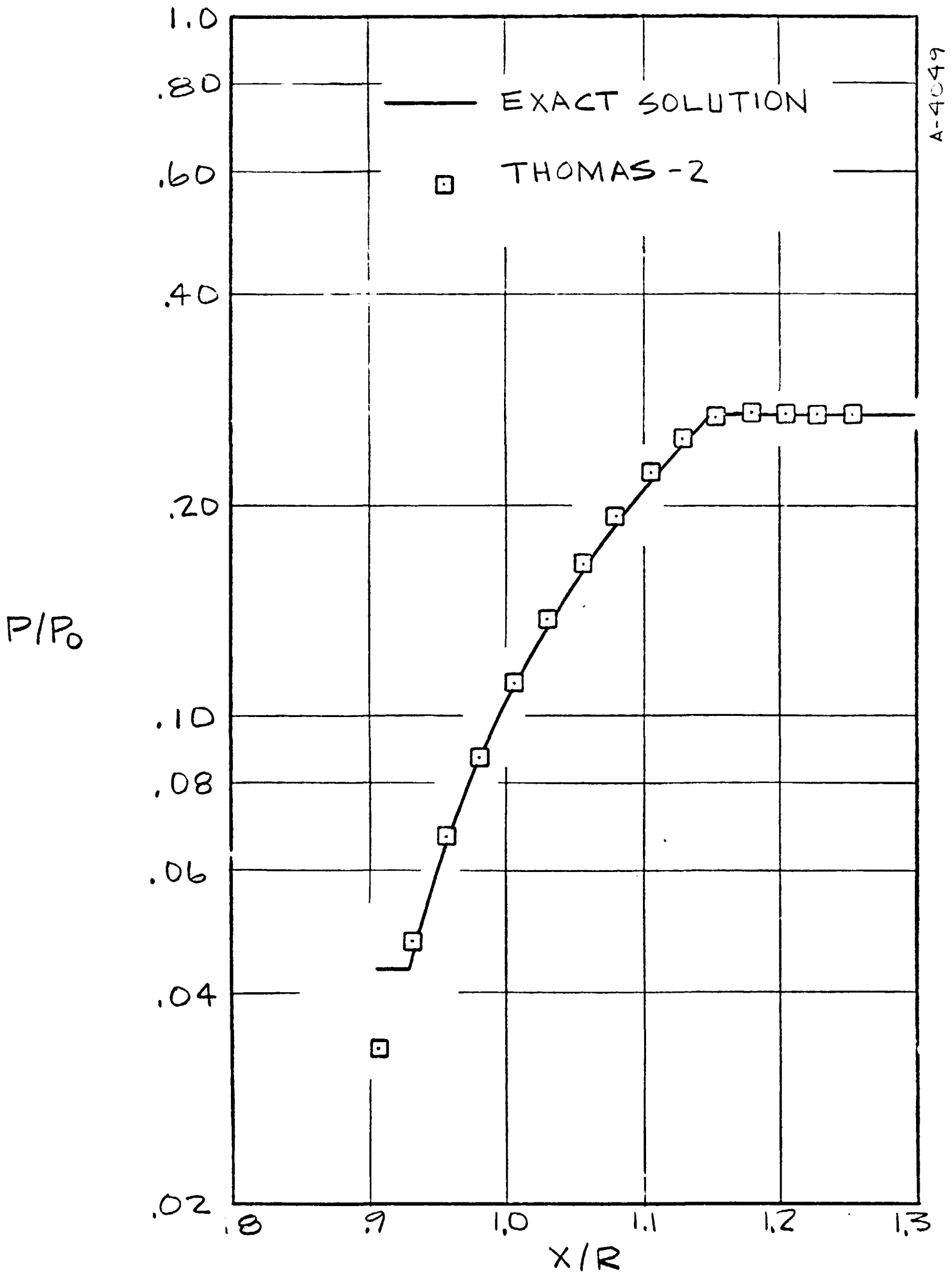

b) SCHEME THOMAS-2

FIGURE 13 (CONCLUDED)

REFERENCES

Abbett, M. J., "Finite Difference Solution of the Subsonic/Supersonic Inviscid Flow Field about a Supersonic, Axisymmetric Blunt Body at Zero Incidence, Analysis and User's Manual, Aerotherm Corporation, Mt. View, California, Report No. UM-71-34, June 30, 1971.

Ames Research Staff, "Equations, Tables, and Charts for Compressible Flow," NACA Report 1135, 1953.

Babenko, K. I., et al., "Three-Dimensional Flow of Ideal Gas Past Smooth Bodies," NASA TTF-380, April 1966. Translation of "Prostranstvennoye obtekaniye gladkikh tel ideal'nym gazom," Izdatel'stvo "Nauka" Moscow, 1964.

Babenko, K. I. and Rusanov, V. V., "Difference Methods for Solving Three-Dimensional Problems in Gas Dynamics," NASA-TTF-10,826, April 1967, translation of "Raznostnyye metody resheniya prostranstvennykh zadach gazovoy dinamiki," in Kolebaniya, Giroskopiya, Teoriya, Mekhanizmov, Zhidkosti i Gaza, 2nd All-Union Proceedings of the Conference on Theoretical and Applied Mechanics, Moscow, 1964.

Barnwell, Richard, "Time Dependent Numerical Method for Treating Complicated Blunt Body Flow Fields, NASA SP-228, 1970.

Barnwell, Richard, "Three Dimensional Flow Around Blunt Bodies with Sharp Corners," AIAA Paper 71-56, presented at Ninth Aerospace Science Meeting, New York, N.Y., January 25-27, 1971.

Bohachevsky, I. and Kostoff, R. N., "Hypersonic Flow Over Cones with Attached and Detached Shock Waves," AIAA Paper No. 71-55, presented at the Ninth Aero. Science Meeting, New York, N.Y., January 25-27, 1971.

Bohachevsky, I. O. and Mates, R. E., "A Direct Method for Calculation of the Flow About an Axisymmetric Blunt Body at Angle of Attack," AIAA Journal, 4, 5, May 1966, 776-782.

Bohachevsky, I. and Rubin, E., "A Direct Method for Computation of Non-Equilibrium Flows with Shock Waves," AIAA Journal, 4, 4, 1966, 600-607.

Burstein, S. Z., "Numerical Methods in Multidimensional Shocked Flows," AIAA Journal, 2, 12, 1964, pp. 2111-2117.

Carriere, Pierre and Capelier, Claude, "Application de la Methode Des Characteristiques Instationnaires au Calcul Numerique d'un Ecoulement Permanent Compressible, AGARD CP 35, Transonic Aerodynamics, September 1968, 12 pp.

Cheng, Sin-I, "Accuracy of Difference Formulation of Navier-Stokes Equation," Physics of Fluids, Supplement II, Proceedings of the International Symposium on High Speed Computing in Fluid Dynamics, 12, 12, December 1969, pp. II-34 through II-41.

Ciment, Melvyn, "Stable Difference Schemes with Uneven Mesh Spacings," New York University, NYO-1480-100, June 1968.

Coakley, James F. and Porter, Robert W., "Characteristics at Boundaries in Numerical Gas Dynamics, Plasma Dynamics Lab., Dept. of Mech. and Aerospace Engr., Illinois Institute of Technology, Chicago, Ill., PDL Note 2-69, Nov. 1969.

Eaton, Roger R., "A Numerical Solution for the Flow Field of A Supersonic Cone - Cylinder Entering and Leaving a Blast Sphere Diametrically, Sandia Laboratories, Albuquerque, New Mexico, SC-CR-67-2532, May 1967.

Edelman, R. B., et al., "Some Aspects of Viscous Chemically Reacting Moderate Altitude Exhaust Plumes," General Applied Science Labs., Westbury, N.Y., Final Report on NASA Contract NAS8-21264, March 1970.

Gary, John, "On Certain Finite Difference Schemes for Hyperbolic Systems," Math. of Computation, 18, January 1964, pp. 1-18.

Godunov, S. K., Zabrodin, A. V., and Prokopov, G. P., "The Difference Schemes for Two-Dimensional Unsteady Problems in Gas Dynamics and the Calculation of Flows with a Detached Shock Wave." J. Comp. Math. Math, Physics, 1, 6, November - December 1961.

Gonidou, René, "Ecoulements Supersonic Autour de Cones en Incidence," La Recherche Aerospatiale, No. 120, September-October 1967, pp. 11-19.

Grossman, B., and Moretti, G., "Time Dependent Computation of Transonic Flow," AIAA Paper No. 70-1322, October 1970.

Johnson, J., ed., "Investigation of the Low Speed Fixed Geometry Scramjet Part I., Inlet Design Practice Manual, General Applied Science Laboratories, Westbury, New York, TR-667, 1967. (Also Issued as AFAPL-TR-68-7).

Kentzer, Czeslaw P., "Discretization of Boundary Conditions on Moving Discontinuities," presented at Second International Conference on Numerical Methods in Fluid Dynamics, University of California, Berkeley, California, September 15-19, 1970.

Kentzer, Czeslaw P., "Computations of Time Dependent Flows on an Infinite Domain," AIAA Paper No. 70-45, January 1970.

Kutler, Paul, "Application of Selected Finite Difference Techniques to the Solution of Conical Flow Problems," Ph.D. thesis, Iowa State University, 1969.

Kutler, Paul and Lomax, Harvard, "A Systematic Development of the Supersonic Flow Fields Over and Behind Wings and Wing-Body Configurations Using a Shock-Capturing Finite Difference Approach," AIAA Paper No. 71-99, presented at the 9th Annual Meeting, New York, N.Y., January 1971.

Kutler, Paul, Lomax, Harvard, and Warming, R. F., "Computation of Space Shuttle Flow Fields Using Noncentered Finite Difference Schemes," to be presented at 10th Aerospace Sciences Meeting, AIAA, San Diego, California, January 1972.

Lapidus, Arnold, "A Detached Shock Calculation by Second-Order Finite Difference," J. Computational Physics, 2, 2, 1967, 159-177.

Lee, Che Ching, "A Theoretical Study of the Interaction of Sonic Transverse Jets with Supersonic External Flows," Ph.D. thesis, University of Alabama, University, Alabama, 1969.

Mac Cormack, Robert W., "Numerical Solution of the Interaction of a Shock Wave with a Laminar Boundary Layer," presented at the Second International Conference on Numerical Methods in Fluid Dynamics, University of California, Berkeley, Calif., September 15-19, 1970.

MacKenzie, D. and Moretti, G., "Time Dependent Calculation of the Compressible Flow About Airfoils," AGARD CP 35, Transonic Aerodynamics, September, 1968.

Magnus, R. and Yoshihara, H., "Inviscid Transonic Flow Over Airfoils," AIAA J., 8, 12, December 1970, pp. 2157-2162.

Masson, Bruce S., "Two Dimensional Flow Field Calculations by the Godunov Method," Aeronutronic Report No. U-4137, Philco Ford Corp., Aeronutronic Div., Newport Beach, Calif., Picatinny Arsenal, Dover, N. J., PA-TR-3575, AD 818379.

Moretti, Gino, "The Importance of Boundary Conditions in the Numerical Treatment of Hyperbolic Equations," The Physics of Fluids, Supplement II, Proceedings of the International Symposium on High-Speed Computing in Fluid Dynamics," 12, 12, December 1969, pp. II-13 through II-20.

Moretti, Gino, "Transient and Asymptotically Steady Flow of an Inviscid, Compressible Gas Past a Circular Cylinder," Polytechnic Institute of Brooklyn, New York, PIBAL Report No. 70-20, April 1970.

Moretti, Gino, "Inviscid Flow Past a Pointed Cone at an Angle of Attack," General Applied Science Labs., Westbury, N.Y., TR 577, December, 1965 (also AIAA J., 4, 5, April 1967, 789-791).

Moretti, Gino, Entropy Layers, Polytechnic Institute of Brooklyn, New York, PIBAL Report No. 71-33, 1971

Moretti, Gino and Abbett, Michael, "A Time-Dependent Computational Method for Blunt Body Flows," AIAA J., 4, 12, December 1966, 2136-2141.

Moretti, G. and Bastianon, R., "Three Dimensional Effects in Intakes and Nozzles," AIAA Paper No. 67-224, 1967.

Rakich, John, and Kutler, Paul, "Application of Shock Capturing and Semi-Characteristics Methods to Shuttle Flow Fields," to be presented at 10th Aerospace Science Meeting, AIAA, San Diego, Calif., January 1972.

Scala, S. M. and Gordon, P., "Solution of the Time Dependent Navier-Stokes Equations for the Flow Around a Circular Cylinder," AIAA Paper 67-221, 1967.

Serra, R. A., "The Determination of Internal Gas Flows by a Transient Numerical Technique," AIAA Paper No. 71-45, presented at the Ninth Aerospace Science Meeting.

Singleton, Robert E., "Lax-Wendroff Difference Scheme Applied to the Transonic Airfoil Problem," AGARD CP 35, Transonic Aerodynamics, September 1968, pp. 2-1 to 2-9.

Skoglund, Victor J. and Gay, Ben Douglas, "Improved Numerical Techniques and Solution of a Separated Interaction of an Oblique Shock Wave and a Laminar Boundary Layer," Bureau of Engineering Research, University of New Mexico, Final Report ME-41(69) S-068, June 1968.

Thomas, P. D., et. al., "Numerical Solution for the Three Dimensional Hypersonic Flow Field of a Blunt Delta Body," AIAA paper 71-596, June 1971.

Thomas, P. D., "On the Computation of Boundary Conditions in Finite Difference Solutions for Multidimensional Inviscid Flow Fields," Lockheed Palo Alto Research Laboratory, Palo Alto, California, LMSC 6-82-71-3, March 2, 1971, Revision A, September 13, 1971.

Thompson, Joe F., "Computer Experimentation with an Implicit Numerical Solution of the Navier -Stokes Equations for an Oscillating Body," AIAA Paper No. 69-185.

Tyler, L. D. and Zumwalt, G. W., "Numerical Solution of the Flow Field Produced by a Shock wave Emerging into a Crossflow," Proceedings of the 1966 Heat Transfer and Fluid Mechanics Institute, ed. by M. Saad and J. Miller, Stanford University Press, Stanford, Calif., 1966, pp. 335-350.

Walker, William F. and Zumwalt, Glen W., "A Numerical Solution for the Interaction of a Moving Shock Wave with a Turbulent Mixing Region, Sandia Corp., SC-CR-67-2531, May 1, 1966.